CLONING, CHARACTERIZATION, AND LOCALIZATION OF AN ABC TRANSPORTER IN THE ROD PHOTORECEPTOR RIMS IMPLICATED IN STARGARDT'S AND AGE-RELATED MACULAR DYSTROPHY

by

MICHELLE ELIZABETH ANNE ILLING

B.Sc. (Hons.), Carleton University, 1987
M.Sc., Carleton University, 1991

A THESIS SUBMITTED IN PARTIAL FULFILLMENT OF

THE REQUIREMENTS FOR THE DEGREE OF

DOCTOR OF PHILOSOPHY

in

THE FACULTY OF GRADUATE STUDIES

(Department of Biochemistry and Molecular Biology)

We accept this thesis as conforming

to the required standard

THE UNIVERSITY OF BRITISH COLUMBIA

December 1997

In presenting this thesis in partial fulfilment of the requirements for an advanced degree at the University of British Columbia, I agree that the Library shall make it freely available for reference and study. I further agree that permission for extensive copying of this thesis for scholarly purposes may be granted by the head of my department or by his or her representatives. It is understood that copying or publication of this thesis for financial gain shall not be allowed without my written permission.

Department of Biochemistry

The University of British Columbia
Vancouver, Canada

Date January 29, 1998

DE-6 (2/88)

ABSTRACT

Outer segments of vertebrate photoreceptor cells contain an abundantly expressed membrane protein that migrates with an apparent molecular mass of 220-290 kDa by SDS gel electrophoresis. Twenty years ago, immunocytochemical studies localized the 290 kDa frog protein to the rims of the photoreceptor disks and since then it has been generally believed that this rim protein is responsible for the filaments observed that link adjacent disks and/or disks to the plasma membrane. Due to its localization and abundance in the outer segment, this protein is likely a good candidate for involvement in retinal disease.

In this study, the primary structure of the bovine 220 kDa protein has been determined by cDNA cloning and direct peptide sequence analysis. A data base homology search showed that it is a new member of the ABC (ATP-binding cassette) transporter superfamily, which includes the cystic fibrosis transmembrane conductance regulator (CFTR), multi-drug resistance proteins P-glycoprotein and MRP, and bacterial transporters. Generally, these proteins utilize the energy of ATP hydrolysis by two nucleotide binding domains (NBDs) for transport of a substrate across the membrane. Clones containing the human 220 kDa orthologue were found to be identical to a recently cloned retina cell-specific ABC transporter (Allikmets *et al.*, Nature Genetics, **15**, 236, 1997). Mutations in the gene encoding this protein (*ABCR*) have been implicated in Stargardt's disease, and more recently, in age-related macular dystrophy.

Studies of immunoaffinity purified 220 kDa protein showed that both ATP and GTP bind this protein with similar affinities. In addition, the protein contains at least one carbohydrate chain and, when solubilized with detergent, does not appear to co-purify with other proteins. Immunocytochemical and biochemical studies have revealed that the 220 kDa glycoprotein is distributed along the rim region and incisures of rod outer segment disk membranes in a pattern similar to that observed for the 290 kDa protein in

frog photoreceptors. Two cytoplasmic fragments each containing one NBD were expressed in *Escherichia coli* and purified. Both of the NBDs were capable of hydrolyzing ATP and GTP at rates comparable to NBDs of other ABC transporters. These experiments suggest that the energy of nucleotide hydrolysis supports active transport of a substrate across the disk membrane.

This study serves as a basis for beginning to define the role of the ABC transporter in rod photoreceptor structure and function and elucidating the molecular basis for how specific mutations in the *ABCR* gene, particularly those in the NBD, lead to either Stargardt's disease or AMD.

TABLE OF CONTENTS

LIST OF TABLES

LIST OF FIGURES

LIST OF ABBREVIATIONS

ABC	ATP binding cassette
ABTS	2,2'-azino-bis(3-ethylbenzthiazolne-6-sulfonic acid)
ADP	adenosine 5'-diphosphate
ADRP	autosomal dominant retinitis pigmentosa
AMD	age-related macular degeneration
ARRP	autosomal recessive retinitis pigmentosa
ATP	adenosine 5'-triphosphate
ATS	active transport signature
BCA	bicinchroninic acid
βME	β-mercaptoethanol
bp	base pairs
BSA	bovine serum albumin
CB	Coomassie Blue
CHAPS	3-[(cholamidopropyl)-dimethylammonio]-1-propanesulfonate
cDNA	DNA reverse-transcribed from an mRNA template (copy DNA)
CFTR	cystic fibrosis transmembrane regulator
cfu	colony forming units
cGMP	guanosine 3',5'-cyclic monophosphate
Ci	Curie
Con A	concanavalin A
CNBr	cyanogen bromide
CTP	cytosine 5'-triphosphate
DAB	diaminobenzidine
DEAE	diethyl aminoethyl
DIC	differential interference contrast

DNA	deoxyribonucleic acid
dNTP	deoxyribonucleoside triphosphate
ECL	enhanced chemiluminescence
EDTA	ethylaminediamine tetraacetic acid
ELISA	enzyme-linked immunosorbant assay
Endo Hf	endoglycosidase Hf
FBS	fetal bovine serum
g	gravity
GAP	GTPase-activating protein
GC	guanylyl cyclase
GCAP	guanylyl cyclase-activating protein
GCL	ganglion cell layer
GDP	guanosine 3'-diphosphate
GST	glutathione-S-transferase
GTP	guanosine 3'-triphosphate
HAT	IMDM media supplemented with hypoxyanthine, aminopterin, and thymidine
HT	IMDM media supplemented with hypoxyanthine and thymidine
Ig	Immunoglobulin
IMDM	Iscove's modified Dulbecco's medium
INL	Inner nuclear layer
IPL	Inner plexiform layer
kb	kilobase
kDa	kilodalton
Km	Michaelis constant (substrate concentration at which the reaction rate is half-maximal)
LCA	Leber's congenital amaurosis

MD	macular degeneration
MDR	multi-drug resistance
MRP	multi-drug resistance related protein
mRNA	messenger RNA
NBD	nucleotide binding domain
ONL	outer nuclear layer
OPL	outer plexiform layer
PAGE	polyacrylamide gel electrophoresis
PBS	phosphate buffered saline
PBST	PBS with 0.05% Tween 20
PDE	phosphodiesterase
pfu	plaque forming units
PMSF	phenyl methyl sulfonyl fluoride
psi	pounds per square inch
rds	retinal degeneration slow
RGS	regulator of G protein signaling
RK	rhodopsin kinase
RNA	ribonucleic acid
ROS	rod outer segment
RPE	retinal pigmented epithelium
S	substrate concentration
SDS	sodium dodecyl sulfate
STGD	Stargardt's disease
TAP	transporter associated with peptide presentation
TCPK	N-Tosyl-L-phenylalanine chloromethyl ketone
TMD	transmembrane domain
Tris	Tris [hydroxymethyl]aminomethane

V	velocity
Vmax	maximal velocity

ACKNOWLEDGMENTS

I am very grateful to my thesis committee members, Dr. Ross MacGillivray and Dr. Michael Hope, for their advice during my study and my written thesis. I would also like to thank Dr. Bob Molday for giving me the opportunity to work in his lab on such an interesting project. The caliber and integrity of his work will be the standard I will attempt to match in my future investigations. I am also grateful to the University of British Columbia and the Killam Foundation for supporting me with University Graduate Fellowships and a Killam Predoctoral Fellowship.

I would like to thank Theresa Hii for performing the hybridoma fusion and her assistance in screening of the fusion and general tissue culture procedures. I would like to thank Laurie Molday for performing the electron microscopy protocols. I am grateful to Dr. Orson Moritz for his expertise and advice in various molecular biology techniques. In addition, the peptide sequencing and amino acid analysis was carried out by Sandy Kielland at the Tripartite Center at the University of Victoria.

I would also like to thank other past and present members of the Molday lab: Dr. Andréa Dosé, Dr. Carol Colville, Dr. Andrew Goldberg, Dr. Delyth Wong, Dr. Yi-Te Hsu, Dr. Shu Hsu, Tom Kim, Dr. Andy Williams, Chris Loewen, Igor Nasonkin, Nancy Mah, René Warren, and Natalie Rundle. They all helped to make my scientific and social time more enjoyable.

Finally, I would like to acknowledge the contribution by my family and Grant Stewart, my best friend; I don't know what I would have done without them.

To:

my parents,

with love

INTRODUCTION

1.1 The Retina:

The vertebrate retina is a delicate extension of the brain which is located at the rear of the eyeball behind protective and nourishing layers of tissue (**Fig 1**). All vertebrate retinas are composed of three layers of cells and two layers of neuronal interconnections (**Fig 2**). The retina is in the reverse orientation to what one might expect: light must pass through the ganglion cell layer and the inner nuclear layer before stimulating the rods and cones of the photoreceptor layer. The photoreceptors transmit their signal to the neurons of the inner retina (bipolar, amacrine, and horizontal cells). These neurons, in turn, transmit their signal to the ganglion cells that comprise the optic nerve, thereby transmitting the signal to the brain (reviewed by Kolb, 1994).

1.2 The Pigment Epithelium:

The retinal pigment epithelium (RPE) is separated from the choroid by Bruch's membrane. The choroid is the vascular layer that provides nutrients to the retina, while Bruch's membrane is a smooth layer which ensures the regular alignment of both the retinal cells and the RPE. The RPE surrounds the outer segments of the photoreceptors (**Fig 2**) and services and maintains them in five ways: (1) absorption of stray light; (2) active transport of metabolites; (3) provision of a blood-retinal barrier; (4) regeneration of visual pigments; and (5) phagocytosis of the photoreceptor outer segments (reviewed by Spalton *et al.*, 1994). These processes become less efficient with age and breakdown products may either become stored in the RPE as lipofuscin or in Bruch's membrane as drusen. Lipofuscin has been shown to be partially composed of a complex between two retinaldehyde molecules and one ethanolamine, presumably derived from phosphotidylethanolamine (Birnbach *et al.*, 1994).

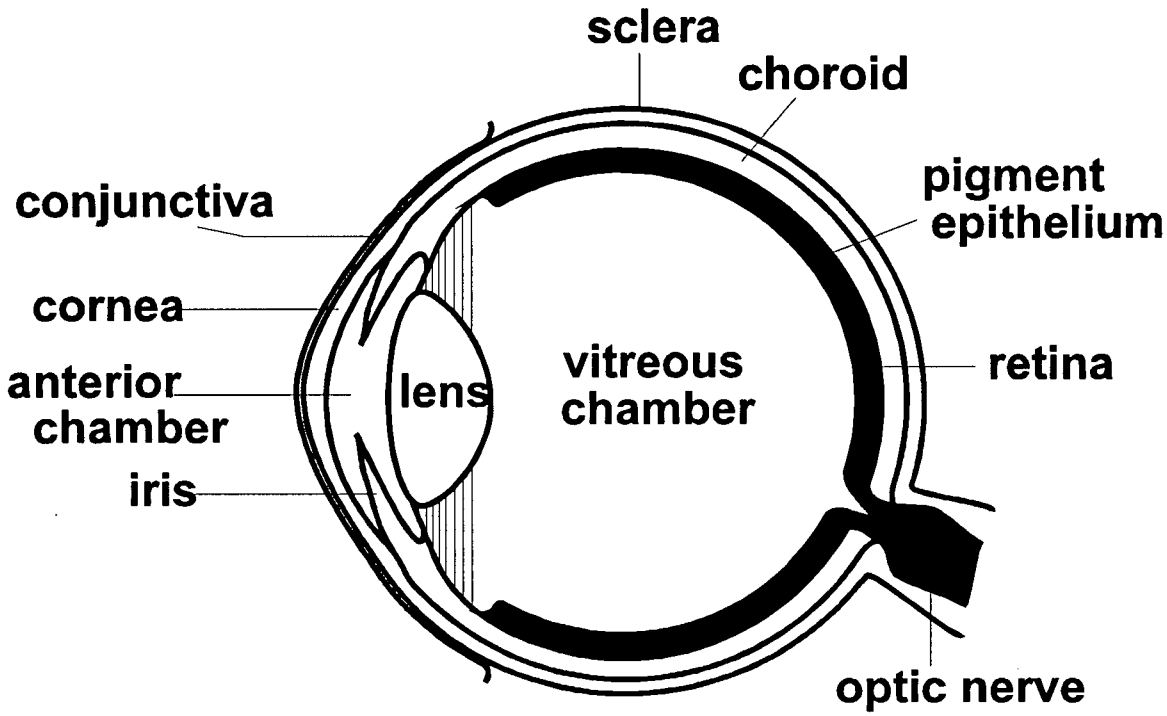

Fig 1. Cross-section of a vertebrate eye. Light enters the eye through two transparent tissues, the conjunctiva and the cornea, and then is focused by the lens onto the retina. The photoreceptor cells of the retina detect light and transmit a signal via the optic nerve to the brain. The cornea is continuous with the sclera, a hard outer layer that protects the eyeball. At the back of the eyeball is the choroid, which is the vascular layer that provides nutrients to the retina. The pigment epithelium is closely associated with the photoreceptor cells and lies between the photoreceptor layer and the choroid. Figure reproduced from Dosé (1995).

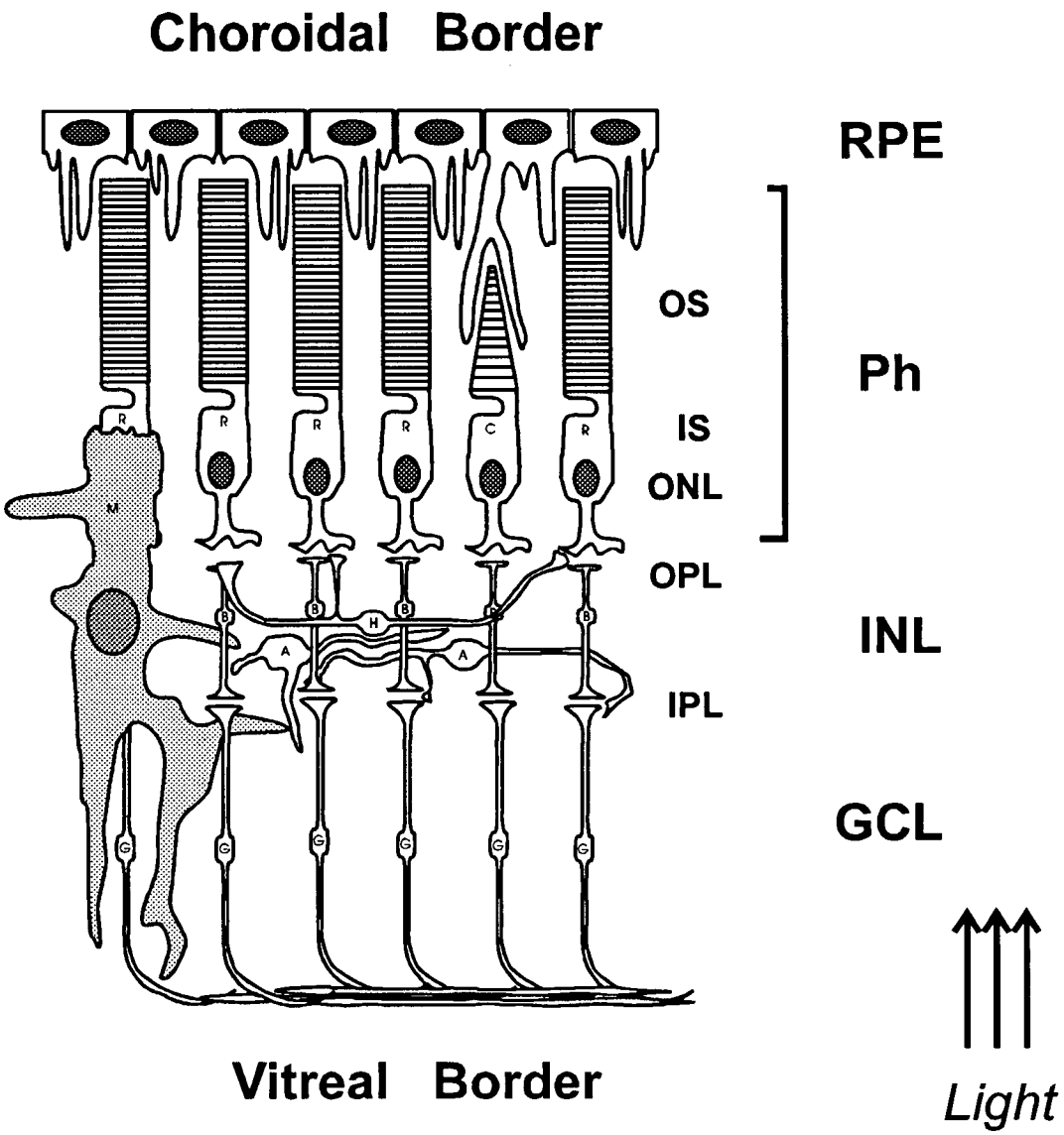

Fig 2. The pigment epithelium and the retinal cell layers. The retinal pigment epithelium (RPE) is responsible for maintenance of the photoreceptor cells. The first layer in the retina is the outer segments (OS) and inner segments (IS) of the photoreceptors (Ph). The nuclei of the photoreceptors make up the outer nuclear layer (ONL). The outer plexiform layer (OPL) is the site of synapse between the photoreceptors and the neurons of the inner nuclear layer (INL), consisting of the bipolar cells (B), amacrine cells (A) and horizontal cells (H). The inner plexiform layer (IPL) is the site of synapse between the cells of the INL and the ganglion cell layer (GCL). The ganglion cell (G) axons form the optic nerve. Also shown are Müller cells (M). Figure modified from Dosé (1995).

1.3 Photoreceptor Cells:

There are two major classes of photoreceptors in the vertebrate retina: the rods and cones. Rod photoreceptors are responsible for vision in dim light, while cones provide colour vision. In most mammalian retinas, the rods outnumber the cones 20 to 1 (Osterberg, 1935), thus making the processes occurring in rod cells better studied than those in cones.

Both rod and cone photoreceptors can be divided into four areas: the outer segment, the inner segment, the cell body, and the synaptic terminus (**Fig 3**). The photoreceptors are named for the shape of their outer segments. The rod outer segment is much more elongated compared to that of the cone, while the cone outer segment is more narrow at its distal end. The outer segment of the rod cell is comprised of a stack of 500-2000 membranous disks surrounded by a plasma membrane. However, the plasma membrane of the cones is continuous with the disk membranes. In both photoreceptor cells, the outer segment is connected to the inner segment by a thin cilium. The inner segment contains the cellular organelles and the cell body houses the nucleus. At the end of the cell is the synaptic terminus, which transmits a signal to the cells of the inner layer of the retina via the neurotransmitter glutamate (reviewed by Massey and Maguire, 1995).

1.4 The Visual Transduction Cascade:

The primary role of the photoreceptors is to convert the energy of a captured photon of light to an electrophysiological signal. In the last ten years, remarkable progress has been made in understanding the rod cell's complex cascade response to light and the steps for restoring the system to the resting state (reviewed by Pugh and Lamb, 1993; Palczewski, 1994; Polans *et al.*, 1996; Koch, 1995).

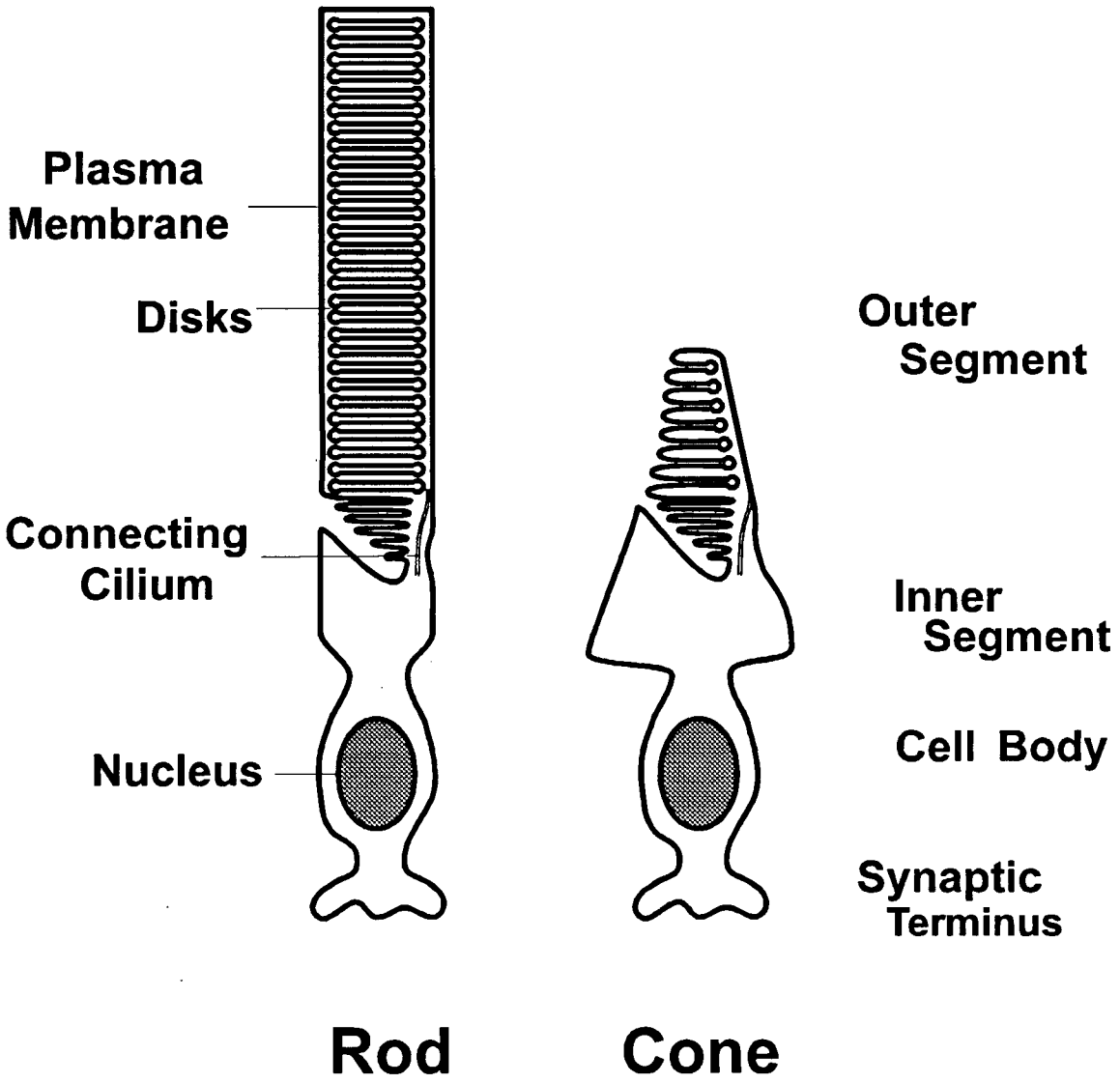

Fig 3. Vertebrate photoreceptors. There are two major classes of photoreceptors in the vertebrate retina, the rods and cones (not drawn to scale). The rod cells have an outer segment which is comprised of a stack of membranous disks surrounded by a plasma membrane. The plasma membrane of the cones, on the other hand, is continuous with the disk membranes. In both photoreceptors, the outer segment is connected to the inner segment by a thin cilium. The inner segment contains the cellular organelles and the cell body houses the nucleus. At the end of the cell is the synaptic terminus, which signals to the cells of the inner layer of the retina. Figure modified from Dosé (1995).

The cascade begins in the outer segment with the interaction of a photon with the chromophore (11-*cis*-retinal) of rhodopsin, causing a series of rearrangements leading to the formation of metarhodopsin II containing all-*trans*-retinaldehyde (**Fig 4**). The signal is then amplified by a cascade involving a G-protein (transducin) and cGMP phosphodiesterase (PDE). Metarhodopsin II binds to and activates transducin: bound GDP is exchanged for GTP and transducin dissociates into Tα and Tβγ subunits. The Tα binds to PDE and stimulates the hydrolysis of cGMP to GMP (Fung *et al.*, 1981). This reaction is slowly terminated by the intrinsic GTPase of transducin, which is in turn accelerated several fold by PDE binding. GTP hydrolysis is also known to be stimulated by a membrane-bound GTPase-activating protein (GAP). Two retina-specific members of a new gene family encoding regulator of G protein signaling (RGS) proteins have recently been cloned (Chen *et al.*, 1996; Faurobert and Hurley, 1997). One or both of these proteins may be responsible for the observed GAP activity in the outer segment.

The reduction in cGMP levels by PDE leads to a change in the conformation of the cGMP-gated channel, which leads to channel closure. Channel closure reduces the conductance of the plasma membrane to cations and results in the hyperpolarization of the plasma membrane, inhibition of neurotransmitter release, and signaling to adjacent neurons. The channel is also regulated by the calcium-binding protein calmodulin (Hsu and Molday, 1993). Calmodulin binding to the channel decreases affinity for cGMP. This decreased affinity results in up to a six fold increase in cation flux at low cGMP levels, and therefore, increased sensitivity of the channel for small changes in cGMP.

Calcium also plays a key role in returning the photoreceptor cell to its resting or dark state by regulating the enzyme guanylyl cyclase. In the dark, the Ca^{2+} concentration is approximately 500 nM and guanylyl cyclase (GC) has low activity. After photoactivation, the channels close and Ca^{2+} levels fall due to the continuing action of the Na^{+}/Ca^{2+}-K^{+} exchanger (**Fig 4**). Low levels of Ca^{2+} activate GC to

Fig 4. The molecular mechanism of phototransduction. Phototransduction begins when rhodopsin molecules capture light and rearrange through several intermediates to metarhodopsin I and metarhodopsin II (step 1). Two opposite processes involve activated rhodopsin: photolyzed rhodopsin triggers a cascade of the amplification reactions and it is inactivated in reactions that involve rhodopsin kinase and arrestin (step 1). Metarhodopsin II catalyses the nucleotide exchange from GDP to GTP in G_t molecules (step 2). The G_t-GTP complex falls apart and α-subunit-bearing GTP binds and activates PDE (step 3), lowering cGMP concentration. Inactivation of this complex occurs when GTP is hydrolyzed to GDP by intrinsic GTPase activity of the α-subunit (step 2). Changes in cGMP (buffered by noncatalytic binding sites of photoreceptor proteins) directly regulate cation channels in the plasma membrane. The combined effects of the cGMP-gated cation channels (closure of the channels impedes calcium flow into the cytosol; step 4) and the Na^+/Ca^{2+}-K^+ exchanger (continues to extrude calcium; step 5) lead to a decrease in intracellular Ca^{2+} concentration and, subsequently, activation of guanylyl cyclase (step 5). Not illustrated are the regulators of G protein signaling proteins (see text for details). The cyclase activity is regulated by a calcium-binding protein M*. Rh, rhodopsin; M, metarhodopsins; K_{Rh}, rhodopsin kinase; 48k, arrestin (S-antigen); G, G-protein; PDE, phosphodiesterase; Cyc, guanylyl cyclase; R, retinal calcium binding protein (recoverin); "buffer", noncatalytic binding sites for cGMP; M*, guanylyl cyclase activating protein (GCAP). Figure reproduced from Palczewski (1994).

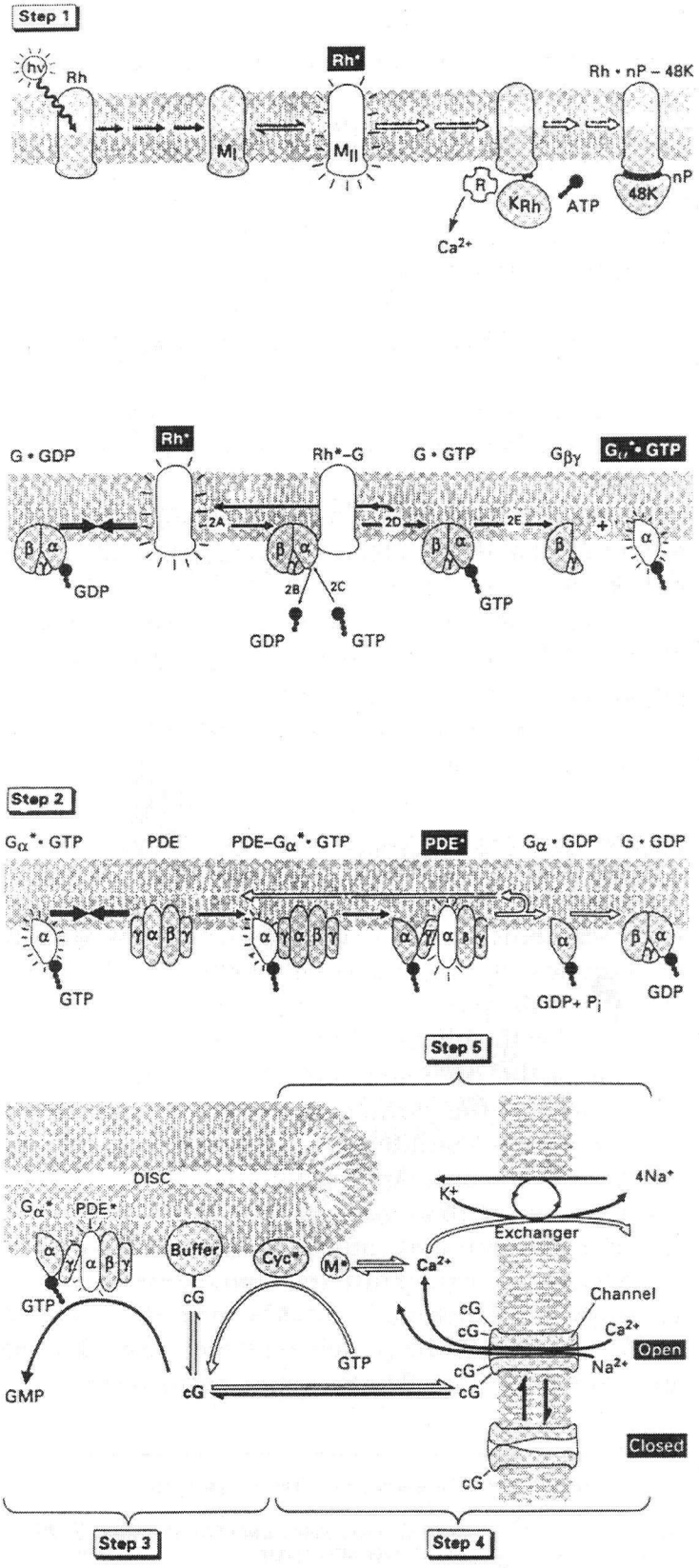
Step 1
hν
Rh
Rh*
Rh • nP – 48K
Mi
MII
R
KRh
ATP
48K
nP
Ca2+
G • GDP
Rh*
Rh*–G
G • GTP
Gβγ
Gα* • GTP
2A
2B
2C
2D
2E
GDP
GTP
GDP
GTP
Step 2
Gα* • GTP
PDE
PDE–Gα* • GTP
PDE*
Gα • GDP
G • GDP
GTP
GDP+ Pi
GDP
Step 5
DISC
Gα*
PDE*
Buffer
Cyc*
M*
Ca2+
4Na+
K+
Exchanger
Channel
cG
Ca2+
Na2+
Open
Closed
GTP
GMP
Step 3
Step 4

produce more cGMP, which reopens the channels and restores the membrane potential. Two GCs have been cloned from retinas: retGC1 and retGC2 (Shyjan *et al.*, 1992; Lowe *et al.*, 1995). To date, only retGC1 has been localized to the outer segments of photoreceptors. These two retGCs are not stimulated by peptides known to stimulate other GCs, but instead are stimulated by two GC activating proteins (GCAPs). GCAP1 (Palczewski *et al.*, 1994) and GCAP2 (Dizhoor *et al.*, 1995) are Ca^{2+}-binding proteins which stimulate GC in their unliganded state (*i.e.* at low Ca^{2+} levels). The precise intracellular locations, roles and interactions of retGC1, retGC2, and the two GCAPs are still under investigation.

Recovery of the cell to the resting state also includes the inactivation of metarhodopsin II. It is inactivated by rhodopsin kinase (RK) catalyzed phosphorylation and binding of the protein arrestin (Wilden *et al.*, 1986). The chromophore is reduced from all-*trans*-retinaldehyde to all-*trans*-retinol by retinol dehydrogenase and released from the inactive rhodopsin. The loss of the chromophore is the final step in the quenching process since the resulting phosphorylated rhodopsin is incapable of binding transducin, RK, or arrestin. The rhodopsin is regenerated by removal of the phosphates by protein phosphatase 2A (Palczewski *et al.*, 1989) and the binding of another molecule of 11-*cis*-retinal. At high calcium concentrations, the lifetime of photoactivated rhodopsin is prolonged by the calcium-binding protein recoverin, which binds to rhodopsin kinase (Gray-Keller *et al.*, 1993). Finally, the all-*trans*-retinol is transported from the disk membrane to the RPE by a poorly understood mechanism that involves the interphotoreceptor retinol binding protein (IRBP). In the RPE, the chromophore is regenerated to the 11-*cis*-retinal configuration and then returned to the disks, most likely using the same mechanism involving IRBP (reviewed by Bok, 1993).

The phototransduction cascade is less well studied in cone cells, which do not respond to the low levels of light that rods are capable of detecting. The transduction cascade appears to occur in much the same manner; however, many of the cone proteins

have cell-specific isoforms. For example, cone subtype-specific opsins have been cloned which are sensitive to red, blue or green wavelengths (Nathans, 1989). In addition, cone-specific isoforms of transducin (Lerea *et al.*, 1986), PDE (Hurwitz *et al.*, 1985) and the cGMP-gated cation channel (Bönigk *et al.*, 1993) have been identified.

1.5 Photoreceptor Outer Segments:

1.5.1 Regeneration of the Outer Segment:

Unlike other neurons, the photoreceptors continually replace a major portion of themselves: their outer segments. In rods cells, new disks are formed at the cilium, progressively pushing the old disks towards the pigment epithelium (Steinberg *et al.*, 1980). Disks are shed in the morning or at the onset of light after prolonged darkness. The shed disks are phagocytosed by the RPE, replacing the entire rod outer segment every 10-14 days. Less is known about cone cells; however, their disks are believed to be regenerated in a similar but slower fashion.

1.5.2 The Plasma Membrane:

Until recently, preparations of isolated disk and plasma membranes were highly impure making protein composition comparison difficult. An affinity density perturbation method employing ricin-gold dextran particles has been developed to address this problem (Molday and Molday, 1987). Briefly, the technique involves purification of outer segment vesicles by sucrose gradient centrifugation. These vesicles are then treated with neuraminidase, which removes sialic acid residues, exposing *Ricinus communis* agglutinin-binding sites on several plasma membrane-specific glycoproteins. The treated vesicles are then incubated with *R. communis* agglutinin ("ricin") which has been conjugated to 8 nm gold-dextran particles. The vesicles are subsequently lysed with hypotonic buffer and treated with dilute trypsin to disrupt plasma membrane-disk interactions. The resultant

preparation is subjected to sucrose gradient centrifugation. The isolated disk membranes form a distinct band in the gradient, separating them from the densely labeled plasma membrane which is found as a pellet at the base of the gradient.

Using this technique and immunohistochemistry, the protein composition of ROS disk membranes has been shown to differ from that of the plasma membrane (see **Table 1** for summary). Although both membranes contain rhodopsin as the major membrane protein, the cGMP-gated channel (Cook *et al.*, 1989), the Na^+/Ca^{2+}-K^+ exchanger (Reid *et al.*, 1990), and the GLUT-1 glucose transporter (Hsu and Molday, 1991) are predominantly, if not exclusively, present in the ROS plasma membrane.

1.5.3 The Disk Membrane and the Rim Region:

The disks are made up of two closely spaced lamellar membranes which are joined at the rims in a highly curved structure (**Fig 5**). The rim region is continuous along the margins of one or more incisures that penetrate toward the center of the disks. The continuous disk membrane encloses a compartment called the disk lumen or intradiskal space. The contents, if any, of the disks is unknown at the present time.

The major membrane protein of the disk lamellar region is rhodopsin. Guanylyl cyclase (Liu *et al.*, 1994) and retinol dehydrogenase are also believed to be localized to the lamellar region; however, conclusive evidence has yet to be obtained. The rim region of the disks appears to have its own complement of proteins. Both the peripherin/rds-rom-1 complex (Molday *et al.*, 1987; Bascom *et al.*, 1992; Moritz and Molday, 1996) and a high molecular weight 290 kDa glycoprotein in frog ROS (Paper-master *et al.*, 1978; Papermaster *et al.*, 1982) are localized to the rim region and incisures of rod and cone disk membranes. The peripherin/rds-rom-1 complex in mammalian ROS and the 290 kDa glycoprotein or rim protein of frog ROS each constitute 3-4% of the total ROS membrane protein (Molday *et al.*, 1987; Bascom *et al.*,

TABLE 1

Rod outer segment proteins[a]

Protein		M_r[b]
Disk membrane proteins		
Peripherin/rds[c]		35,000 (39,000)
Retinol dehydrogenase[d]		37,000
Rhodopsin		38,000
Rim protein[c]		220,000
Rom-1[c]		33,000 (37,000)
Plasma membrane proteins		
α-subunit of the cGMP-gated cation channel complex		63,000
β-subunit of the cGMP-gated cation channel complex		240,000 (155,000)
GLUT-1 glucose transporter		50,000
Na^+/Ca^{2+}-K^+ exchanger		230,000 (130,000)
Rhodopsin		38,000
Ricin-binding sialoglycoprotein		160,000
Ricin-binding sialoglycoprotein		110,000
Guanylyl cyclase (retGC1)[d]		112,000 (120,000)
Guanylyl cyclase (retGC2)[d]		124,000
Soluble and membrane-associated proteins		
Arrestin (S-antigen)		48,000
Calmodulin		20,000 (16,500)
Creatine kinase		43,000
Glutamic acid rich protein (GARP) soluble		140,000 (65,000)
Glutamic acid rich protein (GARP) truncated		62,000 (32,000)
Glyceraldehyde-3-phosphate-dehydrogenase		38,000
Guanylyl cyclase Activating Protein (GCAP1)		24,000
Guanylyl cyclase Activating Protein (GCAP2)		24,000
Phosducin		33,000
Phosphatase 2A		38,000
Phosphodiesterase:	α-subunit	88,000
	β-subunit	84,000
	γ-subunit	11,000
Protein kinase C		85,000
Pyrophosphatase		44,000
Recoverin		26,000 (23,000)
Regulator of G protein signaling protein (RGS-r)		23,000
Regulator of G protein signaling protein (RET-RGS-1)		42,000
Rhodopsin kinase		68,000
Transducin:	α-subunit	39,000
	β-subunit	37,000
	γ-subunit	8,000

[a] Table modified from Molday and Molday (1993). See text also for references.

[b] Subunit M_r values were determined by SDS-PAGE from bovine ROS; values in parentheses were estimated from sequence analysis when they deviate significantly from the M_r estimated by SDS-PAGE.

[c] Localized to the disk rims.

[d] Localization not yet established.

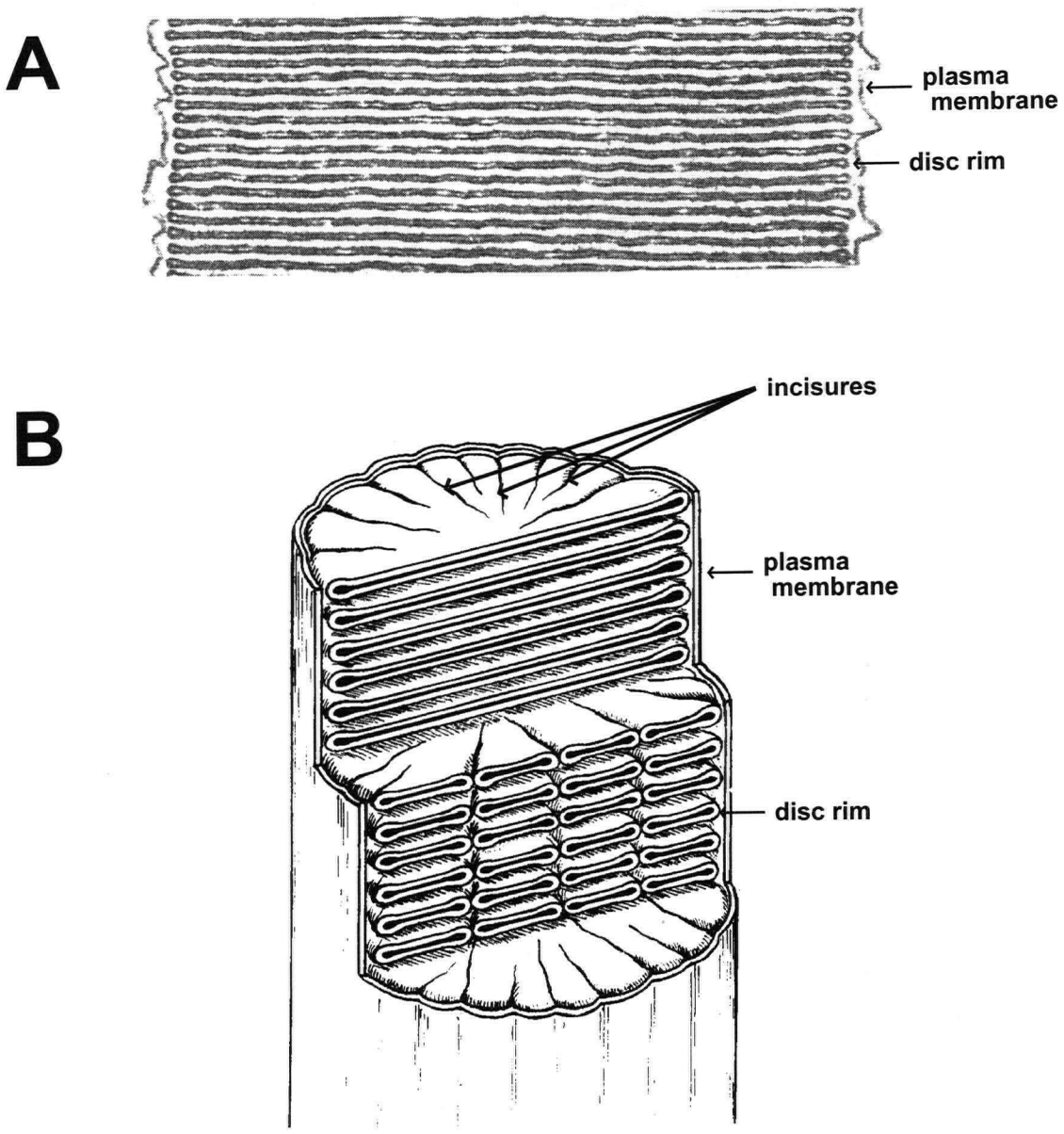

Fig 5. The rim region of the disks. A, Electron micrograph of a longitudinal section through a portion of a rod outer segment of a rhesus monkey, X 75,600. Figure modified from Steinberg *et al.* (1980). **B**, Diagrammatic representation of relationships of ROS disks and the surrounding plasma membrane of a frog retina. Cross sections in the plane of the disk reveal radially oriented incisures. Longitudinal sections reveal a highly curved rim structure present at the edges of the disks which continues into the incisures. Figure modified from Papermaster *et al.* (1978).

1992; Goldberg and Molday, 1996; Moritz and Molday, 1996; Papermaster *et al.*, 1978; Papermaster *et al.*, 1982).

The function of the peripherin/rds-rom-1 complex is not presently known; however, mutations in the gene encoding the peripherin/rds subunit have been implicated in autosomal dominant retinitis pigmentosa and macular dystrophy (see section 1.6). In addition, a digenic disease has been identified where mutations occurring in both genes are implicated (Kajiwara *et al.*, 1994).

The function of the frog rim protein is also not known. It has been reported to undergo a light-activated phosphorylation reaction (Szuts, 1985); however, the role of this reaction in photoreceptor cell function remains to be determined. An abundant 220 kDa membrane glycoprotein is also present in mammalian ROS disk membranes (Molday and Molday, 1979; Converse, 1979) and photoaffinity labeling studies indicates that this protein specifically binds ATP and GTP (Shuster *et al.*, 1988). Although the distribution of the 220 kDa protein in mammalian ROS disk membranes has not yet been determined, it is generally thought that this protein may be the homologue of the frog 290 kDa rim protein. The possibility exists that one or all of the characteristics attributed to this high molecular weight protein may be due to one or more other membrane proteins present in the outer segment because none of these studies have been performed with a purified preparation.

Two filament-like specializations have been shown to be associated with the disk rims: one appears to connect the disks to the plasma membrane while the other appears responsible for disk-disk interactions (Roof and Heuser, 1982; Usukura and Yamada, 1981). While the function of the frog 290 kDa rim protein is not currently known, its large size and distribution along the rim region of ROS disks has led to the suggestion that it may constitute the filament-like structures that link adjacent disks together and/or connect the disks to the plasma membrane (Roof and Heuser, 1982; Corless and Schneider, 1987).

1.6 Retinal Degenerations:

Retinitis pigmentosa and macular degeneration are two groups of heterogeneous inherited human retinal diseases characterized by a progressive degeneration of rod and/or cone photoreceptor cells and a loss in peripheral and central vision. Many of these diseases, including autosomal dominant retinitis pigmentosa (ADRP), autosomal recessive retinitis pigmentosa (ARRP), macular degeneration (MD), and Leber's congenital amaurosis (LCA) have been linked to mutations in the proteins of the outer segment (**Table 2**).

During the course of this study, Allikmets and co-workers (1997a) reported that mutations in the *ABCR* gene encoding a retina cell-specific ATP-binding cassette (ABC) transporter are associated with Stargardt's disease (STGD). This disease is a common form of autosomal recessive macular dystrophy characterized by juvenile onset, central visual dysfunction, perimacular yellow deposits and atrophy of the RPE (**Fig 6**). The yellow deposits are composed of indigestible lipofuscin compounds (Birnbach *et al.*, 1994). In the U.S., 25,000 people have STGD, which usually leads to legal blindness. Fundus flavimaculatus is a clinically similar retinal disorder that often displays later onset and slower progression, but has been linked to the same locus as *ABCR*.

More recently, Allikmets and co-workers reported that mutations in *ABCR* have been implicated in approximately 16% of individuals with age-related macular dystrophy (AMD), the most common cause of central visual loss in the elderly (Allikmets *et al.*, 1997b). AMD is estimated to affect at least 11 million North Americans, with mild forms of AMD occurring in 30% of those 75 years and older and advanced forms occurring in about 7% of people in this age group. AMD can be divided into two groups: (1) 80% of patients have "dry" AMD characterized by the presence of drusen, irregularities in the RPE or geographic atrophy; and (2) 20% of patients have "wet" AMD characterized by serious detachment of the RPE (Spalton *et al.*, 1994). Mutations in *ABCR* are especially frequent in patients with the most common form, "dry" AMD,

TABLE 2

Summary of mutations in retinal proteins involved in human disease

protein (gene)	Disease phenotype[a]	reference
Photoreceptor outer segment proteins:		
α-subunit of the cGMP-gated cation channel (CNCG)	ARRP	Dryja *et al.* (1995)
Guanylyl cyclase (RetGC)	LCA	Perrault *et al.* (1996)
Peripherin/rds	ADRP/MD	Farrar *et al.* (1991) Kajiwara *et al.* (1991) Nichols *et al.* (1993) Wells *et al.* (1993) Weleber *et al.* (1993)
PDE α-subunit (PDEA)	ARRP	Huang *et al.* (1995)
PDE β-subunit (PDEB)	ARRP	McLaughlin *et al.* (1993)
Rhodopsin (RHO)	ADRP/ARRP	Dryja *et al.* (1990) Dryja *et al.* (1991) Keen *et al.* (1991) Sung *et al.* (1991) Rosenfeld *et al.* (1992)
Rod ABC Transporter (ABCR)	STGD/AMD	Allikmets *et al.* (1997a) Nasonkin *et al.* (1997) Allikmets *et al.* (1997b)
Other retinal proteins:		
guanine nucleotide exchange factor (RPGR)	RP3	Meindl *et al.* (1996)
metalloproteinase-3 inhibitor (TIMP3)	Sorsby's fundus dystrophy	Weber *et al.* (1994)
myosin VIIa (USH1B)	Usher's syndrome	Weil *et al.* (1995)
XLRS1 protein (XLRS1)	X-linked juvenile retinoschisis	Sauer *et al.* (1997)

[a] ADRP, autosomal dominant retinitis pigmentosa; AMD, age-related macular degeneration; ARRP, autosomal recessive retinitis pigmentosa; LCA, Leber's congenital amaurosis; MD, macular degeneration; STGD, Stargardt's disease; RP3, X-linked retinitis pigmentosa.

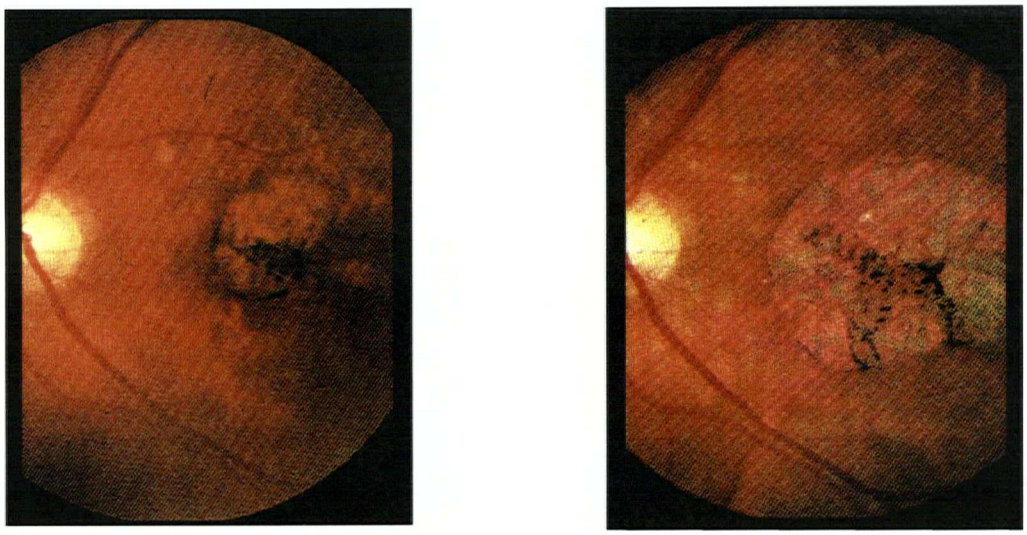

Fig 6. Fluorescein angiogram of a retina from a patient with Stargardt's disease. Signs of progressive macular atrophy can be seen in these photographs taken 6 years apart. Note the presence of yellow perimacular deposits. Figure reproduced from Spalton *et al.* (1994).

with mutations found throughout the protein. On the other hand, a relatively large number of disease causing missense mutations, particularly those linked to Stargardt's disease, reside within the nucleotide binding domains (NBDs) of the rod ABC transporter (Allikmets *et al.*, 1997a and 1997b).

1.7 The Superfamily of ABC Transporters:

1.7.1 Function of the ABC Transporters:

The ABC (ATP-binding cassette) superfamily is a large and diverse family of eukaryotic and prokaryotic membrane proteins that share a conserved nucleotide binding domain (NBD). The major function of these proteins is the transport of substrate across the membrane by utilizing the energy of ATP hydrolysis (reviewed by Higgins, 1992; Doige and Ames, 1993). The ABC transporters have received considerable attention recently because they are involved in many important cellular processes and clinical disorders, including cystic fibrosis, multi-drug resistance, and antigen presentation. There is an enormous variety of substrates transported including peptides, amino acids, sugars, inorganic ions, polysaccharides, and proteins. Some ABC transporters import the substrate while others export it. To date, no transporter has been identified that transports in both directions. ABC transporters have been identified in eukaryotes and prokaryotes mediating substrate transport both across cell (eukaryotic and prokaryotic) or internal (eukaryotic) membranes.

1.7.2 Domain Organization:

The ABC proteins may be classified by the organization of four modules: two transmembrane domains and two cytoplasmic NBDs which may be fused in a variety of ways (**Fig 7A**). Many of the prokaryotic ABC transporters, such as the histidine permease (Shyamala *et al.*, 1991), the maltose permease (Nikaido, 1994), and the

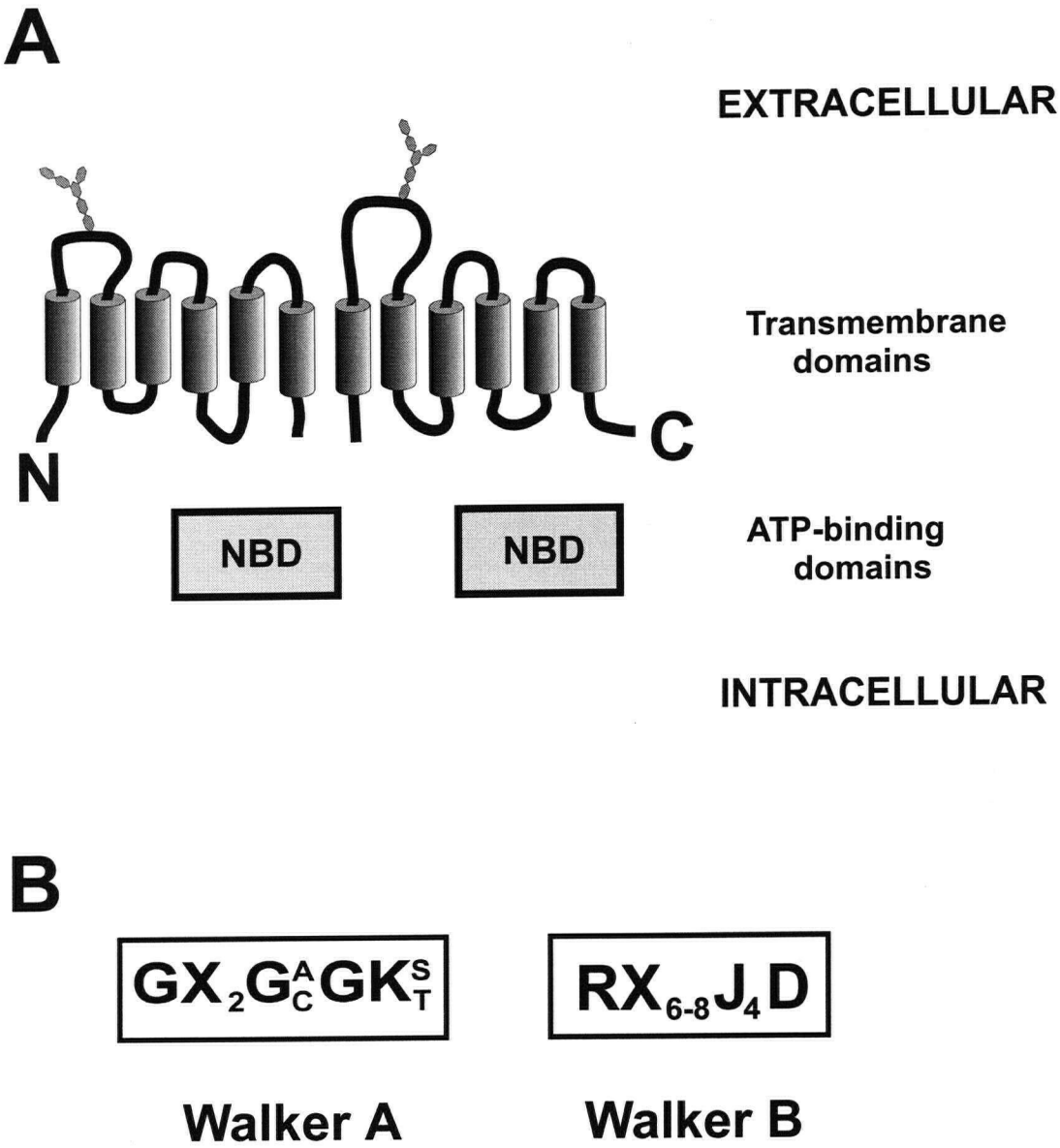

Fig 7. Structural organization of a typical ABC transporter. A, The core domains of a typical ABC transporter are diagrammed as separate polypeptides, although they can also be fused together (see text). The two transmembrane domains are predicted to span the membrane 4-8 times. Potential glycosylation sites (shown by *hexagons*) are on the extracellular face of the membrane. The ATP- or nucleotide binding domains (*NBD*) are peripherally located on the cytoplasmic face of the membrane and may interact with each other or the transmembrane domains. Figure adapted from Higgins (1992). **B**, The sequences of the two conserved nucleotide binding motifs (Walker A and B motifs) in the cytoplasmic NBDs. *X*, any amino acid; *J*, hydrophobic residues. Figure adapted from Luciani *et al.* (1994).

oligopeptide permease (Gallagher *et al.*, 1991), have subunits which are encoded by separate genes but are assembled together to form the complete transporter. Many eukaryotic ABC transporters contain all four modules in a single polypeptide, including the cystic fibrosis transmembrane conductance regulator (CFTR; Riordan *et al.*, 1989), the major multi-drug resistance proteins P-glycoprotein (Chen *et al.*, 1986) and MRP (Cole *et al.*, 1992), the sulfonylurea receptor (SUR; Aguilar-Bryan *et al.*, 1990), and the a-factor mating pheromone transporter in *Saccharomyces cerevisae* (STE6; McGrath and Varshavsky, 1989). Many eukaryotic ABC transporters are also encoded as half molecules that assemble in pairs, including the peptide transporters involved in antigen presentation (TAP1 and TAP2; Monaco *et al.*, 1990) and the *Drosophila* genes white (*w*), brown (*bw*), and scarlet (*st*) which transport pigment precursors responsible for eye colour (Ewart *et al.*, 1994).

The two transmembrane domains (TMD) of the ABC transporters are highly hydrophobic. Hydropathy plots predict that these domains consist of multiple α-helical segments that may span the membrane. Comparison of amino acid sequences of the TMD of one of the ABC transporters with another reveal little or no sequence similarity. The TMDs likely play a role in the transport of the substrate across the membrane by the formation of a pore or by interaction with other domains. Indeed, mutations in the TMDs of P-glycoprotein have been found to interfere with drug transport (Gros *et al.*, 1991; Loo and Clarke, 1996). The TMDs of an ABC transporter are generally more closely related to each other than they are to the equivalent domains of other proteins in the family, likely reflecting a gene duplication event (Higgins, 1992).

Unlike the TM domains, the NBDs of the ABC transporters exhibit common features. Each NBD is approximately 200 amino acids long and is usually 20-50% similar in sequence (Higgins, 1992; Hyde *et al.*, 1990). Like the TMDs, the sequence similarity is usually greater between the domains of a single transporter than between domains of different transporters (Hughes, 1994). Within the domains are two short ATP-binding

motifs, referred to as Walker motifs, associated with many nucleotide binding proteins (**Fig 7B**) and an active transport signature (Walker *et al.*, 1982; Higgins *et al.*, 1986). The sequence similarity extends over the entire NBD, which clearly defines the ABC proteins from other nucleotide binding proteins that contain Walker motifs.

1.7.3 Mechanism of Transport:

Understanding of the mechanism of transport by the ABC proteins at the molecular level is superficial at the present time mainly because little structural information is available. Models have been proposed in which the TMDs are packed into two sets of blocks with solute translocation occurring at the interface between these blocks (Higgins, 1992); however, little experimental evidence has been provided. Recent models on the mechanism of action of P-glycoprotein challenge some aspects of this model in suggesting an interaction of the substrate between the lipid bilayer and the TMDs (Shapiro and Ling, 1995). The natural substrate of P-glycoprotein has yet to be identified; however, the protein is capable of recognizing and transporting a plethora of structurally unrelated, hydrophobic compounds which partition mostly into the membrane. The proposed mechanism of action is the "hydrophobic vacuum cleaner" hypothesis: compounds are pumped directly from the bilayer out of the cell (Shapiro and Ling, 1995). However, many of the ABC transporter substrates do not partition into the membrane. Therefore, new models may be required to describe transport mechanisms of other members of the family.

Nucleotide hydrolysis by the NBDs plays a critical but poorly understood role in the substrate transport by the ABC proteins. For example, mutations in the highly conserved Walker motifs severely disrupt or completely inhibit transport activity in P-glycoprotein (Beaudet and Gros, 1995) and the histidine permease (Shyamala *et al.*, 1991). There have been many studies examining the nucleotide hydrolysis capability of various ABC proteins and their isolated NBDs (see discussion for more details).

However, the mechanism of nucleotide hydrolysis coupled to substrate transport is still poorly understood. Interactions between the TMDs and the NBDs and the TMDs with each other (Loo and Clarke, 1995), and between the NBDs themselves (Loo and Clarke, 1995; Nikaido *et al.*, 1997) have been reported. The most likely mechanism for substrate transport would involve a conformational change with nucleotide hydrolysis that is transmitted to the transmembrane domains.

The great majority of ABC transporters mediate active transport; however, expression of CFTR in heterologous cells can generate channel activity (Anderson *et al.*, 1991). Investigators have tried to measure channel activity for other ABC transporters such as P-glycoprotein but much of the data is inconclusive. To date, no transporter function has been associated with CFTR; however, a general mechanism of channel function has been proposed. CFTR has an extra R (regulatory) domain between the two halves of the protein. Recent studies have shown that serine residues in this domain must be phosphorylated by cAMP-dependent protein kinase for CFTR to enter its open state (Ma *et al.*, 1997; Winter and Welsh, 1997). In addition, intracellular ATP must bind the NBDs and subsequently be hydrolyzed. Functional studies of CFTR containing site-directed mutations in its two NBDs suggest that they have different roles in gating of the CFTR channel. Based on these studies, it has been proposed that ATP hydrolysis at the N-terminal NBD initiates a burst of activity and that hydrolysis at the C-terminal NBD terminates a burst of open events (reviewed by Ma *et al.*, 1997). However, more studies are required to elucidate these events and show them to be applicable to a general mechanism of transport for other members of the ABC protein superfamily.

1.8 Thesis Investigations:

At the start of this study, little was known about the rim protein from frog ROS and whether it was a homologue of the 220 kDa protein detected in mammalian ROS. Due to its abundance and apparent localization in the outer segment, the mammalian protein appeared to be a good candidate for involvement in retinal disease.

In order to begin to characterize the 220 kDa protein in bovine photoreceptor outer segments, monoclonal and polyclonal antibodies were generated. These antibodies were used to screen bovine retinal cDNA libraries and the primary structure for the bovine 220 kDa protein was predicted. In addition, the protein was immunopurified using the monoclonal antibody. Direct peptide sequencing from the immunopurified protein confirmed the amino acid sequence deduced from the cDNA cloning. Using both immunocytochemical and biochemical techniques, antibodies were used to localize the protein both in the retina and within the photoreceptor cells. The bovine 220 kDa glycoprotein was identified as a novel member of the ATP binding cassette (ABC) transporter superfamily and, like the frog rim protein, it is localized to the rim region of bovine ROS disk membranes.

The immunopurified 220 kDa protein was characterized with respect to its extent of glycosylation and its interaction with other proteins in detergent. In addition, the nucleotide binding characteristics of the whole purified protein were investigated by photoaffinity labeling with 8-azido-ATP.

To begin to examine the function of the rod ABC transporter in photoreceptor cells, each of its nucleotide binding domains was overexpressed and purified as a glutathione-S-transferase fusion protein in *Escherichia coli*. The kinetics of nucleotide hydrolysis by these two domains were determined and compared with the NBDs of several other members of the ABC transporter superfamily.

MATERIALS AND METHODS

2.1 Materials:

Fresh bovine eyes were obtained from J&L Meats (Surrey, BC) and frozen bovine retinas were purchased from J&W Lawson (Lincoln, Nebraska). Human donor eyes were received from the UBC Eyebank within 16 h post-mortem while eyes from all other species were dissected immediately post-mortem.

The λZAPII oligo(dT)-primed bovine retinal cDNA library and the λgt10 oligo(dT)-primed human retinal cDNA library were generous gifts of W. Baehr (University of Utah) and J. Nathans (Johns Hopkins University), respectively. The pcDNAII random-primed bovine cDNA library was made from bovine retinal poly(A) mRNA by Invitrogen. The FastTrack® 2.0 mRNA Isolation Kit and the TA Cloning™ Kit were also obtained from Invitrogen. Taq DNA Polymerase and pGEX vectors were purchased from Pharmacia, while restriction enzymes were obtained from Pharmacia, New England Biolabs, or Promega.

Sheep anti-mouse and donkey anti-rabbit Ig-F(ab')$_2$ fragment conjugated to horseradish peroxidase, ECL reagent, and Rapid-hyb buffer were obtained from Amersham. Goat anti-mouse and goat anti-rabbit Ig conjugated to Cy3 and the BCA protein assay were purchased from Pierce. Concanavalin A conjugated to horseradish peroxidase was obtained from Sigma. The [α^{35}S]-dATP (3000 Ci/mmole) and the [α^{32}P]-dCTP (3000 Ci/mmole) were purchased from NEN. Sepharose 2B and DEAE-Sephacel were obtained from Pharmacia. DEAE-Fractogel TSK was purchased from Supelco, while Ultragel AcA 54 was procured from LKB.

For immunohistochemistry studies, the following reagents were used: LR white resin (Polysciences); gluteraldehyde, paraformaldehyde, and Reynold's lead citrate stain (JB EM Services); goat anti-rabbit Ig-10 nm gold conjugate (British BioCell

International); O.C.T.™ embedding compound (Tissue Tek); and ImmunoPure® Metal Enhanced DAB Substrate (Pierce).

For Western blotting, Immobilon was purchased from Millipore, while nitrocellulose was obtained from Schliecher & Schuell. Endoproteinase Lys-C (sequencing grade) and endoglycosidase Hf were purchased from Boehringer Mannheim Biochemicals and New England Biolabs, respectively. The 8-azido-[α^{32}P]-ATP (15 Ci/mmole) was obtained from ICN. The cDNA library screening was performed with HATF nitrocellulose filters (Millipore) or Hybond N nylon filters (Amersham). Hybond N membrane (Amersham) was also used for Northern blot protocols.

Freund's adjuvant (complete and incomplete), IMDM, FBS, goat serum, and IPTG were obtained from BRL Gibco. Reagents for peptide synthesis were purchased from NovaBiochem and Aminotech. All other reagents were obtained from Sigma or Fisher Scientific. The recipes for the standard buffers used in this study are presented in the Appendix.

2.2 Preparation of ROS and Disk Membranes:

Bovine ROS were isolated under dim red light from fresh or previously frozen retinas by continuous sucrose-gradient centrifugation (Molday and Molday, 1987). For other species, ROS were isolated under normal light from freshly dissected retinas by the same method. The ROS membranes were isolated by hypotonic lysis of ROS in 0.01 M Tris·HCl, pH 7.4, 100 μM PMSF followed by centrifugation at 12,000 rpm for 10 min. at 4 °C in a Sorvall SS-34 rotor (Dupont). The membranes were washed twice in the same buffer and either used immediately or stored at -70 °C at a protein concentration of 8-10 mg/ml in light-tight vials. Disk membranes were dissociated from ricin-gold-dextran labeled plasma membranes by mild trypsin digestion and isolated by sucrose gradient centrifugation (Molday and Molday, 1987).

2.3 Monoclonal and Polyclonal Antibodies:

2.3.1 Preparation of Antigen for Monoclonal Antibody Production:

The immunogen was prepared by solubilizing ROS membranes in 0.02 M Tris·HCl, pH 7.4, 18 mM CHAPS and 0.15 M NaCl and passing this solution through a DEAE-Fractogel TSK column equilibrated in the same buffer. The flow-through fraction (immunogen) containing the 220 kDa protein, rhodopsin and other minor proteins was devoid of the cGMP-gated channel and the Na^+/Ca^{2+}-K^+ exchanger (Cook *et al.*, 1987).

2.3.2 Generation of Monoclonal Antibody Rim 3F4:

BALB/c mice were immunized with 50 μg of the above immunogen in 50 μl of PBS mixed 1:1 with Freund's adjuvant. Complete Freund's adjuvant was used in the initial injection while incomplete Freund's was used in subsequent injections. After four immunizations, the serum was assayed by Western blotting against ROS proteins for binding to the high molecular weight 220 kDa protein. Two mice, giving a positive response, were sacrificed and their spleens removed for the following fusion procedure adapted from Galfre *et al.* (1979). The author would like to thank Theresa Hii for performing the fusion and subsequent tissue culture protocols.

NS-1 myeloma cells were grown in IMDM 10% FBS (fusion grade). On the day of the fusion, 6 X 10^6 cells were collected by centrifugation at 400 X g (5 min., room temperature. The cells were resuspended in serum-free IMDM and washed twice by centrifugation. The final pellet was made up in 20 ml IMDM. Splenocyte feeder cells were collected from a non-immunized mouse. Briefly, the spleen was removed and washed in sterile IMDM in a small petri dish. The spleen was then perforated with two IMDM-filled 1 ml syringes fitted with 26 gauge needles. The released splenocytes were washed once by centrifugation, resuspended in 80 ml of HAT medium and kept at 37 °C. The immunized mouse spleen was removed and treated similarly, except the cells were

collected in serum-free IMDM. These cells were centrifuged and resuspended in 20 ml serum-free IMDM and pooled with the myeloma cells. The pooled cells were centrifuged at 400 X g and the supernatant was removed. The pellet was loosened in the remaining medium by gentle tapping of the tube. The tube was placed at 37 °C and 800 µl of 50% PEG was added while the tube was simultaneously swirled for one min. After 1 min., 1 ml of serum-free IMDM was added dropwise over 1 min. Finally, 20 ml of serum-free IMDM was added slowly over 5 min. with occasional swirling. The cells were centrifuged at 400 X g for 5 min. and resuspended in the 80 ml of HAT medium containing the splenocyte feeder cells. The suspension was then divided into eight 96-well plates and the cells were grown at 37 °C. The cells were treated with HAT the next day and with HT after 5 days when the hybridomas were visible.

The hybridomas were initially screened for antibody production by an ELISA procedure (MacKenzie and Molday, 1982). Briefly, ROS membranes were solubilized at 0.1 mg/ml in 0.2% Triton X-100, 0.15 M NaCl in PBS and allowed to adsorb overnight at 4 °C to 96-well microtiter plates (Nunc), with 100 µl per well. The wells were washed 3 times with PBS and then blocked for 30 min. with 0.2% (w/v) Carnation evaporated milk powder in PBS. A 100 µl aliquot of the hybridoma supernatant was added to a well for 30 min. after which it was transferred to a clean 96-well plate for further analysis. The microtiter plates were then washed 3 times with PBS and 100 µl of sheep anti-mouse Ig-F(ab')$_2$ fragment conjugated to horseradish peroxidase diluted 1:5000 in blocking buffer was added for 30 min. The wells were washed as above and 100 µl of the substrate (0.5 µg/ml ABTS in PBS, containing 0.009% H_2O_2) was added and the absorbance monitored at 410 nm. If the well tested positive (*i.e.* more than 0.2 absorbance units higher than the control), the supernatant was tested by Western blotting of ROS membranes. Positives were subcloned twice and screened for antibody production using Western blotting. A hybridoma cell line was isolated which produced an anti-220 kDa antibody (Rim 3F4).

2.3.3 Generation of Polyclonal Antibody PrimT1:

Polyclonal antibody PrimT1 was obtained by immunizing a New Zealand white rabbit with 50 μg of the 220 kDa rim protein purified on a Rim 3F4 antibody-Sepharose 2B column (see below) in 450 μl of PBS mixed 1:1 with Freund's adjuvant. Complete Freund's adjuvant was used for the first injection, while incomplete Freund's adjuvant was used in subsequent injections. The rabbit was bled 8-12 days after injection and the blood was centrifuged at 5,000 X g for 10 min. For use in Western blotting, immunocytochemistry and library screening, residual contaminating antibodies to other ROS proteins were removed by treating 5 ml of the antiserum, containing 1% Triton X-100, with 2 ml of CNBr-activated Sepharose 2B conjugated to 4 mg of Triton X-100-solubilized ROS proteins, in which the 220 kDa protein had been removed by passage through a Rim 3F4 antibody-Sepharose 2B column (PrimT1). For electron microscopy, the PrimT1 antibody was purified by the method of Burton *et al.* (1989). Briefly, the immunoaffinity purified 220 kDa rim protein was subjected to SDS-polyacrylamide gel electrophoresis and electrophoretically transferred to nitrocellulose membranes. Strips containing the 220 kDa rim protein were blocked with 0.5% (w/v) Carnation evaporated milk powder in PBS for 30 min. and then incubated for 1 h at 25 °C with 1 ml of the PrimT1 antiserum diluted 1:500 in 0.01 M Tris·HCl, pH 7.4, 0.15 M NaCl, and 2% bovine serum albumin. The strips were washed in the same buffer and then rinsed in distilled water. The antibody was eluted from the strips with 1.0 ml of 0.2 M glycine·HCl, pH 2.3, and dialyzed against PBS.

2.3.4 Other Monoclonal Antibodies:

Monoclonal antibodies PMc 1D1 and PMs 4B2 against the α- and β-subunits of the bovine cGMP-gated channel, respectively, and PMe 2D9 against the Na^+/Ca^{2+}-K^+ exchanger have been reported (Cook *et al.*, 1989; Molday *et al.*, 1990; Reid *et al.*, 1990).

2.4 Peptide Sequencing and Amino Acid Analysis:

For N-terminal peptide sequencing and amino acid analysis, 100-200 μg of the immunoaffinity purified 220 kDa rim protein or its 115 kDa and 120 kDa tryptic fragments (see below) were subjected to SDS polyacrylamide gel electrophoresis and electrophoretically transferred to Immobilon membranes. The immobilized protein was subjected to acid hydrolysis for amino acid analysis or Edman degradation for N-terminal microsequencing.

For internal peptide sequences, 80 mg of purified ROS membranes were resuspended in 10 ml of 0.02 M Tris·HCl, pH 7.4, and 0.02 M $CaCl_2$. Ten ml of TCPK-trypsin (0.4 μg/ml) were added and the reaction was allowed to proceed for 5 min. at room temperature and then for 30 min. on ice. The membranes were sedimented at 12,000 rpm in a Sorvall SS34 rotor for 10 min. and subsequently washed 3 times with 20 ml each of 10 μg/ml soybean trypsin inhibitor in the same buffer. The final pellet was solubilized at 2 mg/ml in 0.02 M Tris·HCl, pH 7.4, 0.15 M NaCl, 1% Triton X-100 and 10 μg/ml soybean trypsin inhibitor and incubated with 1 ml of Rim 3F4 antibody-Sepharose 2B (see below) for 1 h. After the matrix was washed in the same buffer containing 0.2% Triton X-100, the tryptic fragments of the 220 kDa protein were eluted with 0.6 ml of 0.1 M glycine·HCl, pH 3.5, 0.15 M NaCl, and 0.2% Triton X-100. The eluted fraction was concentrated to 0.1 ml using a Centricon 30 (Amicon).

The 120 kDa and 115 kDa tryptic fragments and the immunoaffinity purified rim protein were electrophoretically transferred to nitrocellulose membrane and digested with endoproteinase Lys-C by standard methods (Aebersold *et al.*, 1987). The nitrocellulose was stained with Ponceau S (0.1% in 1% acetic acid) to visualize the protein bands, which were excised and washed extensively with water. The nitrocellulose was blocked with 0.5% PVP-40 in 0.1 M acetic acid for 30 min. at 37 °C, and then cut into 1 X 1 mm fragments which were placed in 50 μl of 25 mM Tris·HCl, pH 8.5, containing 1 mM EDTA and 1 μg endoproteinase Lys-C at overnight at 37 °C. Peptides were isolated by

high pressure liquid chromatography using a narrow-bore C18 reverse-phase column and subjected to N-terminal microsequencing.

Amino acid analysis and N-terminal peptide gas-phase sequencing were carried out by the Tripartite Microanalytical Center at the University of Victoria.

2.5 Cloning of Bovine and Human cDNA of the 220 kDa Protein:

2.5.1 Isolation of Bovine cDNA Clones:

A λZAPII oligo(dT)-primed bovine retinal cDNA library was screened with the preadsorbed PrimT1 polyclonal antibody by the method of Helfman *et al.* (1983) as modified by Sambrook *et al.* (1989). For titering and phage screening, an overnight culture of *E. coli* XL-1 Blue cells in LB containing 50 μg/ml ampicillin (LB/amp) was used as the bacterial lawn. Initial screens were performed with 25,000 pfu/150-mm petri dish while subsequent screens were performed with 100-500 pfu/90-mm petri dish. The phage were allowed to infect the bacterial lawn for 4 h at 42 °C. Sterile HATF nitrocellulose filters, impregnated with 10 mM IPTG, were laid over the plaques, which were then placed at 37 °C for 6 h. A second IPTG impregnated filter was laid over the plaques at 37 °C overnight, when duplicates were made. Filters were marked with water insoluble India ink prior to removal. The filters were washed in PBST with 0.02% sodium azide for 30 min. and blocked in 0.2% (w/v) Carnation evaporated milk powder in PBS for 30 min. They were then incubated with the preadsorbed PrimT1 polyclonal antibody (1:5000) and washed 3 times with PBS for 10 min. each. The filters were subsequently incubated with the secondary donkey anti-rabbit Ig-F(ab')$_2$ fragment conjugated to horseradish peroxidase (1:5000), and washed as above. Antibodies were diluted in 0.1% (w/v) Carnation evaporated milk powder in PBS and incubated for 30 min. at room temperature. Positives were detected by adding 0.5 mg/ml DAB in PBS, containing 0.009% H_2O_2 until a dark brown precipitate was visible. Plaques were identified and

removed from the original agar plate and placed in 1 ml of SM containing 50 μg chloroform for rescreening until a preparation containing a single plaque was obtained. Approximately 100,000 pfu were screened and of the 11 positive clones detected, 6 were subcloned by rescue of the BluescriptII plasmid (see section 2.14) and sequenced (see below), and found to contain identical sequences.

To obtain longer clones from the oligo(dT)-primed library, an oligonucleotide obtained from the 5' end of the longest clone (λ2) was used to rescreen the library by the method of Benton and Davis (1977) as modified by Sambrook *et al.* (1989). The location of oligonucleotide probes in the isolated clones and the whole cDNA sequence is summarized in **Table 3**. Plaques were allowed to infect an *E. coli* XL-1 Blue lawn (see above) overnight at 37 °C. Sterile Hybond N nylon filters were laid over the plaques, marked, and removed immediately for processing. The filters were denatured in 1.5 M NaCl and 0.5 M NaOH for 2 min.; then neutralized for 5 min. in 0.5 M Tris·HCl, pH 8.0, containing 1.5 M NaCl; and finally, washed twice for 30 sec. each in 0.2 M Tris·HCl, pH 7.5, containing 2X SSC. The filters were then air-dried and cross-linked with long-wavelength UV light for 3 min. The filters were pre-washed in a 500 ml solution of 5X SSC, 0.5% SDS, and 1 mM EDTA for 30 min. at 50 °C, after which, they were gently wiped with a tissue soaked in the same solution. Filters were hybridized at 65 °C for 2 h in Rapid-hyb buffer with a [^{32}P]-labeled probe synthesized by random priming (Pharmacia T7Quick Prime Kit). Typically, 25 ng of DNA was labeled at a specific activity of 0.5-1 X 10^9 dpm/μg with [α^{32}P]-dCTP. Approximately 125,000 pfu were screened and of 33 positives identified, 15 were subcloned by rescue of the BluescriptII plasmid (see section 2.14) and sequenced (see below), and found to contain identical sequences.

An Eco RI/Apa I fragment (**Table 3**) from the 5' end of the longest resulting clone (λ27) was used to screen the pcDNAII-random primed bovine retinal cDNA library by the method of Grunstein and Hogness (1975). For titering and screening procedures, the

TABLE 3

Oligonucleotide probes used in screening the cDNA libraries and Northern blots.

Clone[a]	restriction sites[b]	location[c] in clone	location[c] in whole cDNA
λ2	Afl II/Sph I	5-518	5805-6318
λ27	Eco RI/Apa I	-6-534[d]	4243-4771
p41	Eco RI/Sac I	-6-322[d]	3722-4038
p55	Eco RI/Hpa II	84-367	2497-2780
p72	Eco RI/Rsa I	-6-205[d]	1506-1705
p76	Eco RI/Xho I	-6-218[d]	1245-1457
p90	Eco RI/Apa I	-6-215[d]	1098-1307
p103	Not I/Pst I	-25-228[d]	413-616

[a] Clones λ2 and λ27 were isolated from the λZAPII oligo(dT)-primed bovine retinal cDNA library, while all others were isolated from the pcDNAII random-primed bovine retinal cDNA library.

[b] Restriction enzymes used to digest the clones and produce the probes (see text).

[c] Numbers refer to the nucleotide position in the clones and in the whole rod ABC transporter cDNA.

[d] Negative numbers indicate that a portion of the multiple cloning site of the vector (BluescriptII or pcDNAII) was included in the probe.

library was plated on LB/Amp agar at 20,000 cfu/150-mm or 100-500 cfu/90-mm petri dish. Sterile Hybond N nylon filters were laid on the agar and the appropriate amount of cfu in 0.5 ml/150-mm or 0.2 ml/90-mm petri dish was spread on the filter and incubated overnight at 37 °C. A sterile numbered filter was then laid over the bacteria, marked, and removed immediately. The original filters were transferred, bacteria side up, to fresh LB/amp agar containing 25% glycerol, incubated at 37 °C for 4 h, sealed with Parafilm®, and kept at -70 °C. The replica filters were placed colony side up on fresh LB/amp agar and incubated at 37 °C for 4 h. The filters were then removed and impregnated colony

side up with the following solutions for 5 min. each by laying them on 3MM paper (Whatman) saturated with: (1) 10% SDS; (2) 0.5 M NaOH, 1.5 M NaCl; (3) 0.5 M Tris·HCl, pH 8.0, containing 1.5 M NaCl; and (4) 2X SSC. The filters were then air-dried, cross-linked with UV light, pre-washed, and labeled with DNA probes as above. Overlapping clones were identified and sequenced (see below) until the entire cDNA was cloned (see **Table 3** for probes used).

Clones were sequenced in both directions by a modified method of Sanger *et al.* (1977), by a combination of the dideoxy chain termination method using [α^{35}S]-dATP and the Sequenase™ Quick Denature™ Plasmid Sequencing Kit (United States Biochemical) and automated fluorescent sequencing (Licor, Inc.).

2.5.2 Isolation of Human cDNA Clones:

An Afl II/Sph I fragment from clone λ2 (**Table 3**) from the bovine 220 kDa cDNA cloning was used to screen approximately 100,000 pfu from a λgt10 oligo(dT)-primed human retinal cDNA library by the method of Grunstein and Hogness (1975), outlined in section 2.5.1. Of 37 positive clones, 5 were subcloned by PCR (see section 2.14) and sequenced, and found to contain overlapping sequences. Clones were partially sequenced by the dideoxy chain termination method using [α^{35}S]-dATP and the Sequenase™ Quick Denature™ Plasmid Sequencing Kit (United States Biochemical).

2.6 Northern Blot Analysis:

Northern blots were carried out essentially as described by Ausubel *et al.* (1994) using formaldehyde denaturing agarose gels, 10 μg of total RNA per lane, and capillary transfer onto Hybond N nylon membranes. The membranes were hybridized at 65 °C for 2 h in Rapid-hyb buffer with [^{32}P]-labeled probes synthesized by random-priming (Pharmacia ^{T7}Quick Prime Kit) as described in section 2.5.1. The blots were washed once with 2X SSC, 0.1% SDS and then twice with 0.1X SSC, 0.1% SDS. All washes

were performed at 65 °C for 20 min. each. Probes were derived from an Eco RI/Sac I fragment of clone p41 and an Eco RI/Hpa II fragment of clone p55 (**Table 3**) and blotting was performed in duplicate.

2.7 Immunohistochemistry:

2.7.1 Immunofluorescence Microscopy:

For light microscopy, bovine retinas were obtained within 1 h post-mortem. After removal of the cornea, lens and vitreous humor, the whole eye cup was fixed in 4% paraformaldehyde, 1% sucrose, 0.1 M sodium phosphate, pH 7.4 for 1 h. The retina was removed and fixed in the same solution for another 1-2 h and then washed three times in 1% sucrose, 0.1 M sodium phosphate, pH 7.4 for 1 h each at room temperature. Sections of retina were flash frozen in O.C.T.™ embedding compound and sectioned at 8-10 μm thickness using a cryostat. The cryosections were blocked with PBS containing 0.1% goat serum and 0.05% Triton-X100 for 30 min. The sections were then labeled with Rim 3F4 (1:10) or PrimT1 (1:500) antibodies for 30 min. followed by three 10 min. washes of PBS containing 0.2% BSA. The secondary goat anti-mouse or goat anti-rabbit Ig antibodies conjugated to Cy3, or sheep anti-mouse or donkey anti-rabbit Ig conjugated to horseradish peroxidase, were applied at 1:5000 dilution for 30 min. and then the sections were washed as above. All antibodies were diluted in the blocking buffer. Horseradish peroxidase labeling was visualized by addition of ImmunoPure® Metal Enhanced DAB Substrate. The reaction was monitored visually through the microscope and stopped by washing off the unused substrate with excess PBS. In control studies, to measure nonspecific binding, Rim 3F4 antibody labeling was carried out in the presence of excess 3F4 peptide (0.1 mg/ml; see section 2.8.1).

For electron microscopy, a post-embedding protocol modified from Lewis *et al.* (1991) was utilized. The author would like to thank Laurie Molday for performing the electron microscopy tissue preparation, sectioning and labeling techniques. Briefly, bovine retina was obtained within 1 h post-mortem and fixed in 0.1 M sodium phosphate, pH 7.2, containing 2% gluteraldehyde and 1% paraformaldehyde for 1 h. Small sections of retina were then washed 3 times for 10 min. each with 0.1 M sodium phosphate, pH 7.2. The tissue was then washed sequentially in 15%, 30% and 50% methanol for 10 min. each, and transferred to 70% methanol containing 2% uranyl acetate for 30 min. Finally, the tissue was washed sequentially in 85%, 95% and 100% methanol for 10 min. each, then placed in a 1:1 mixture of LR-White resin and methanol overnight at 4 °C. The next day, the tissue was transferred to 100% LR White resin at
4 °C for 2 h and subsequently immersed in fresh resin in a gelatin capsule for 4 h at room temperature. The resin was allowed to polymerize overnight at 52-57 °C. Small pieces of embedded retina were cut out of the LR blocks and reoriented in Epon/Araldite resin. Thin sections were cut with a microtome equipped with a diamond knife and collected on nickel grids.

The sections were immuno-gold labeled following a modified protocol of Moritz and Molday (1996) by incubating the grids on small drops of the following solutions:

1) 0.1 M Tris, pH 7.5, 5 min.

2) 4% BSA, 0.1 M Tris, pH 7.5, 10 min.

3) 20 mM glycine, 0.1 M Tris, pH 7.5, 15 min.

4) purified Prim T1 (see section 2.3.3) in 1% BSA, 0.1 M Tris, pH 7.5, 30 min.

5) 0.1 M Tris, pH 7.5, 6 X 1 min.

6) Secondary antibody (10 nm diameter gold conjugate) 5X dilution in 1% BSA, 0.1 M Tris, pH 7.5, 30 min.

7) 0.1 M Tris, pH 7.5, 6 X 1 min.

8) distilled water, 6 X 1 min.

9) Saturated uranyl acetate, 10 min.

10) distilled water, 6 X 1 min.

11) Reynold's lead citrate stain, 1 min.

12) distilled water, 6 X 1 min.

13) air dry overnight.

2.8 Generation of the Monoclonal Antibody Rim 3F4 Immunoaffinity Matrix:

2.8.1 Mapping of the Rim 3F4 Epitope and Synthesis of the 3F4 Peptide:

A glutathione-S-transferase (GST) fusion peptide containing the C-terminal 128 amino acid residues of the bovine rim ABC transporter was first used to localize the epitope for the Rim 3F4 antibody. This was carried out by subcloning a Bam HI/Xho I (blunt) fragment of clone λ4 (nucleotides 6458-7609; **Fig 11**) into pGEX-1 pre-digested with Bam HI/Sma I (**Fig 8**). The 39 kDa GST fusion peptide was expressed in *E. coli* and purified by glutathione affinity chromatography (Smith and Johnson, 1988; see section 2.12.2) for analysis of Rim 3F4 antibody binding by Western blotting. Synthetic peptides were used to map the epitope for Rim 3F4 antibody more precisely. Briefly, overlapping peptides (9 amino acids long, 2 amino acid overlap) spanning the C-terminal 128 amino acids were synthesized using the Epitope Scanning Kit (Cambridge Research Biochemicals), and Rim 3F4 antibody binding was measured by ELISA. A 9 amino acid peptide (3F4 peptide) corresponding to amino acids 2253-61 of the rim protein sequence and containing the epitope for the Rim 3F4 antibody was synthesized by standard solid phase peptide synthesis procedures (Merrifield, 1963) using a BioLynx synthesizer (LKB).

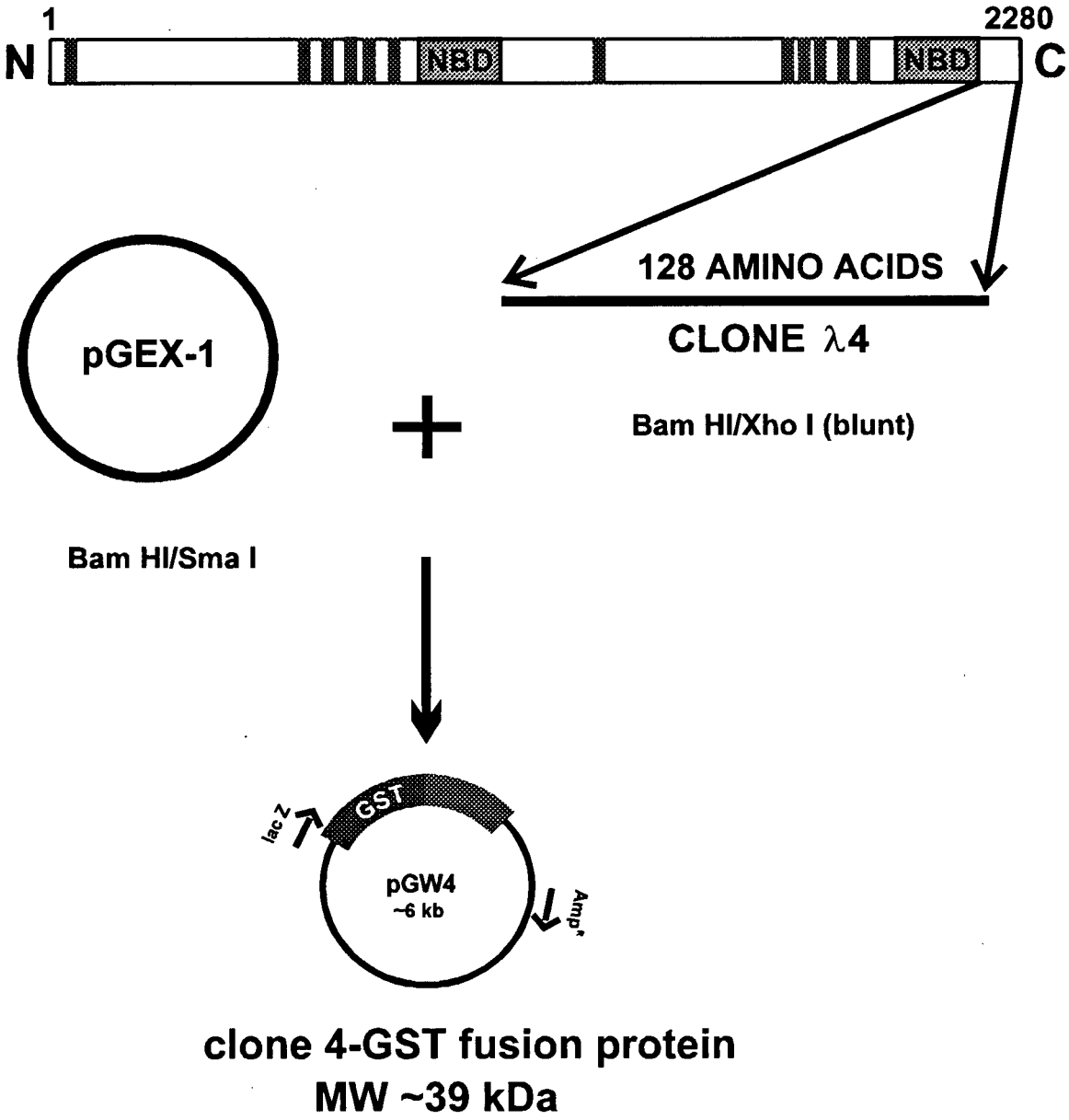

Fig 8. Construction of the GST fusion protein for mapping the Rim 3F4 epitope. The 128 C-terminal amino acids of the bovine rim ABC transporter contained in clone λ4 (**Fig 11**) was expressed in *E. coli* as a GST fusion protein. The numbers refer to the amino acid sequence of the bovine rod ABC transporter. Positions of possible transmembrane segments are shown as *black bars* and the nucleotide binding domains are indicated as *NBD*.

2.8.2 Production of the Rim 3F4 Immunoaffinity Matrix:

Ascites fluid was raised by injection of the hybridoma cell line producing the Rim 3F4 antibody into pristane-primed BalbC mice. The antibody was purified from the ascites fluid by precipitation with 50% ammonium sulfate at 4 °C followed by DEAE-Sephacel ion exchange chromatography (Goding, 1986). The purified antibody was coupled to CNBr-activated Sepharose 2B at a concentration of 2 mg protein per ml of packed beads overnight in 20 mM sodium borate buffer, pH 8.4. CNBr activated Sepharose was prepared as described by Cuatrecasas (1970).

2.9 Immunoaffinity Purification of the 220 kDa Rim Protein:

The 220 kDa rim protein was purified by incubating 1 mg of ROS membranes solubilized in 0.5 ml of 0.02 M Tris·HCl, pH 7.4, 5 mM $MgCl_2$, and 18 mM CHAPS or 1% Triton X-100 with 50 µl of Rim 3F4-Sepharose 2B beads at 4 °C for 1 h. The unbound fraction was isolated by low speed centrifugation through an Ultrafree filter unit (Millipore), and the beads were then washed twice with 0.5 ml of solubilization buffer. Finally, the bound protein was dissociated by incubation of the beads in 0.1 ml solubilization buffer containing 0.1 mg/ml 3F4 synthetic peptide for 15 min. at 25 °C and collected by low speed centrifugation.

2.10 Endoglycosidase Hf Treatment of the 220 kDa Rim Protein:

For endoglycosidase treatment, 100 µl of 1.5 mg/ml ROS membranes solubilized in 0.02 M Tris·HCl, pH 7.4, 10 mM CHAPS, and 5 mM $MgCl_2$ was treated with endoglycosidase Hf according to the manufacturer's instructions (New England Biolabs) and subjected to SDS polyacrylamide gel electrophoresis and Western blotting.

2.11 Labeling of the 220 kDa Rim Protein with 8-Azido-[α^{32}P]-ATP:

The 220 kDa rim protein was photoaffinity labeled with 8-azido-[α^{32}P]-ATP (15 Ci/mmole) using a modified procedure of Shuster *et al.* (1988). All steps were performed at 4 °C under dim red light. Briefly, 2 μg of ROS membranes or 0.5 ng of Triton X-100 solubilized, immunoaffinity purified 220 kDa rim protein (each in 0.02 M Tris·HCl, pH 7.4, 0.5 mM $ZnCl_2$ and 0.5 mM $MgCl_2$) containing the indicated concentration of unlabeled nucleotide was placed in microtiter plate wells. After 5 min., 8-azido-[α^{32}P]-ATP (3 μM final concentration) was added. The samples were incubated for 3 min. and then irradiated for 5 min. with ultraviolet light (Mineralight UV Lamp; 254 nm) at a distance of 3 cm. The reaction was terminated by turning off the UV lamp and adding 25 μl of SDS buffer for SDS gel electrophoresis. Gels were stained with Coomassie Blue, dried, and exposed to either X-ray film or a phosphoimaging screen. Phosphoimages were analyzed quantitatively by normalizing the intensity of the bands relative to the sample which contained no competitive nucleotide.

2.12 Glutathione-S-Transferase (GST) Fusion Proteins With the Two Nucleotide Binding Domains (NBDs) of the Bovine Rim ABC Transporter:

2.12.1 Construction of the Expression Plasmids of Fragments FNBD1 and FNBD2 Containing the Two NBDs:

Clone p55 in pcDNAII and clone λ2 in BluescriptII were isolated during the cloning of the bovine rod ABC transporter (**Fig 11**). Clone p55 codes for a fragment (FNBD1) from Thr806 to Ala1310 and contains the first NBD (NBD1); clone λ2 encodes a fragment (FNBD2) from Ile1935 to Gly2280 and includes the second NBD (NBD2) near the C-terminus of the protein (**Fig 9**). Each clone was excised from BluescriptII with Bam HI and Xho I, and after blunt ending the Xho I site, the clone was ligated in frame with GST into pGEX-2T or pGEX-1 vectors, that had been predigested with Bam

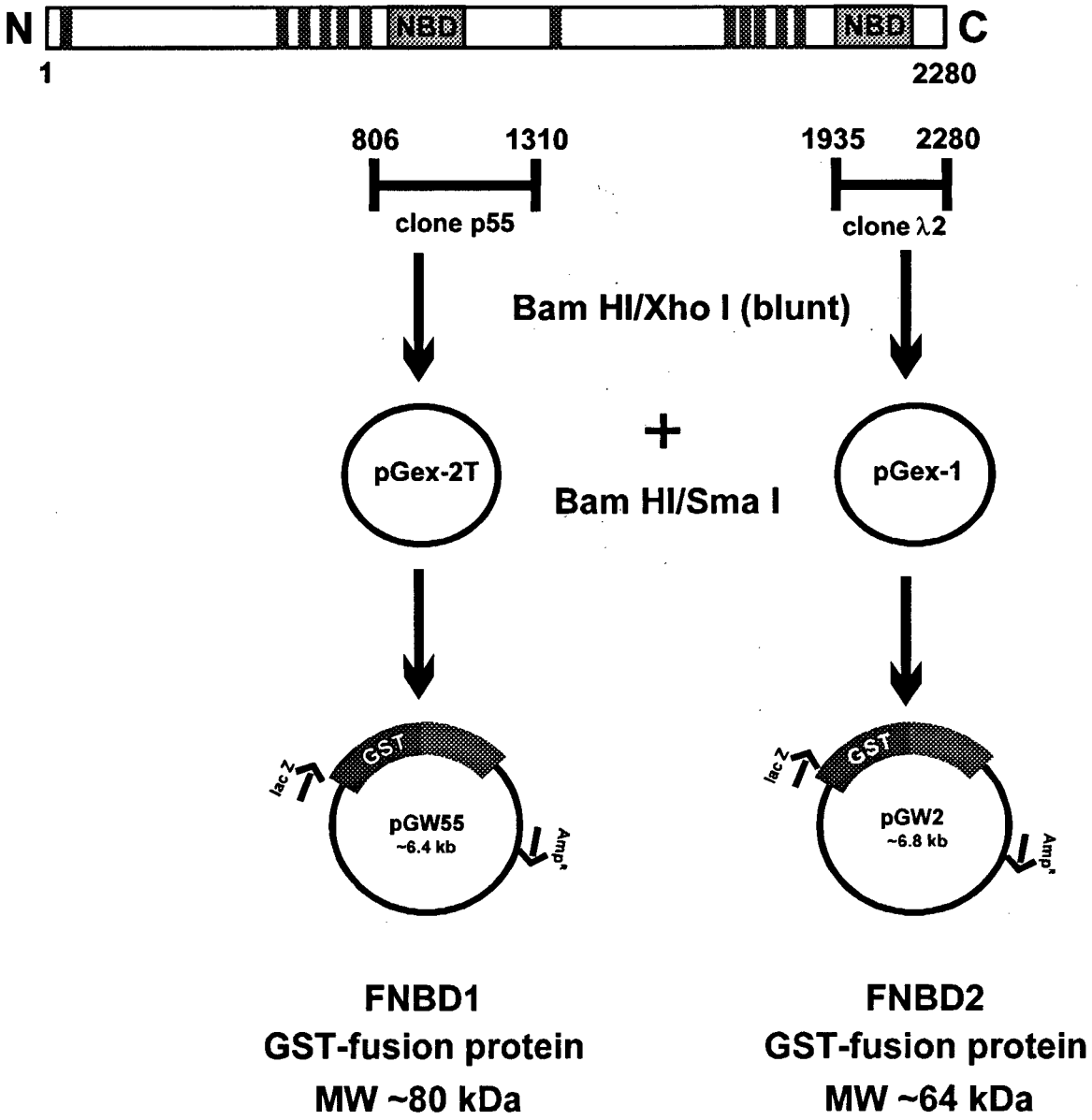

Fig 9. Diagram showing the location of the FNBD1 and FNBD2 fragments of the rod ABC transporter expressed as GST fusion proteins. Fragments FNBD1 and FNBD2 were encoded by clone p55 and clone λ2 (**Fig 11**), respectively, and expressed in *E. coli* as GST fusion proteins. The numbers refer to the amino acid sequence of the bovine rod ABC transporter. Positions of possible transmembrane segments are shown as *black bars* and the nucleotide binding domains are indicated as *NBD*.

HI and Sma I. The ligation mixtures were used to transform competent *E. coli* XL-1 Blue cells, and clones were screened by restriction digests and DNA sequencing.

2.12.2 Overexpression and Purification of GST-Fusion Proteins Containing the NBDs:

Proteins were expressed and purified by glutathione affinity chromatography as described by Smith and Johnson (1988). Briefly, XL-1 Blue cells containing the appropriate plasmids were grown in LB/amp broth at 37 °C until the A_{600} was 0.6. The culture was then induced with 0.2 mM IPTG and harvested 3 h later at 6,000 x g for 15 min. The cells were resuspended in PBS containing 100 μM PMSF, 2 μg/ml aprotinin, and 5 mM EDTA and lysed with a SLM-Aminco French pressure cell press at 12,600 psi. The cell homogenate was centrifuged at 15,000 x g for 15 min., and the supernatant was subjected to glutathione-Sepharose 4B affinity chromatography. The fusion protein was eluted from the column with 5 mM reduced glutathione in 0.05 M Tris·HCl, pH 8.0. For nucleotide hydrolysis activity measurements, the isolated fusion protein was dialyzed overnight at 4 °C against 3 changes of 0.05 M Tris-HCl, pH 8.0, containing 5 mM $MgCl_2$.

For some studies, the fusion proteins were further purified by gel filtration chromatography on a 41 ml Ultragel AcA 54 column to remove low molecular weight proteins. Fractions containing the fusion protein were pooled and dialyzed against 0.05 M Tris-HCl, pH 8.0 containing 5 mM $MgCl_2$.

2.12.3 Measurement of Nucleotide Hydrolysis Activity Using a Colorimetric Assay:

Nucleotide hydrolysis was measured by the release of inorganic phosphate using a colorimetric assay (Fiske and Subarrow, 1925). A 0.1 ml sample of purified GST fusion protein in 0.05 M Tris·HCl, pH 8.0, containing 5 mM $MgCl_2$ was incubated at 37 °C. The reaction was initiated by adding 5 μl of ATP, GTP, CTP, ADP, GDP, ATP-γ-S (adenosine-5'-O-[3-thiophosphate]), or GTP-γ-S (guanosine-5'-O-[3-thiophosphate]) to give the final indicated concentration. The reaction was allowed to

proceed up to 60 min., the interval over which the release of phosphate was linear with time. The reaction was terminated by the addition of 0.5 ml of 0.25% ammonium molybdate in 0.25 M H_2SO_4 and reduction was carried out by the addition of 20 µl of 13.3% 1-amino-2-naphthol-4-sulfonic acid, 1.3% sodium sulfite, and 1.3% sodium bisulfite. After 10 min. at 25 °C, the absorbance was read at 825 nm. Assays were performed in triplicate.

2.13 SDS-Gel Electrophoresis, Western Blotting and Protein Determination:

SDS-gel electrophoresis was carried out using the Laemmli buffer system (Laemmli, 1970). Samples were made up in an equal volume of SDS-PAGE loading buffer, containing 4% SDS, 40% sucrose, 8% βME, 0.05 M Tris·HCl, pH 7.4. Gels were either stained in Coomassie Blue or transferred onto Immobilon membranes using a Bio-Rad semi-dry apparatus and the buffer system of Towbin *et al.* (1979). The membranes were blocked in 0.5% (w/v) Carnation evaporated milk powder in PBS for 30 min., followed by incubation with the primary antibody for 1 h at room temperature. Typically, Rim 3F4 was diluted at 1:40 and PrimT1 was used at 1:1000. The blots were washed with three 10 ml aliquots of PBS for 10 min. each, followed by incubation with 1:5000 diluted secondary sheep anti-mouse or donkey anti-rabbit Ig-$F(ab')_2$ fragment conjugated to horseradish peroxidase (Amersham). Alternatively, blots were labeled with 1:5000 diluted concanavalin A conjugated to horseradish peroxidase. All antibodies were diluted in the blocking buffer and antibody binding was detected using the ECL system. Protein concentrations were determined using the BCA assay with BSA as the standard.

2.14 Molecular Biology Techniques:

Protocols for the routine molecular biology techniques used in this study can be found in Sambrook *et al.* (1989). The *E. coli* strains used were obtained from Pharmacia (XL-1 Blues) and Invitrogen (Top 10F'). Plasmid purifications were performed with Qiagen Plasmid Kits (Qiagen). Restriction enzyme digestions and ligations were carried out according to the manufacturer's instructions (Pharmacia, New England Biolabs, Promega). Digested DNA fragments and PCR products were separated by electrophoresis and purified using a Bio 101 Geneclean® Kit (Bio/Can Scientific).

E. coli cells were transformed by mixing plasmid DNA with transformation competent cells ($CaCl_2$ method; Sambrook *et al.*, 1989) on ice for 30 min. The DNA/cell mixture was heat-shocked at 42 °C for 90 sec. and then placed on ice. The mixture was added to 800 µl LB/Amp and incubated at 37 °C for 45 min. with shaking. The cells were then plated on LB/Amp agar.

BluescriptII inserts from isolated λZAPII library clones were rescued by the protocol supplied by the manufacturer (Stratagene). Inserts from the λgt10 library were recovered by Polymerase Chain Reaction (PCR) in a TwinBlock™ System thermocycler (Ericomp, Inc.). The reaction volume was 50 µl of 0.01 M Tris·HCl, pH 9.0, containing 0.05 M KCl, 2 mM $MgCl_2$, 16 pmoles of each primer, 6 µmoles of each dNTP, and 1.25 units of Taq DNA Polymerase. The following program was used for the PCR: 5 min. at 95 °C for 1 cycle; 1 min. at 95 °C, 1 min. at 60 °C, 2 min. at 72 °C, for 40 cycles; and 5 min. at 72 °C for 1 cycle. The forward and reverse primers for the λgt10 library were purchased from Promega. DNA fragments generated by PCR were purified (see above) and subcloned using the TA Cloning™ Kit.

For RNA isolation, bovine eyes were obtained within 1 h post-mortem; the retinas were dissected and placed in small vials and frozen immediately in liquid nitrogen. For construction of the pcDNAII library, poly(A) mRNA was isolated from retinal tissue using the FastTrack® 2.0 mRNA Isolation Kit. For Northern blot analysis, total RNA was

isolated from retinal tissue using a protocol involving solubilization in guanidinium isothiocyanate followed by ultracentrifugation in cesium chloride as described by Chirgwin *et al.* (1979).

RESULTS

3.1 Specificity of Monoclonal and Polyclonal Antibodies:

Monoclonal antibody Rim 3F4 and polyclonal antibody PrimT1 were used as probes to clone, characterize and localize the major 220 kDa protein of bovine ROS membranes. The specificities of these antibodies are shown by Western blotting in **Fig 10**. Both antibodies labeled a single protein having an apparent molecular weight of 220,000 in both ROS membranes and the flow through (unbound fraction) obtained when Triton X-100 solubilized ROS membranes were passed through a DEAE anion exchange column. The labeled protein co-migrated with the prominent Coomassie Blue stained 220 kDa protein present in both these samples. In contrast, monoclonal antibodies PMe 2D9 against the 230 kDa Na^+/Ca^{2+}-K^+ exchanger (Reid *et al.*, 1990) and PMs 4B2 against the 240 kDa β-subunit of the cGMP-gated channel (Molday *et al.*, 1990; Körschen *et al.*, 1995) each labeled a high molecular weight polypeptide in ROS membranes, but not in the unbound DEAE fraction (**Fig 10**).

3.2 Cloning and Primary Structure of the Bovine 220 kDa Protein:

cDNA clones of the 220 kDa protein were identified by screening an oligo(dT)-primed bovine retinal cDNA expression library with the PrimT1 antibody. Of the six cDNA clones isolated in the initial screen, the longest clone (λ2) was 1.8 kb in length and had a polyadenylation signal and a poly(A) tail. Rescreening of the oligo(dT)-primed library and a random primed retinal cDNA library with oligonucleotide probes resulted in the isolation of several overlapping clones (**Fig 11**). Upstream clone (p114) contained an ATG start codon with an adjacent upstream Kozak consensus sequence (Kozak, 1991). The nucleotide sequence immediately downstream from this ATG coded for an amino acid sequence that was identical to that determined by direct N-terminal sequencing of the isolated 220 kDa protein (see section 3.5.1). The bovine ABC transporter nucleotide

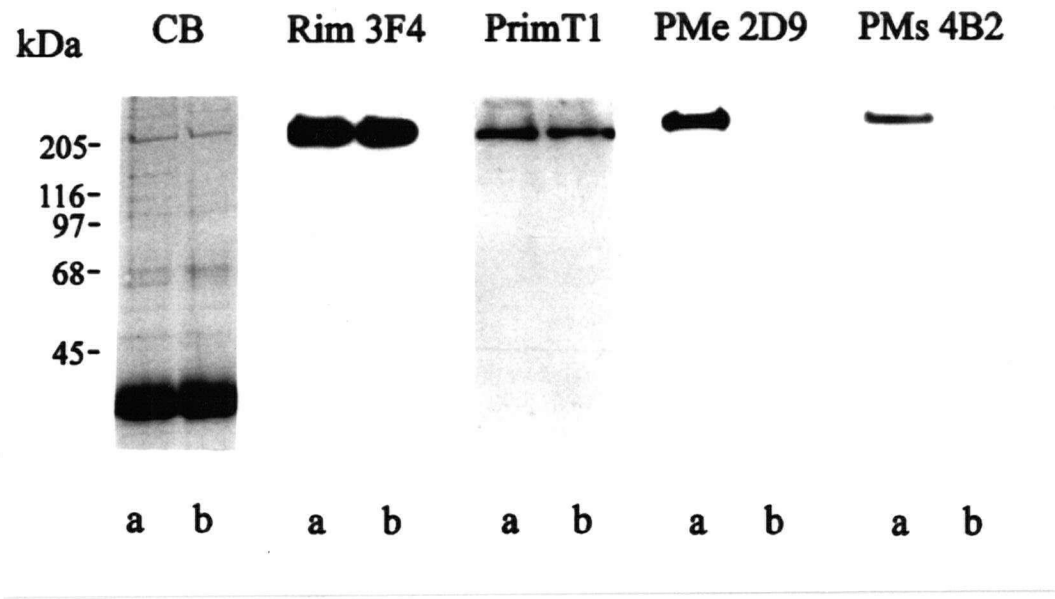

Fig 10. Western blot analysis of ROS proteins labeled with a monoclonal and polyclonal antibody to the 220 kDa protein. Triton X-100 solubilized ROS membranes were passed through a DEAE-Fractogel TSK column and the unbound fraction was collected. Solubilized ROS membranes (*lane a*) and the unbound DEAE fraction (*lane b*) were subjected to SDS-gel electrophoresis (10 μg protein/well). Gels were stained with Coomassie Blue (CB) and Western blots were labeled with antibodies to the 220 kDa protein (monoclonal antibody Rim 3F4 or polyclonal antibody PrimT1) and monoclonal antibodies to the 230 kDa Na^+/Ca^{2+}-K^+ exchanger (PMe 2D9) and the 240 kDa β-subunit of the cGMP-gated channel (PMs 4B2) for comparison. The 220 kDa protein was present in both fractions; the exchanger and channel were only present in the ROS membrane fraction.

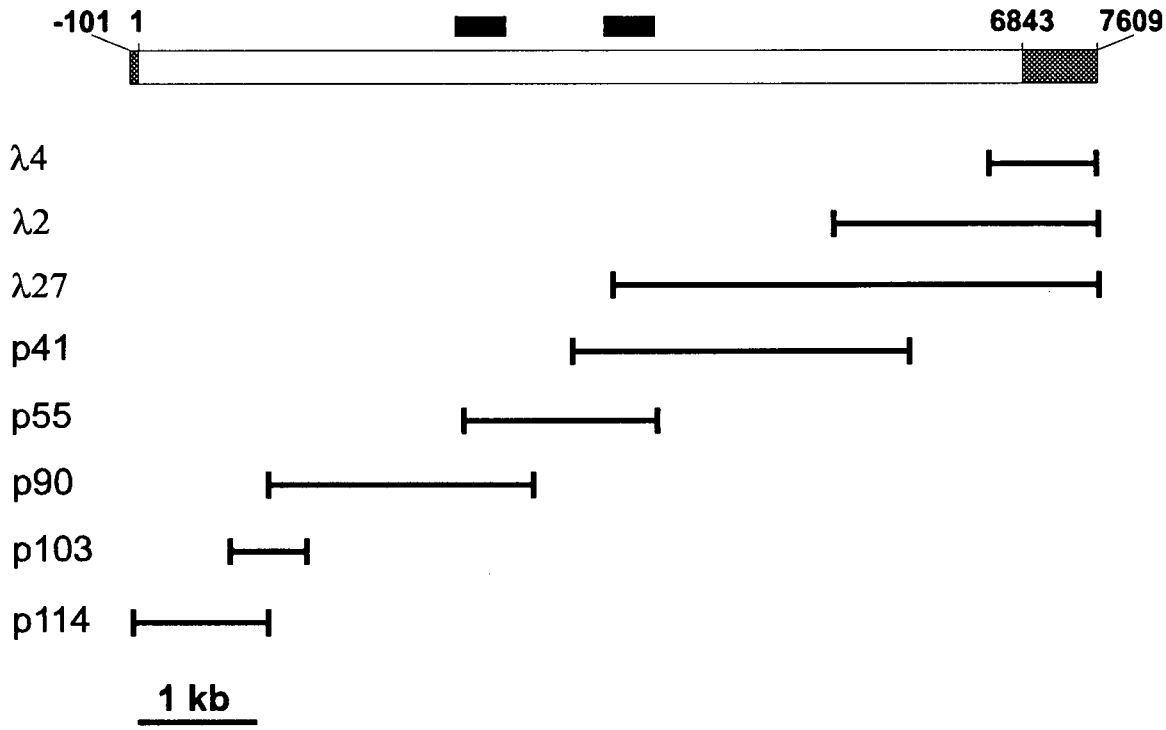

Fig 11. Diagram showing overlapping clones used to define the full length cDNA of the 220 kDa protein. The open reading frame is shown in white and the untranslated regions are in gray. Clones λ2, λ4, and λ27 were isolated from an oligo(dT)-primed library and contain a poly(A) tail. Other clones were isolated from a random primed library. The most 5' clone (p114) contains the ATG start codon designated position 1. The location of two probes used to label Northern blots are shown by *small black bars*.

and protein sequences have been submitted to the GenBank™/EBI Data Bank with accession numbers U90126 and g1943947, respectively (Illing *et al.*, 1997).

The overlapping clones contained an open reading frame of 6843 bp that encodes a protein of 2280 amino acids having a calculated molecular mass of 257,000 daltons (**Fig 12**). This value is 14% higher than the apparent mobility of 220 kDa predicted from SDS-PAGE. The Na^+/Ca^{2+}-K^+ exchanger has a mobility of 230 kDa as estimated by SDS-PAGE; however, its cDNA predicts a molecular mass of 130 kDa. This discrepancy has been attributed to the extensive glycosylation of the protein (Reilander *et al.*, 1992). On the other hand, the β-subunit of the cGMP-gated cation channel complex has a calculated molecular mass of 155 kDa from analysis of its cDNA although it has an apparent mobility of 240 kDa by SDS-PAGE. It has been suggested that this discrepancy is due to the high number of acidic residues in the protein (Körschen *et al.*, 1995). The discrepancy in apparent molecular mass for the 220 kDa protein is probably not due to extensive glycosylation (see section 3.9.2) or charged residues (**Fig 12**) but more likely reflects the inherent inaccuracy of SDS-PAGE to predict molecular mass for high molecular weight proteins.

The predicted amino acid sequence for the 220 kDa protein consists of two structurally related halves arranged in tandem. Each half of the protein has a cluster of hydrophobic segments followed by a conserved ATP-binding cassette (Walker *et al.*, 1982). Hydropathy profiles (Kyte and Doolittle, 1982; Eisenberg *et al.*, 1984) predict 12-14 transmembrane segments, 6-7 in each half of the protein. Fourteen consensus sequences for N-linked glycosylation are also present (**Fig 12**).

Data base homology searches indicate that the ROS 220 kDa protein is a member of the ABC (ATP binding cassette) transporter superfamily. Overall, it is 40-50% identical in amino acid sequence to the ABC1 and ABC2 proteins from a mouse macrophage cell line (Luciani *et al.*, 1994) and 37% identical to ABC-c, a putative transporter recently cloned from a human medullary thyroid carcinoma cell line

Fig 12. Amino acid sequence of the 220 kDa bovine ABC transporter of ROS. The two putative ATP-binding cassettes (*double underline*) and the hydrophobic segments (*single underline*) predicted to be potential transmembrane segments by hydropathy plots (Kyte and Doolittle, 1982; Eisenberg *et al.*, 1984) are indicated. N-terminal peptide sequences derived from the 220 kDa protein or proteolytic fragments of the 220 kDa protein are indicated by a *single overtype line*. The 115 kDa and 120 kDa fragments were obtained by trypsin digestion of the 220 kDa protein in ROS membranes. Peptides 4 and 5 were obtained from endoproteinase Lys C digestion of the purified, detergent solubilized 220 kDa protein, while peptide 25 was isolated from endoproteinase Lys C digestion on the 120 kDa tryptic fragment. All other peptides were obtained by endoproteinase Lys C digestion of the 115 kDa fragment. The 11-amino acid epitope for monoclonal antibody Rim 3F4 is also indicated. Consensus sequences for N-glycosylation are denoted with an *asterisk* (*).

220 kDa/120 kDa

1 MGFARQIKLLLWKNWTLRKRQKIRFVVELVWPLSLFLVLIWLRNVNPLYSKHECHFPNKAMPSAGMLPWLQGIFCNVNNPCFQSPTAGESPGIVSNYNNS

101 ILARVYRDFQELLMDAPESQHLGQVWRELRTLSQLMNTLRMHPERIAGRGIRIREVLKDDEMLTLFLVKNIGLSDSVVYLLVNSQVRPEQFARGVPDLML

201 KDIACSEALLERFLIFPQRRAAQTVRGSLCSLSQGTLQWMEDTLYANVDFFKLFHVFPRLLDSRSQGMNLRSWGRILSDMSPRIQEFIHRPSVQDLLWVT

301 RPLVQTGGPETFTQLMGILSDLLCGYPEGGGSRVFSFNWYEDNNYKAFLGIDSTRKDPIYSYDERTTTFCNALIQSLESNPLTKIAWRAAKPLLMGKILF

peptide #25

401 TPDSPATRRILKNANSTFEELERVRKLVKVWEEVGPQIWYFFDKSTQMSMIRDTLENPTVKAFWNRQLGEEGITAEAVLNFLYNGPREGQADDVDNFNWR

501 DIFNITDRALRLANQYLECLILDKFESYDDEFQLTQRALSLLEENRFWAGVVFPDMHPWTSSLPPHVKYKIRMDIDVVEKTNKIKDRYWDSGPRADPVED

601 FRYIWGGFAYLQDMVEHGITRSQAQEEVPVGIYLQQMPYPCFVDDSFMIILNRCFPIFMVLAWIYSVSMTVKSIVLEKELRLKETLKNQGVSNRVIWCTW

701 FLDSFSIMSMSICLLTIFIMHGRILHYSNPFILFLFLLAFSIATIMQCFLLSTFFSRASLAAACSGVIYFTLYLPHILCFAWQDRITADMKMAVSLLSPV

801 AFGFGTEYLAXFEEQGVGLQWSNIGNSPMEGDEFSFLMSMKMMLLDAALYGLLAWYLDQVFPGDYGTPLPWYFLLQESYWLGGEGCSTREERALEKTEPI

901 TEEMEDPEYPEGINDCFFERELPGLVPGVCVKNLVKIFEPYGRPAVDRLNITFYESQITAFLGHNGAGKTTTLSIMTGLLPPTSGTVLVGGKDIETNLDA

========== ATP-binding cassette========

1001 IRQSLGMCPQHNILFHHLTVAEHILFYAQLKGRSWDEAQLEMEAMLEDTGLHHKRNEEARDLSGGVQRKLSVAIAFVGDAKVVVLDEPTSGVDPYSRRSI

==========

1101 WDLLLKYRSGRTIIMSTHHMDEADILGDRIAIISQGRLYCSGTPLFLKNCFGTGFYLTLVRRMKTIQSQGRGREATCSCASKGFSVRCPACAEAITPEQV

1201 LDGDVNELTDMVHHHVPEAKLVECIGQELIFLLPNKNFKQRAYASLFRELEETLADLGLSSFGISDTPLEEIFLKVTEDLDSGHLFAGGTQQKRENINLR

115 kDa

1301 HPCSGPSEKAGQTPQGSSSHPGEPAAHPEGQPPPEREGHSRLNSGARLIVQHVQALLVKRFQHTIRSHKDFLAQIVLPATFVFLALMLSLIIPPFGEYPA

peptide#5

1401 LTLHPWMYGQQYTFFSMDQPDSEWLSALADVLVNKPGFGNRCLKEEWLPEFPCGNSSPWKTPSVSPDVTHLLQQQKWTADQPSPSCRCSTREKLTMLPEC

peptide #27 peptide #21

1501 PEGAGGLPPPQRIQRSTEILQDLTDRNVSDFLVKTYPALIRSSLKSKFWVNEQRYGGISVGGKLPAPPFTGEALVGFLSDLGQLMNVSGGPMTREAAKEM

peptide #22

1601 PAFLKQLETEDNIKVWFNNKGWHALVSFLNVAHNAILRASLHKDKNPEEYGITVISQPLNLTKEQLSEITVLTTSVDAVVAICVIFAMSFVPASFVLYLI

1701 QERVNKAKHLQFVSGVSPTTYWLTNFLWDIMNYTVSAALVVGIFIGFQKKAYTSSENLPALVALLMLYGWAVIPMMYPASFLFDIPSTAYVALSCANLFI

1801 GINSSAITFVLELFENNRTLLRINAMLRKLLIIFPHFCLGRGLIDLALSQAVTDVYAQFGEAHSSNPFQWDLIGKNLAAMAVEGVVYFLLTLLIQYQFFF

peptide #24 peptides #4/26

1901 SRWTTEPAKEPITDEDDDVAEERQRIISGGNKTDILRLNELTKVYSGTSSPAVDRLCVGVRPGECFGLLGVNGAGKTTTFKMLTGDTAVTSGDATVAGKS

==========

2001 ILTNISDVHQSMGYCPQFDAIDDLLTGREHLYLYARLRGVPAEEIERVTNWSIQSLGLSLYADRLAGTYSGGNKRKLSTAIALIGCPPLVLLDEPTTGMD

==========ATP-binding cassette==========

2101 PQARRMLWNTIMGIIREERAVVLTSHSMEECEALCTRLAIMVKGAFQCLGTIQHLKSKFGDGYIVTMKIRSPKDDLLPDLGPVEQFFQGNFPGSVQRERH

peptide #28

3F4 epitope

2201 YNTLQFQVSSSSLARIFRLLVSHKDSLLIEEYSVTQTTLDQVFVNFAKQQNETYDLPLHPRTAGASRQAKEVDKGNSAPQG

(Klugbauer and Hofmann, 1996). The ABC binding domains of these proteins display an even higher degree of identity (>60%), particularly within the two short stretches of the Walker motifs and the active transport signature (ATS) located upstream of the Walker B pattern (Walker *et al.*, 1982). The ROS 220 kDa protein is more distantly related to other well-studied members of the ABC transporter superfamily such as the cystic fibrosis transmembrane regulator (CFTR; Riordan *et al.*, 1989) and the multi-drug resistance protein (MDR1 or P-glycoprotein; Chen *et al.*, 1986), showing a sequence identity of 20-22% overall and 20-26% for the ABC domains. A 43% sequence identity is observed between the N- and C-terminal ABC domains of the bovine ROS 220 kDa protein, a value similar to that between the two cassettes within ABC1 and MDR1 P-glycoprotein.

3.3 Partial Sequence of Human 220 kDa Protein Clones:

The human orthologue to the bovine 220 kDa protein was partially cloned and sequenced. Clones were found to have an overall 92% identity and another 5% similarity to the bovine sequence at the amino acid level (**Fig 13**) and 100% identity to a recently cloned ABC transporter from retina (Allikmets *et al.*, 1997a). This transporter maps to chromosome 1p22 and mutations in the gene (*ABCR* or *STG1*) have been linked to Stargardt's disease, a common inherited autosomal recessive macular degeneration (Kaplan *et al.*, 1993; Weber *et al.*, 1996; Allikmets *et al.*, 1997a; Nasonkin *et al.*, 1997). More recently, mutations in *ABCR* have been found in 16% of patients displaying age-related macular degeneration (AMD), the most common cause of central vision loss in the elderly (Allikmets *et al.*, 1997b).

3.4 Northern Blot Analysis of Bovine mRNA:

The size of the mRNA transcripts for the 220 kDa protein was estimated by Northern blotting. As shown in **Fig 14**, an Eco RI/Sac I fragment from clone p41 (**Fig 11**) hybridized to transcripts of ~9.5 kb and 6.8 kb in length. An upstream fragment from

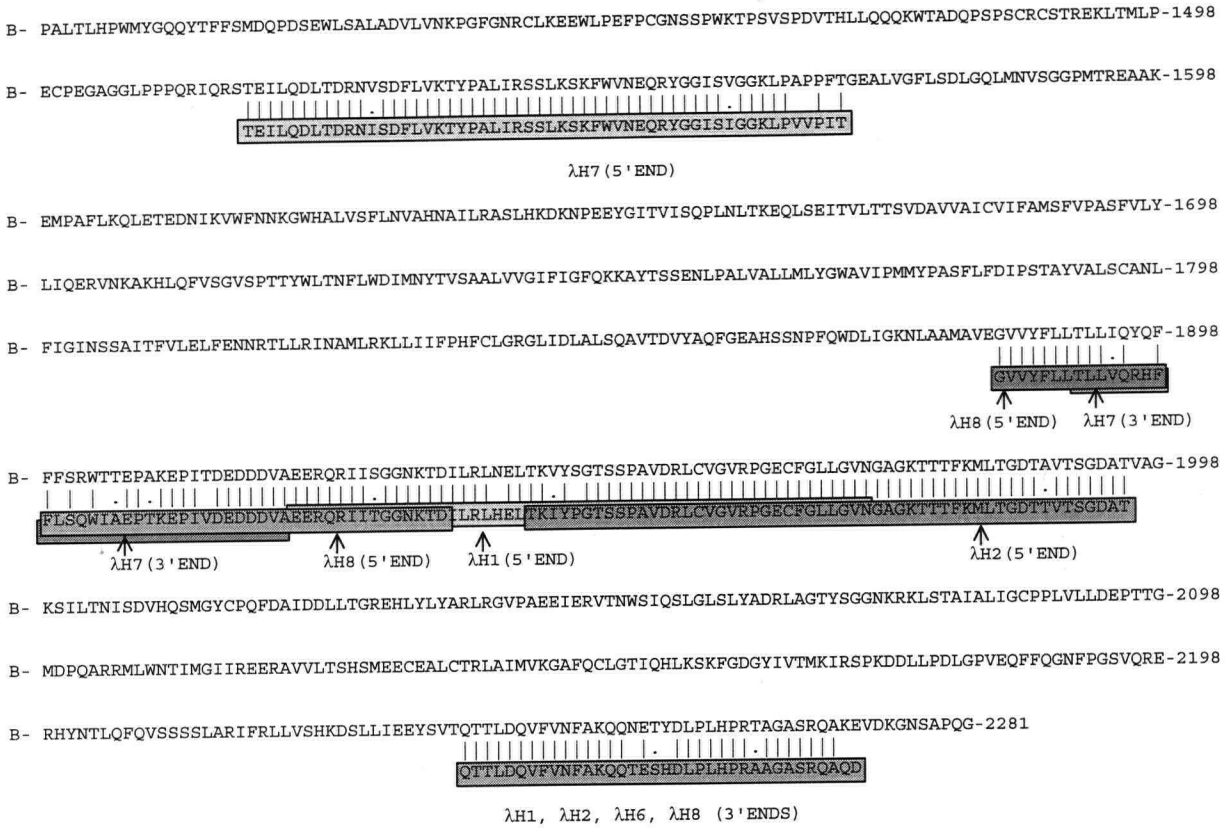

Fig 13. Partial sequence of human 220 kDa clones. Clones were isolated from a λgt10 human retinal cDNA library by screening with an Afl II/Sph I fragment of clone λ2 (**Fig 11**) isolated in the bovine 220 kDa cloning. Five clones (*λH1, λH2, λH6, λH7,* and *λH8*) were isolated and partially sequenced (*boxes*; see section 2.4.2) that contain overlapping sequences. The deduced amino acid sequence of the human clones was aligned (NALIGN program; PC Gene, IntelliGentics, Inc.) with the bovine amino acid sequence (*B*) deduced from the cDNA. Clones were found to have a 92% identity and another 5% similarity at the amino acid level.

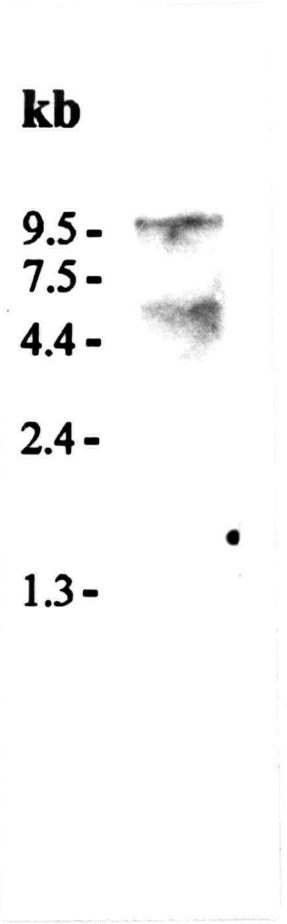

Fig 14. Northern blot analysis of the 220 kDa protein transcripts from bovine retinal RNA. Total bovine retinal RNA (10 μg) was probed with the Eco RI/Sac I restriction fragment of clone p41 (**Fig 11**). A prominent band at ~9.5 kb and a less intensely stained band at 6.8 kb are evident.

clone p55 gave a similar labeling pattern (data not shown). The smaller labeled fragment could be an alternately spliced mRNA product or the mRNA of a related transporter from rod cells or another cell of the retina. The stringency of the washes was quite high (65 °C; 0.1X SSC), therefore, cross-hybridzation would only be likely if the mRNA showed a high degree of homology.

3.5 Peptide Sequencing and Amino Acid Composition of the Bovine 220 kDa Protein:

3.5.1 Generation of Internal Peptide Sequences:

Peptide sequencing of the 220 kDa ROS protein was carried out in order to confirm that the cDNA clones code for the protein sequence of the major 220 kDa protein of bovine ROS membranes. The N-terminal 18 amino acids of the immunoaffinity purified 220 kDa protein were found to be identical to a sequence contained in clone p114 and immediately downstream from a methionine (**Fig 12**).

Mild trypsin digestion of the 220 kDa protein in ROS membranes followed by purification on a Rim 3F4 antibody affinity column resulted in two large peptide fragments having apparent molecular masses of 120 kDa and 115 kDa (**Fig 15**). N-terminal sequencing of the 120 kDa fragment produced more than one sequence. One of these sequences was found to be identical to the N-terminal sequence of the full-length 220 kDa while the others were difficult to assign (data not shown). The sequence of the 115 kDa fragment was identical to a sequence starting at position 1311, close to the middle of the 220 kDa protein (**Fig 12**). Western blot analysis with Rim 3F4 indicated that the lower band contained the epitope of the antibody and was the C-terminus of the protein (see section 3.7), while a fragment at 120 kDa is most likely the N-terminal half of the protein. Rim 3F4 labeling at 120 kDa is unlikely due to cross-reactivity with the N-terminal half of the protein for two reasons: (1) the epitope is not repeated in the primary structure of the

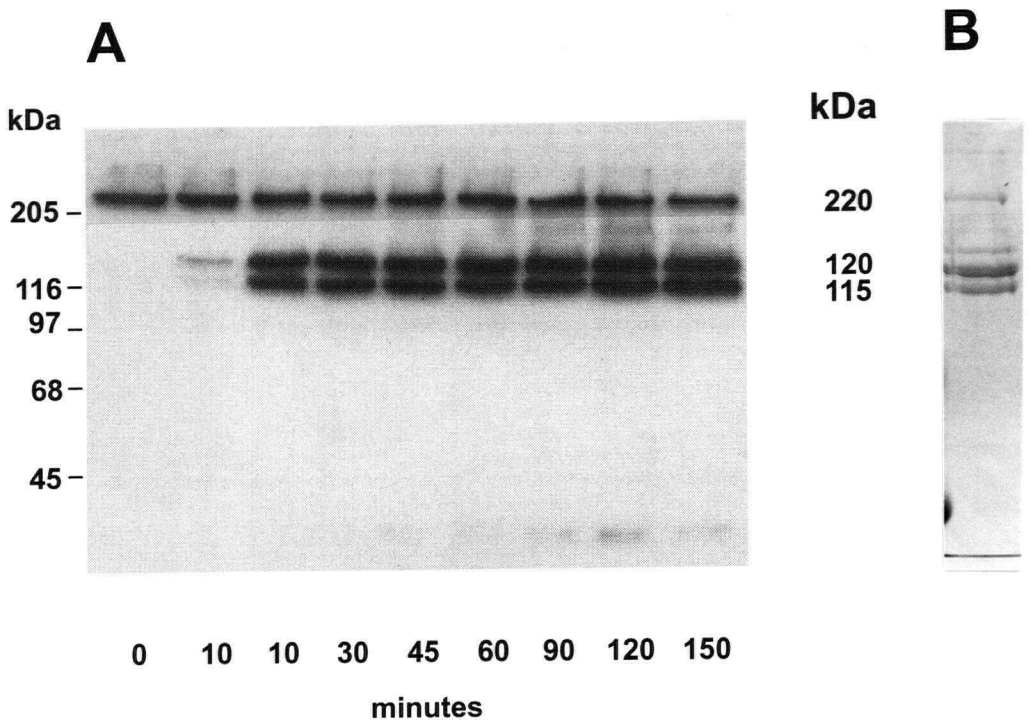

Fig 15. Generation of the 115 and the 120 kDa fragments of the 220 kDa protein. A, Hypotonically lysed ROS (8 mg/ml) were treated with 0.4 μg/ml TPCK-treated trypsin in 0.02 M Tris·HCl, pH 7.4, and 0.02 M $CaCl_2$ at room temperature and 0.1 ml fractions were removed over time. The reaction was stopped by washing with one 1 ml aliquot of 10 μg/ml soybean trypsin inhibitor in the same buffer and the pellet was made up in 0.1 ml of the inhibitor buffer. A 20 μl sample was subjected to SDS gel electrophoresis and transferred onto Immobilon and stained with the monoclonal antibody Rim 3F4. The 220 kDa protein is stained in addition to two lower (115 and 120 kDa) fragments. **B**, The lightly trypsinized ROS were subjected to Rim 3F4-affinity chromatography and the protein was eluted with a low pH buffer (see Methods). Approximately 10 μg of the eluted protein was subjected to SDS gel electrophoresis and stained with Coomassie Blue. Two bands of 115 and 120 kDa, corresponding to the Rim 3F4 labeled bands, are visible as well as the undigested 220 kDa protein.

protein (**Fig 12**); and (2) the relative intensity of Rim 3F4 staining of the two fragments varies greatly with the preparation while staining with Coomassie Blue remains constant (see also **Fig 19**). Therefore, labeling of the upper band appears to be due to an alternate cleavage site which produces a slightly larger C-terminal fragment that co-migrates with the N-terminal fragment. These results indicate that limited digestion with trypsin produces fragments corresponding to the two homologous domains, which remain associated in detergent and co-purify with Rim 3F4 affinity chromatography. Trypsin digestion has also been reported to split MDR1 P-glycoprotein into two homologous halves which remain associated after cleavage (Senior *et al.*, 1995).

Nine smaller peptide fragments were derived from endoproteinase Lys C digestion of the purified, detergent solubilized 220 kDa protein and its purified 115 kDa and 120 kDa fragments (**Fig 16**). The N-terminal sequences of these peptides were identical to sequences found within the 220 kDa protein sequence deduced from cDNA cloning (**Fig 12**). The sequence of peptide #21 was of particular interest. Although 36 of the 37 amino acids of this peptide correspond to positions 1564-1600 of the full length 220 kDa protein sequence, the amino acid at position 23 of the peptide sequence (position 1586 of the 220 kDa sequence) could not be identified. Since this residue is an Asn that is part of a N-linked glycosylation consensus sequence, it is likely that this residue is covalently modified with an oligosaccharide chain, and therefore, not identifiable by sequencing.

3.5.2 Amino Acid Composition and N-terminal Sequence:

Further evidence that the immunoaffinity purified 220 kDa protein is the same as the protein encoded by the cloned cDNA was obtained from amino acid analysis. As indicated in **Table 4**, the experimentally determined amino acid composition of the purified 220 kDa protein is in good agreement with the amino acid composition determined from the deduced protein sequence.

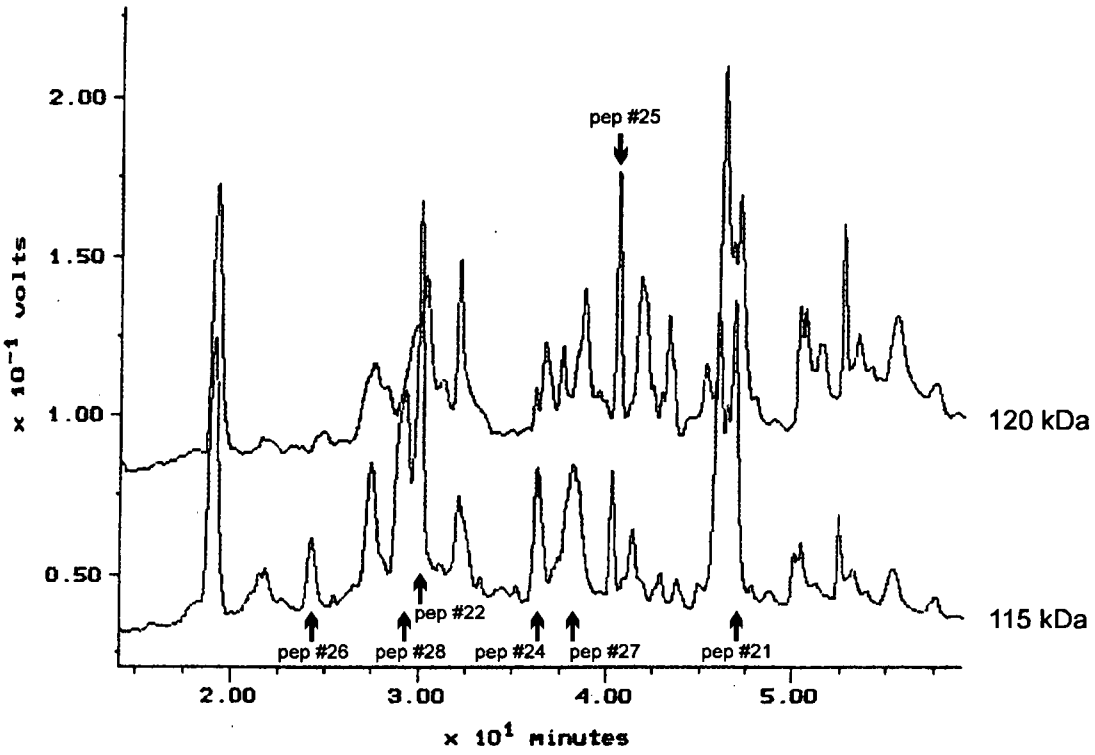

Fig 16. Purification of peptides from the 120 and 115 kDa fragments of the bovine 220 kDa protein. The 120 and 115 kDa fragments of the bovine 220 kDa protein (**Fig 15**) were transferred to nitrocellulose and digested with endoproteinase Lys C. The resulting peptides were isolated by high pressure liquid chromatography using a narrow bore C18 reverse-phase column. A linear gradient of 5-65% acetonitrile, containing 0.05% trifluoroacetic acid, was applied at a flow rate of 0.25 ml per min. The flow through was monitored at 214 nm and fractions were collected manually. Peptides (indicated by *arrows*) were subjected to Edman degradation and numbering corresponds to that in **Fig 12**.

TABLE 4

Amino acid analysis of the 220 kDa protein.

The values are a percentage of the total amino acids. Tryptophan is degraded in the presence of 6M HCl and is not detectable. The low value for cysteine is also attributed to degradation.

Amino acid	Theoretical value[a]	Experimental value	Exp/theoretical
Asx[b]	8.9	10.0	1.1
Glx[c]	10.4	12.4	1.2
Ser	7.1	6.4	0.9
Gly	6.6	7.2	1.1
His	2.0	2.0	1.0
Arg	5.4	5.6	1.0
Thr	6.0	5.3	0.9
Ala	6.3	6.8	1.1
Pro	5.3	4.4	0.8
Tyr	2.8	3.3	1.2
Val	6.1	5.9	1.0
Met	2.8	3.9	1.4
Cys	1.8	0.5	0.3
Ile	5.6	4.8	0.9
Leu	11.8	11.9	1.0
Phe	5.4	5.7	1.1
Lys	4.0	3.9	1.0
Trp	1.9	---	---

[a] Calculated from the predicted amino acid composition of the 220 kDa protein.
[b] Asx; aspartic acid + asparagine
[c] Glx; glutamic acid + glutamine

3.6 Cellular and Subcellular Distribution of the Bovine 220 kDa Protein:

3.6.1 Immunofluorescence Microscopy of Bovine Retina:

The distribution of the 220 kDa protein in retina tissue was examined using immunocytochemical labeling methods. The Rim 3F4 antibody labeled the outer segments of rod, but not cone, photoreceptor cells in bovine retinal cryosections labeled

with either the fluorescent probe Cy3 (**Fig 17**) or the colourimetric DAB substrate (data not shown). Weak staining was observed in the inner segment layer, but no staining was detected in other retinal cells. A similar pattern of labeling was observed in rat retina (data not shown). Labeling was specific since addition of excess 3F4 peptide inhibited antibody labeling (**Fig 17C**). Labeling with the PrimT1 polyclonal antibody gave similar results.

3.6.2 Immunogold Labeling of Bovine Retina for Electron Microscopy:

The subcellular distribution of the 220 kDa protein in ROS was studied using immunogold labeling methods for electron microscopy. When LR White resin embedded retinal sections were labeled with the PrimT1 antibody, immunogold particles were observed to be distributed along the edges of the ROS where the rim region of the disks are in close proximity to the plasma membrane and incisures (**Fig 18**). This labeling pattern is similar to that described by Papermaster *et al.* (1978) for a 290 kDa rim protein in frog outer segments. The Rim 3F4 monoclonal antibody did not label these sections presumably due to inaccessibility of the epitope in resin embedded samples.

3.6.3 Biochemical Analysis of Disk and Plasma Membranes:

Since postembedding immunogold labeling studies could not unambiguously establish whether the 220 kDa protein was localized to the rim region of disk membranes or the plasma membrane, disk membranes were isolated from trypsin treated ROS (Molday and Molday, 1987) for Western blot analysis. As shown in **Fig 19**, the Rim 3F4 monoclonal antibody intensely labeled the 220 kDa protein in ROS membranes and its 115 kDa tryptic fragment in isolated disk membranes. A less intensely labeled 120 kDa fragment was also observed in the disk membrane fraction; this fragment is most likely derived from trypsin cleavage at a secondary site within the 220 kDa (see section 3.5.1).

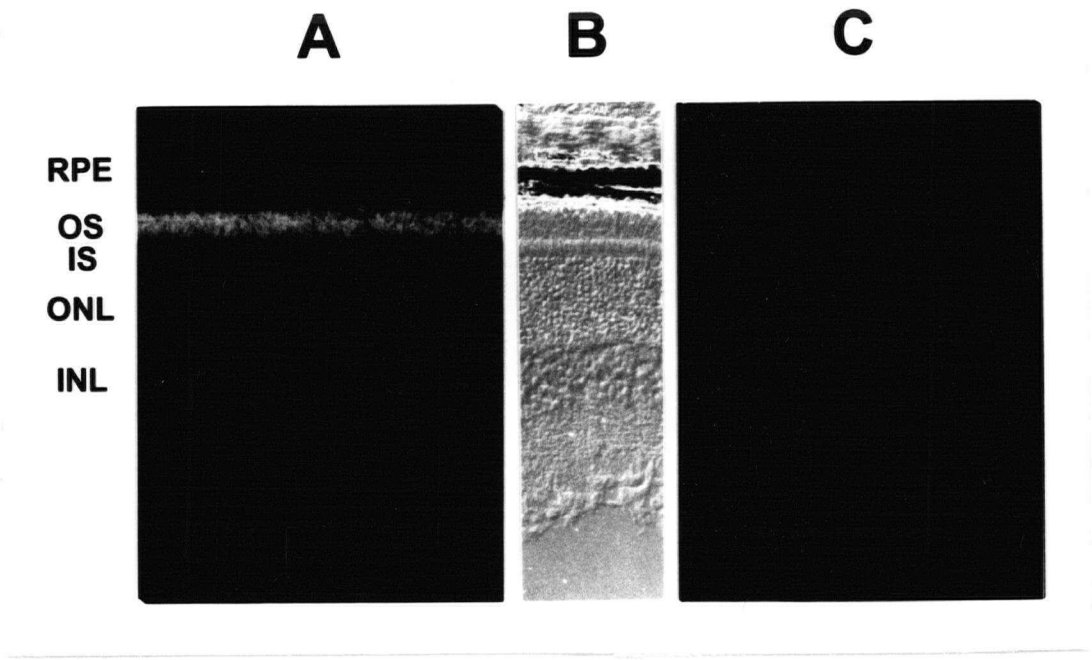

Fig 17. Retinal cellular localization of the 220 kDa protein. Light micrographs of bovine retina cryosections labeled with the Rim 3F4 monoclonal antibody against the 220 kDa protein and goat anti-mouse Ig-Cy3 in the absence **(A)** and in the presence **(C)** of the 3F4 peptide. In the absence of competing peptide, intense labeling is observed in the rod outer segment (OS) layer. The DIC image is shown in **B**. Low levels of labeling can be detected in the inner segment. No labeling is observed in the retinal pigmented epithelium (RPE), the outer nuclear layer (ONL), or the inner nuclear layer (INL). Figure provided by L.L. Molday.

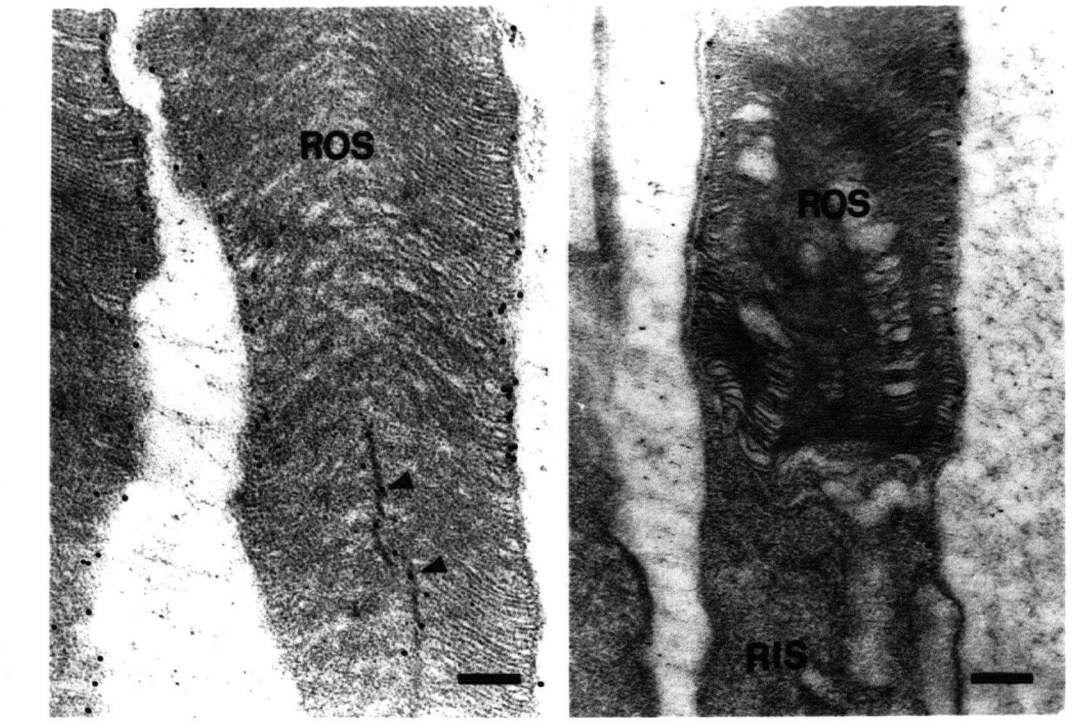

Fig 18. Subcellular localization of the 220 kDa protein in the retina. Electron micrographs of a LR White resin embedded rod photoreceptor cells labeled with the PrimT1 antibody and immunogold particles. Labeling is restricted to the peripheral region of the rod outer segment and to the incisures (*arrowheads*). The rod inner segments (RIS) are not labeled. Bar, 200nm. Figure provided by L.L. Molday.

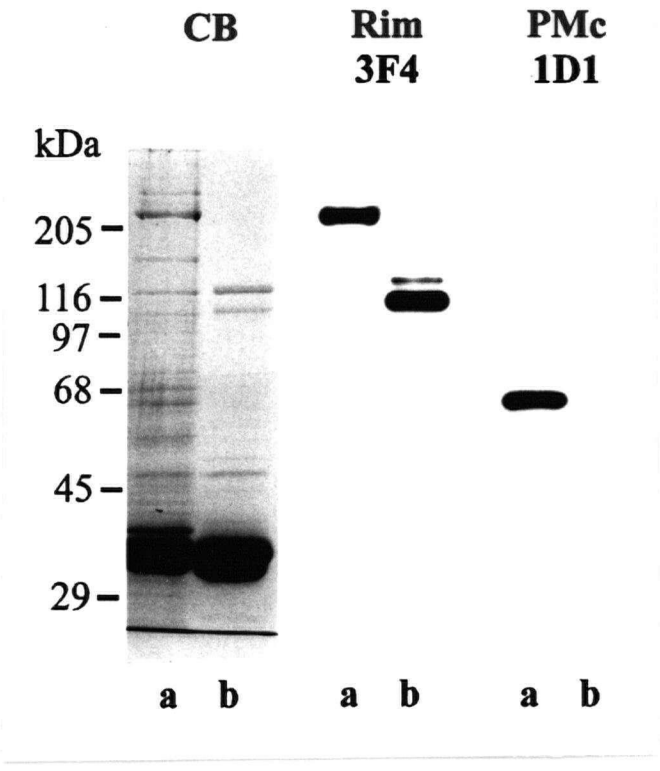

Fig 19. Localization of the 220 kDa protein to the disk membranes of ROS. Disk membranes were separated from the ricin-gold-dextran labeled plasma membrane after mild trypsin treatment by sucrose gradient centrifugation (Molday and Molday, 1987). Untreated ROS membranes (*lane a*) and trypsin-treated disk membranes (*lane b*) were subjected to SDS-polyacrylamide gel electrophoresis. Gels were stained with Coomassie Blue (CB) and Western blots were labeled with the Rim 3F4 antibody against the 220 kDa protein and the PMc 1D1 antibody against the α-subunit of the cGMP-gated channel. The 220 kDa protein is cleaved by trypsin to 120 kDa and 115 kDa fragments as visualized by Coomassie Blue staining; the latter is intensely stained with the Rim 3F4 antibody in isolated disk membranes. Absence of PM 1D1 labeling in the disk fraction confirms that the disk fraction is not contaminated with plasma membrane from ROS as previously reported (Cook *et al.*, 1989).

Absence of plasma membrane contamination in the disk fraction was verified in labeling studies employing a plasma membrane specific cGMP-gated channel antibody (Cook *et al.*, 1989). As shown in **Fig 19**, the anti-channel antibody PMc 1D1 labeled the 63 kDa α-subunit of the cGMP-gated channel in ROS membranes, but no labeling of the trypsinized channel subunit (Cook *et al.*, 1989) was observed confirming its absence in the disk fraction. The immunocytochemical and biochemical studies taken together indicate that the bovine 220 kDa protein is preferentially, if not exclusively, localized to the rim and incisures of ROS disks.

3.7 Mapping of the Epitope of the Monoclonal Antibody Rim 3F4:

Peptide mapping studies using a combination of glutathione-S-transferase fusion proteins and synthetic peptides revealed that the epitope for the Rim 3F4 monoclonal antibody is localized near the C-terminus of the protein. Initially, the C-terminal 128 amino acids of the bovine rim ABC transporter were expressed as a fusion protein with GST, and fortuitously, the affinity-purified protein was reactive to Rim 3F4 as shown by Western blotting (**Fig 20A**). The epitope was further narrowed down to an 11 amino acid stretch based on immunoreactivity with overlapping synthetic peptides (**Fig 20B**). A 9 amino acid peptide corresponding to this epitope was synthesized (residues 2253-2262) and used in immuno-purification studies (section 3.8).

3.8 Immunoaffinity Purification of the Bovine 220 kDa Protein:

The 220 kDa protein could be efficiently purified from detergent solubilized ROS on a Rim 3F4-Sepharose 2B column. As shown in **Fig 21**, the 220 kDa protein was completely adsorbed to a Rim 3F4-Sepharose column and competitively eluted with the 9 amino acid peptide corresponding to the Rim 3F4 epitope to yield a highly pure protein as determined by SDS polyacrylamide gel electrophoresis and Western blot analysis.

Fig 20. Mapping of the epitope of the Rim 3F4 monoclonal antibody. A, The GST fusion protein with the C-terminal 128 amino acids of the bovine rim ABC transporter was induced with IPTG as described in Materials and Methods. Samples of non-induced and induced cell culture (10 μg protein) were solubilized in SDS-sample buffer, electrophoresed, transferred onto Immobilon and stained with the monoclonal antibody Rim 3F4. An intensely stained band at 39 kDa, corresponding to the predicted molecular mass of the fusion protein, was present in the induced cells. **B**, The epitope was further refined by synthesizing overlapping peptides, 9 amino acids long with a 2 amino acid overlap (represented by *lines*), and probing with the Rim 3F4 antibody. Near the C-terminus of the protein, two overlapping peptides were labeled corresponding to the amino acid residues 2251-61. The 9 amino acid "3F4 peptide" (*box*) was synthesized and used in subsequent experiments. Numbers refer to the amino acid sequence of the bovine rod ABC transporter.

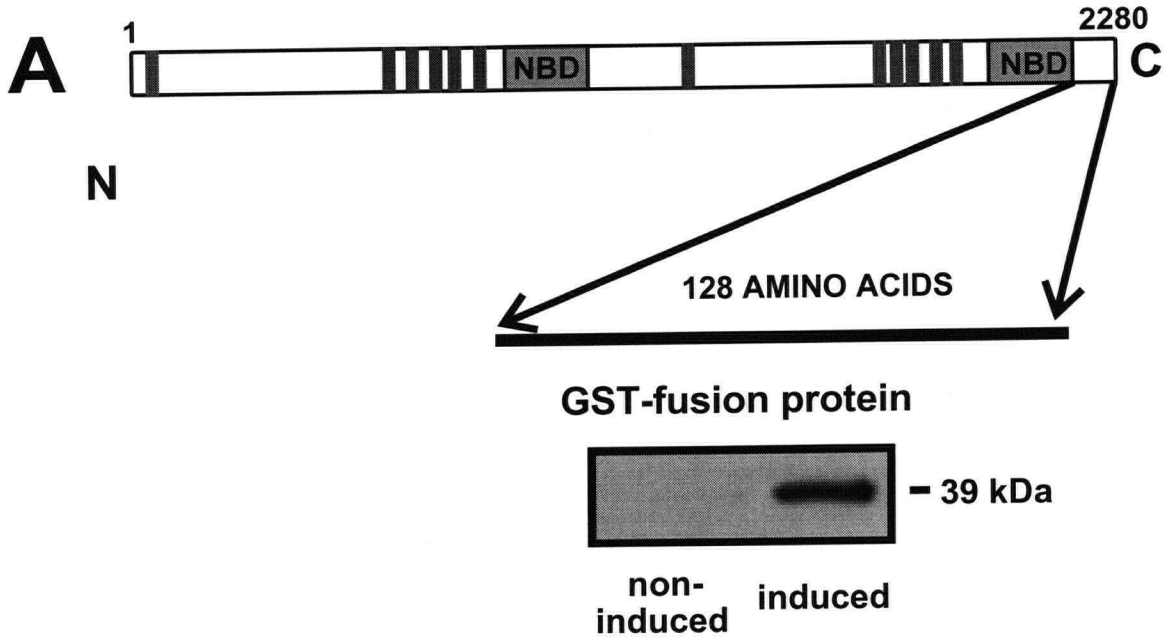
A
1
2280
NBD
NBD
C
N
128 AMINO ACIDS
GST-fusion protein
39 kDa
non-induced
induced

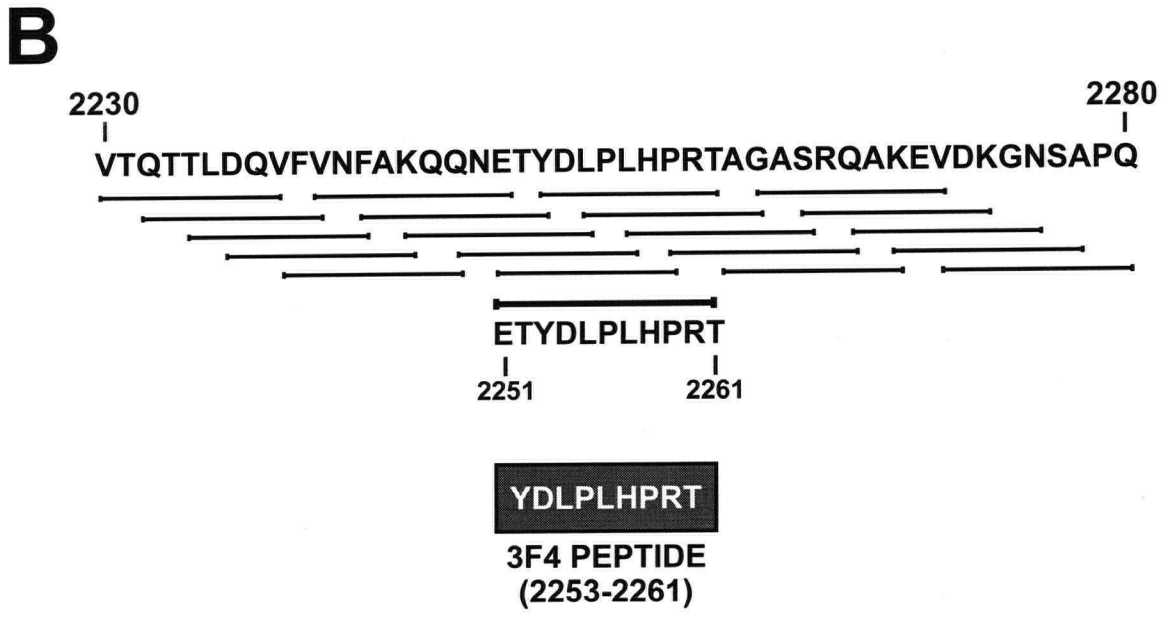
B
2230
2280
VTQTTLDQVFVNFAKQQNETYDLPLHPRTAGASRQAKEVDKGNSAPQ
ETYDLPLHPRT
2251
2261
YDLPLHPRT
3F4 PEPTIDE
(2253-2261)

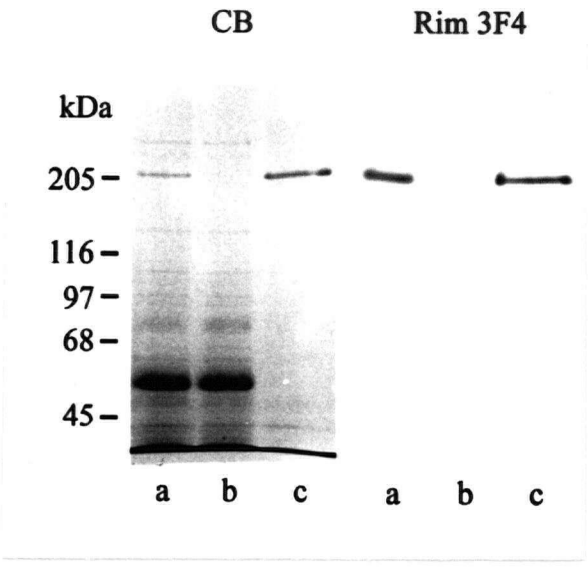

Fig 21. Immunoaffinity purification of the 220 kDa protein. Triton X-100 solubilized ROS membranes were applied to a Rim 3F4 antibody-Sepharose 2B column. The unbound fraction was collected and the bound fraction was subsequently eluted with the 3F4 peptide. The solubilized ROS membranes (*lane a*), unbound fraction (*lane b*) and the bound fraction (*lane c*) were subjected to SDS gel electrophoresis on a 8% polyacrylamide gel and either stained with Coomassie Blue (CB) or electrophoretically transferred to Immobilon membranes and labeled with monoclonal antibody Rim 3F4. The Coomassie Blue stained 220 kDa protein present in the ROS membrane fraction (*lane a*) and the bound fraction (*lane c*) was labeled by the Rim 3F4 antibody.

3.9 Characterization of the 220 kDa Protein:

3.9.1 Expression of the Rim ABC Transporter in Various Species:

Western blotting was used to investigate the presence of the rim ABC transporter in ROS isolated from retinas of different vertebrate species. The monoclonal antibody 3F4, generated against the bovine rim ABC transporter, labeled the corresponding 220 kDa protein in human, mouse, rat, and dog ROS (**Fig 22**). No labeling was observed in chicken and frog preparations, presumably due to lack of cross-reactivity with non-mammalian proteins.

3.9.2 The Bovine 220 kDa Protein is Glycosylated:

Concanavalin A labeling and endoglycosidase H digestion were carried out to determine if the ROS 220 kDa protein is glycosylated. As shown in **Fig 23**, concanavalin A labeled the 220 kDa protein in both ROS membranes and immunoaffinity purified preparations, but not in the unbound fraction from the immunoaffinity column. Monomeric and oligomeric forms of rhodopsin are also labeled with concanavalin A in the ROS sample and in the unbound fraction from the affinity column. The immunoaffinity purified 220 kDa protein fraction appears to be largely free of rhodopsin.

Endoglycosidase digestion was carried out to further evaluate the extent to which the 220 kDa protein is glycosylated. As shown in **Fig 24**, only a slight increase in mobility of the 220 kDa protein was observed after treatment with endoglycosidase H. These results indicate that the 220 kDa protein contains at least one N-linked, high mannose oligosaccharide chain, but it is unlikely to be highly glycosylated.

3.9.3 Photoaffinity Labeling of the 220 kDa Protein with 8-Azido-ATP:

Photoaffinity labeling was carried out to determine if the putative ATP binding domains of the 220 kDa protein bind nucleotides. As shown in **Fig 25**, 8-azido-[α^{32}P]-

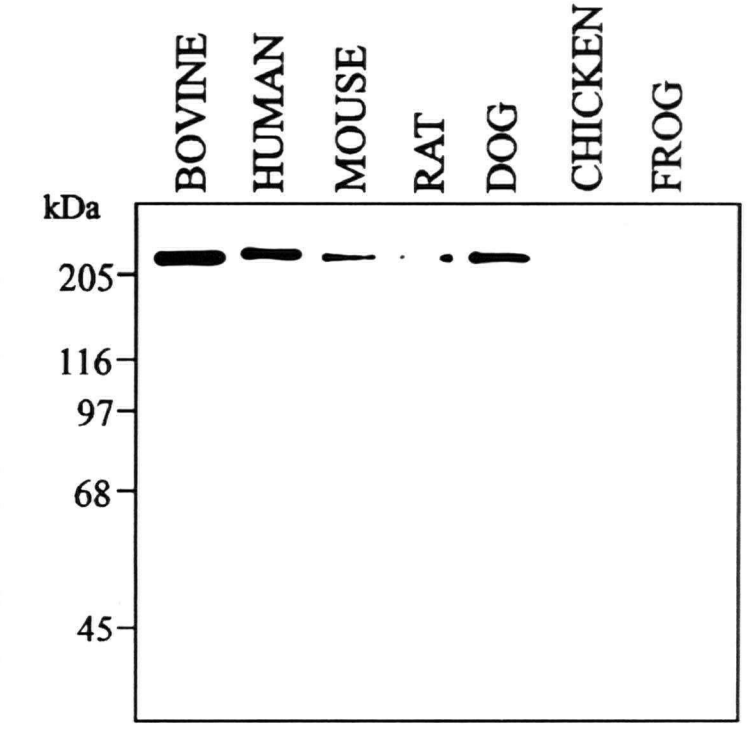

Fig 22. Western blot analysis of rod outer segment proteins from various species labeled with the Rim 3F4 monoclonal antibody. A 220 kDa polypeptide corresponding to the rod rim ABC transporter is stained in all the mammalian species; no staining was observed for frog or chicken preparations.

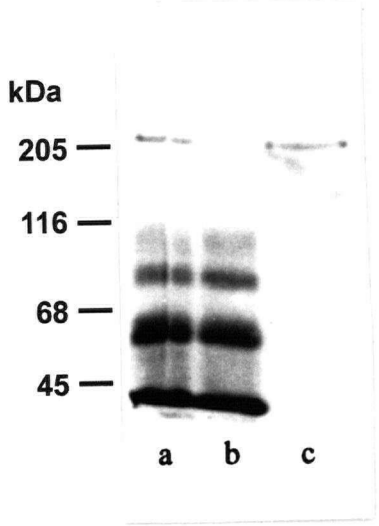

Fig 23. The 220 kDa protein is glycosylated: concanavalin A labeling. The 220 kDa protein was immunoaffinity purified as described in **Fig 21**. The solubilized ROS membranes (*lane a*), unbound fraction (*lane b*) and the bound fraction (*lane c*) were subjected to SDS gel electrophoresis on a 8% polyacrylamide gel and electrophoretically transferred to Immobilon membranes and labeled with concanavalin A. The Coomassie Blue stained 220 kDa protein (**Fig 21**) present in the ROS membrane fraction (*lane a*) and the bound fraction (*lane c*) was labeled by concanavalin A; oligomers of rhodopsin were also labeled by concanavalin A (*lanes a* and *b*).

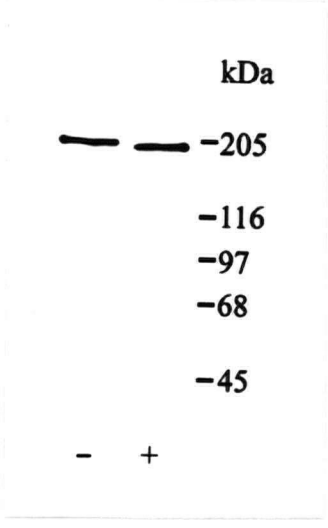

Fig 24. The 220 kDa protein is glycosylated: endoglycosidase Hf digestion.
Detergent solubilized ROS membranes were treated with endoglycosidase Hf for 1 hour at 37°C and Western blots were labeled with the Rim 3F4 antibody (—, untreated; +, endoglycosidase-treated).

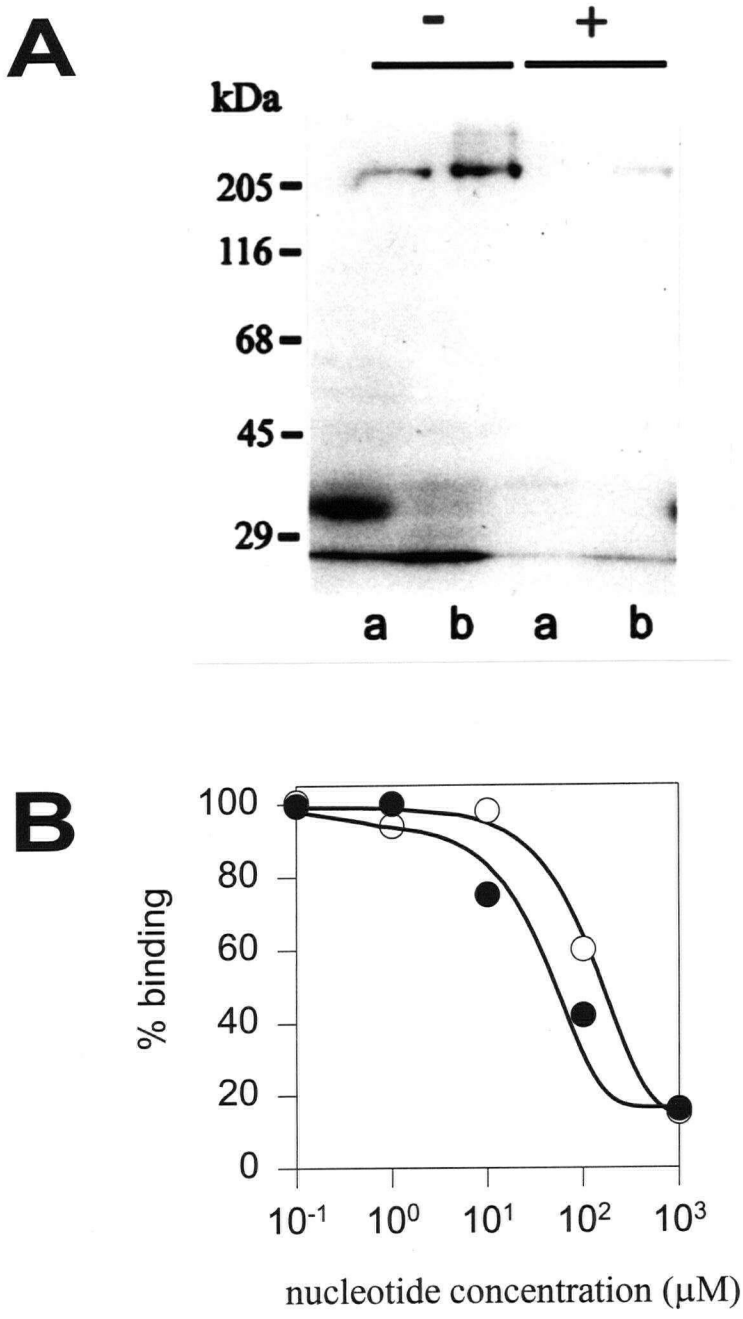

Fig 25. Photoaffinity labeling of the 220 kDa protein with 8-azido-ATP. **A**, Purified ROS membranes (*lane a*) and immunoaffinity purified 220 kDa protein (*lane b*) were labeled with 8-azido-[α^{32}P]-ATP in the absence (-) and presence (+) of 1 mM unlabeled ATP. **B**, Inhibition of 8-azido-[α^{32}P]-ATP by varying concentrations of unlabeled ATP (-○-) and GTP (-●-).

ATP covalently labeled the 220 kDa protein in both ROS membranes and immunoaffinity purified preparations. Labeling could be largely inhibited by the addition of 1 mM unlabeled ATP or 1 mM GTP (**Fig 25A&B**). These studies are in agreement with the earlier studies of Shuster *et al.* (1988) indicating that a high molecular weight polypeptide in ROS is covalently labeled by this reagent.

Inhibition studies were carried out to determine the binding specificity of the ROS 220 kDa protein for ATP and GTP. As shown in **Fig 25B** both ATP and GTP inhibited 8-azido-[α^{32}P]-ATP labeling. Half-maximum inhibition occurred at a slightly lower GTP concentration (~70 μM) than ATP concentration (~95μM), in general agreement with an earlier study (Shuster *et al.*, 1988). These results further support the view that the ROS 220 kDa protein is an ABC transporter capable of binding both ATP and GTP.

3.10 Hydrolysis Activity of the Nucleotide Binding Domains:

3.10.1 Expression and Purification of Fusion Proteins Containing the NBDs of the Bovine Rod ABC Transporter:

Fragments of the bovine rod ABC transporter containing NBD1 and NBD2, referred to as FNBD1 and FNBD2, respectively, were overexpressed as GST fusion proteins in *E. coli* after induction of the lacZ promoter with IPTG (**Fig 26**). On SDS gels, the FNBD1-GST and FNBD2-GST proteins migrated with apparent molecular masses of 85 kDa and 62 kDa, respectively, values that are in close agreement with their predicted molecular masses. A substantial fraction of each fusion protein was recovered in the soluble fraction after lysis of the bacterial cells. Affinity chromatography on a glutathione-agarose column yielded a FNBD1-GST fusion protein that was estimated to be 26% pure by laser densiotometry and a FNBD2-GST protein that was 17% pure. Low molecular weight proteins could be effectively removed by gel filtration chromatography

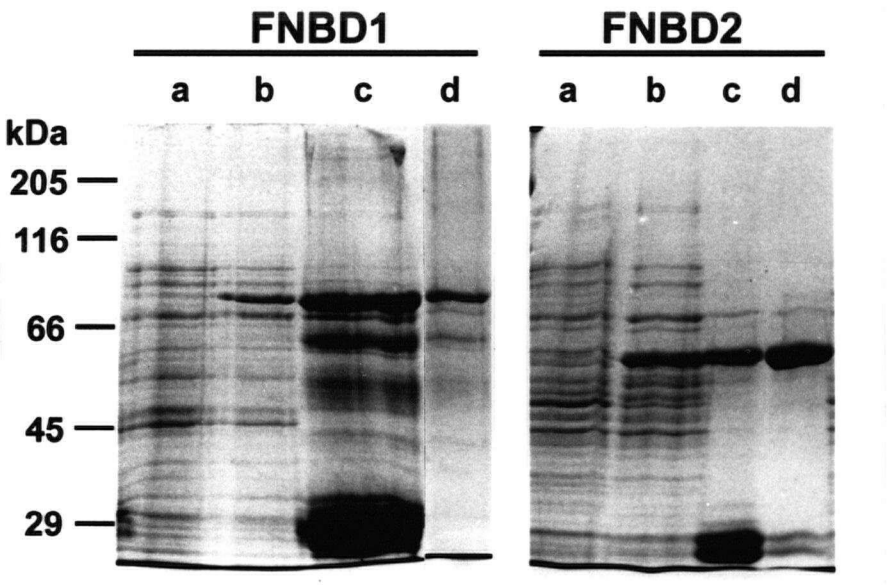

Fig 26. Expression and purification of the FNBD1-GST and FNBD2-GST fusion proteins. *E. coli* transformed with the pGEX vector containing the appropriate insert were induced with IPTG. The cells were lysed in a French press and the supernatant fraction was subjected to affinity chromatography on a glutathione-agarose column and gel filtration chromatography. Samples were analyzed by SDS gel electrophoresis on a 8% polyacrylamide gel. *Lane a*: extract from uninduced cells; *lane b*: extract from IPTG induced cells; l*ane c*: fusion protein purified by glutathione affinity chromatography; and *lane d*: fusion protein purified on a gel filtration column after glutathione affinity chromatography.

resulting in the FNBD1-GST protein that is estimated to be 92% pure and a FNBD2-GST protein that is approximately 80% pure. Removal of these low molecular weight contaminants did not affect the enzymatic activity of the fusion proteins and as a result most enzyme activity measurements were made on the affinity purified fusion proteins.

3.10.2 Nucleotidase Activity of the Fusion Proteins:

The nucleotide hydrolysis activity of the two FNBD1-GST and FNBD2-GST proteins was found to be linear over an initial 60 min. interval and dependent on Mg^{2+} (data not shown). The dependence of activity with nucleotide concentration is illustrated in **Fig 27**. Both fusion proteins were observed to hydrolyze ATP and GTP with similar kinetics (**Table 5**).

The effect of various nucleotide substrates and inhibitors on the ATPase activity of the FNBD2-GST protein was investigated. As shown in **Fig 28**, CTP was hydrolyzed, but significantly less efficiently than either ATP or GTP, and only a background level phosphate release was measured when ADP or cGMP was used as substrate. The nonhydrolyzable nucleotide analogues, ATPγS and GTPγS, were effective inhibitors, whereas ouabain, a specific inhibitor for Na^+/K^+ ATPase, showed no inhibition of the FNBD2-GST ATPase activity. Similar results were obtained for the FNBD1-GST protein (data not shown).

Several studies were also carried out to determine if the FNBD1-GST and FNBD2-GST fusion proteins were capable of interacting with one another. The FNBD2-GST immobilized on Sepharose did not bind the FNBD1-GST fusion protein. Likewise, by far western blotting, the FNBD1-GST fusion protein immobilized on Immobilon membranes following SDS gel electrophoresis did not bind the FNBD2-GST protein when probed with the Rim 3F4 antibody. Finally, no inhibition or stimulation of ATPase activity was observed when the fusion proteins were mixed together.

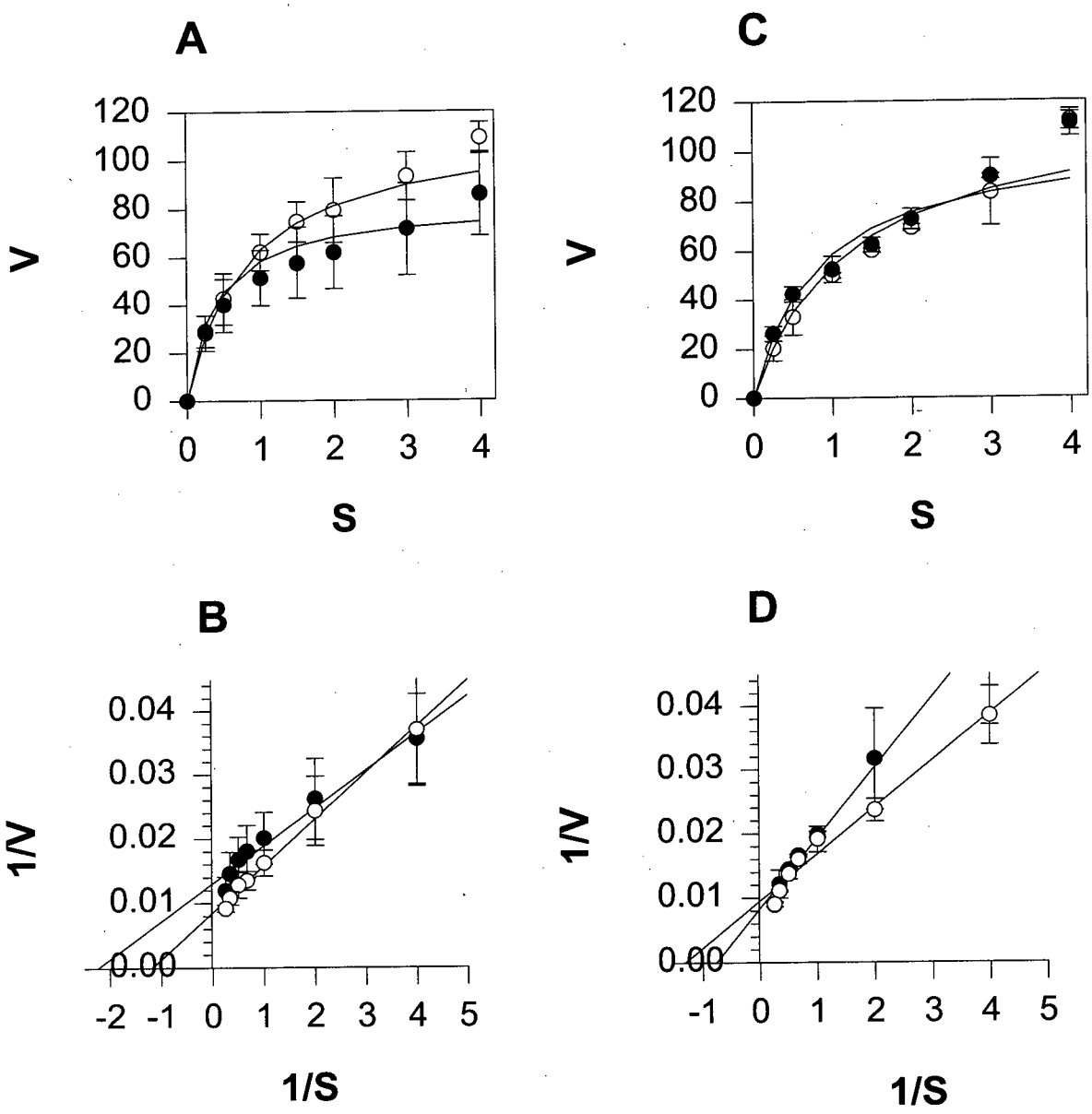

Fig 27. Kinetics of Mg^{2+}-nucleotidase activity for the FNBD1- and the FNBD2-GST fusion proteins. Panel **A&C**, 20 μg of either GST fusion protein was incubated with varying amounts of nucleotide in 50 mM Tris·HCl, pH 8.0, containing 5 mM $MgCl_2$ for 60 min. at 37 °C. Panel **B&D**, Lineweaver Burke double reciprocal plots. -●-, ATP; -○-, GTP; FNBD1-GST, panels **A&B**; FNBD2, panels **C&D**.

TABLE 5

Summary of kinetic data for nucleotidase activity by the two NBD GST fusion proteins. The values were calculated from the axes of the Lineweaver Burke plots in **Fig 27**. There is a fairly high error (10-15%) involved in these calculations as the Fiske-Subbarow phosphate assay was near its lower limit for many of the readings.

	ATP		GTP	
Fusion protein	Km (mM)	Vmax (nmole/ min/mg)	Km (mM)	Vmax (nmole/ min/mg)
N-terminal (FNBD1-GST)	.44 ± .02	80 ± 17	.80 ± .17	125 ± 10
C-terminal (FNBD2-GST)	.97 ± .12	116 ± 13	.75 ± .18	102 ± 19

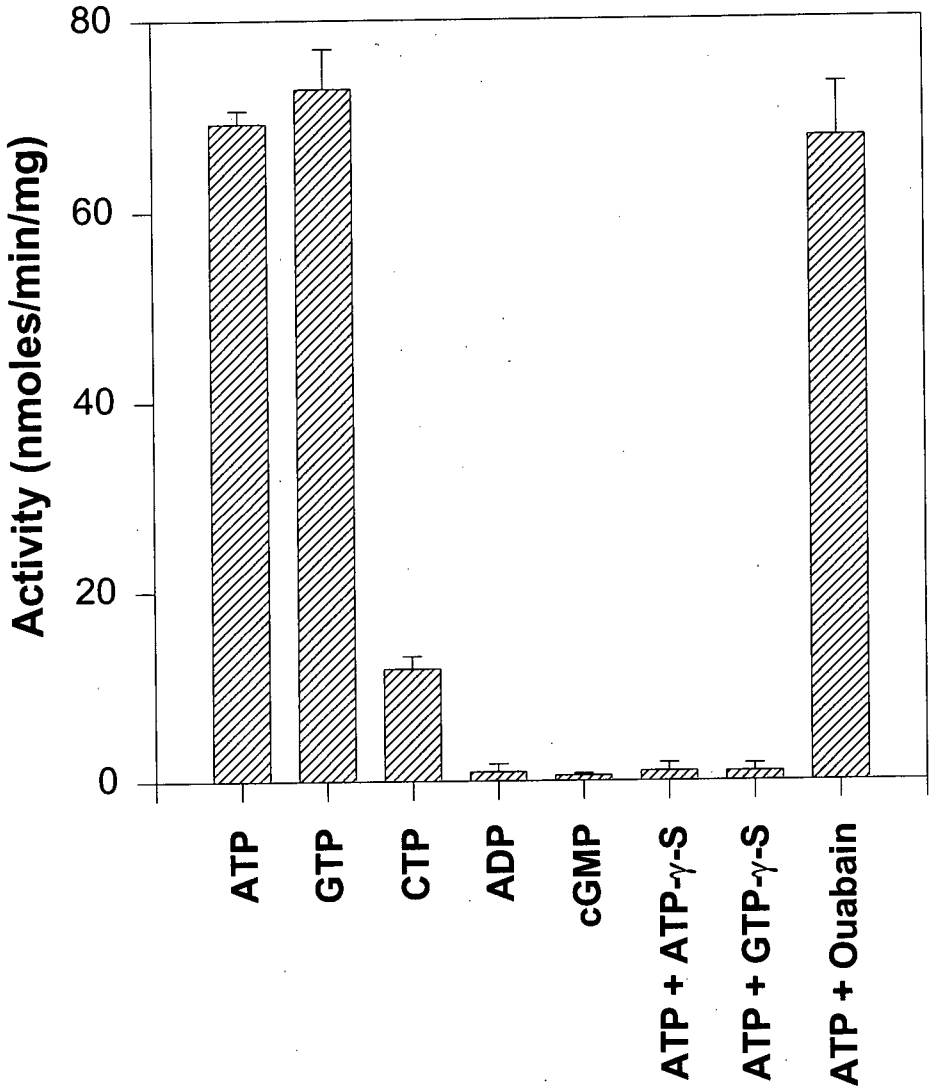

Fig 28. The effect of different substrates and inhibitors on Mg^{2+}-dependent nucleotidase activity of the FNBD2-GST fusion protein. Activity assays were carried out for 60 min. at 37 °C with 2 mM nucleotide (ATP, GTP, CTP, ADP or cGMP) in absence or presence of 2 mM inhibitor (ATPγS, GTPγS, or ouabain) as indicated.

DISCUSSION

4.1 Localization of the 220 kDa Protein to the Rims of the Disks of Rod Photoreceptors:

Although the high molecular weight rim protein had been shown to be a major membrane protein of ROS almost twenty years ago (Papermaster *et al.*, 1978), no detailed studies have been reported on its structural properties since that time. In this study, the bovine ROS 220 kDa glycoprotein has been localized to the rim region and incisures of bovine ROS disk membranes by a combination of immunogold labeling and biochemical techniques. On this basis, this protein is most likely the mammalian homologue of the 290 kDa frog rim protein first reported by Papermaster *et al.* (1978). However, a notable difference in labeling of photoreceptors is apparent. Whereas a polyclonal antibody to the frog rim protein labels both frog rod and cone outer segments (Papermaster *et al.*, 1982), antibodies against the bovine rod protein used in the present study label only outer segments of rod photoreceptors. Recent investigations in human retinas with *in situ* hybridization (Allikmets *et al.*, 1997a) and immunofluorescence labeling (Sun and Nathans, 1997) have also indicated the absence of the rim protein in cone photoreceptors. It appears that either mammalian cone photoreceptors do not express a rim protein, or more likely, the cone rim protein is different from the rod rim protein and may be encoded by a separate gene.

4.2 Purification and Characterization of the 220 kDa Protein:

The Rim 3F4 monoclonal antibody has been used to purify the rim protein from Triton X-100 and CHAPS solubilized ROS in a single step. Analysis of the purified protein by SDS gel electrophoresis indicates that no other intensely stained proteins are present in this preparation. Furthermore, the amino acid composition of the purified rim protein is in close agreement with the composition calculated from its sequence. These

results suggest that the rim protein is composed of a single type of subunit and, at least in detergent solution, is not tightly associated with other proteins in stoichiometric amounts. It remains to be determined if the rim protein exists as a single polypeptide or as a protein complex consisting of several identical subunits.

4.3 Primary Structure of the 220 kDa Protein:

Primary structural analysis indicates that the rim protein is a new member of the superfamily of ABC transporters. Like other eukaryotic ABC transporters (Higgins, 1992), the rod rim protein consists of two structurally related halves, each half consisting of a hydrophobic domain with multiple predicted membrane spanning segments followed by a highly conserved ATP binding cassette. The presence of nucleotide binding sites is consistent with earlier photoaffinity labeling studies (Shuster *et al.*, 1988) and studies carried out here, indicating that the rim protein specifically binds both ATP and GTP with similar affinities. The large size of the rim protein (2280 amino acids; calculated M_r ~257,000) makes this protein one of the largest ABC transporters reported to date.

4.4 Predicted Membrane Topology of the 220 kDa Protein:

Current models of most eukaryotic ATP transporters have twelve transmembrane segments, six in each hydrophobic domain, and both the ATP binding cassettes and the N and C terminus localized on the cytoplasmic side of the membrane (Higgins, 1992). However, a recent model for the structure of MRP predicts the presence of an additional membrane spanning region and an N-terminus that is extracellular (Tusnády *et al.*, 1997; Hipfner *et al.*, 1997), indicating that all the members of the ABC transporter superfamily may not have similar membrane topologies.

At least twelve membrane spanning segments (**Fig 12**) are predicted for the rim protein from hydropathy plots (Kyte and Doolittle, 1982; Eisenberg *et al.*, 1984). The rim protein is glycosylated like other well characterized ABC transporters. However, the

number of N-linked oligosaccharide chains is likely to be small since digestion with endoglycosidase H has only a minor effect on the mobility of the rim protein on SDS gels. Although the site(s) of glycosylation has yet to be determined directly, the inability to detect Asn1586 in peptide #21 by direct peptide sequencing strongly suggests that this residue, which is part of a consensus sequence for N-linked glycosylation, is covalently bound to an oligosaccharide chain. This consensus sequence is conserved in both the human and the mouse orthologues (see next section), providing additional evidence that it is important.

Glycosylation suggests that this segment probably resides on the intradiskal or lumen side of the disk membrane. In addition, removal of the sugar moiety by endoglycosidase H suggests that it has a high mannose content and likely has not been processed in the Golgi. A similar shift is observed when peripherin/rds is treated with endoglycosidase H (Connell and Molday, 1990). When the cDNA for peripherin/rds is heterologously expressed in COS-1 cells, the resultant protein is targeted to the endoplasmic reticulum and not the plasma membrane (Goldberg *et al.*, 1995). Targeting of peripherin/rds to an internal organelle is consistent with its localization in the disk membranes. The co-localization of the 220 kDa protein suggests that its glycosylation would also be immature (or unprocessed by the Golgi). Heterologous expression of the cDNA for the 220 kDa protein may provide more evidence for this argument.

On the basis of these studies, a working model is proposed for the organization of the rim protein in the disk rim membrane as shown in **Fig 29**. A novel aspect of this model is the presence of a large intradiskal loop between each of the first two membrane spanning segments for each half of the protein. Such segments are not predicted in models for other ABC transporters such as P-glycoprotein and CFTR and contribute to the unusually large size of the rim protein relative to most other ABC transporters. Relatively large intradiskal segments are also found in the peripherin/rds and rom-1

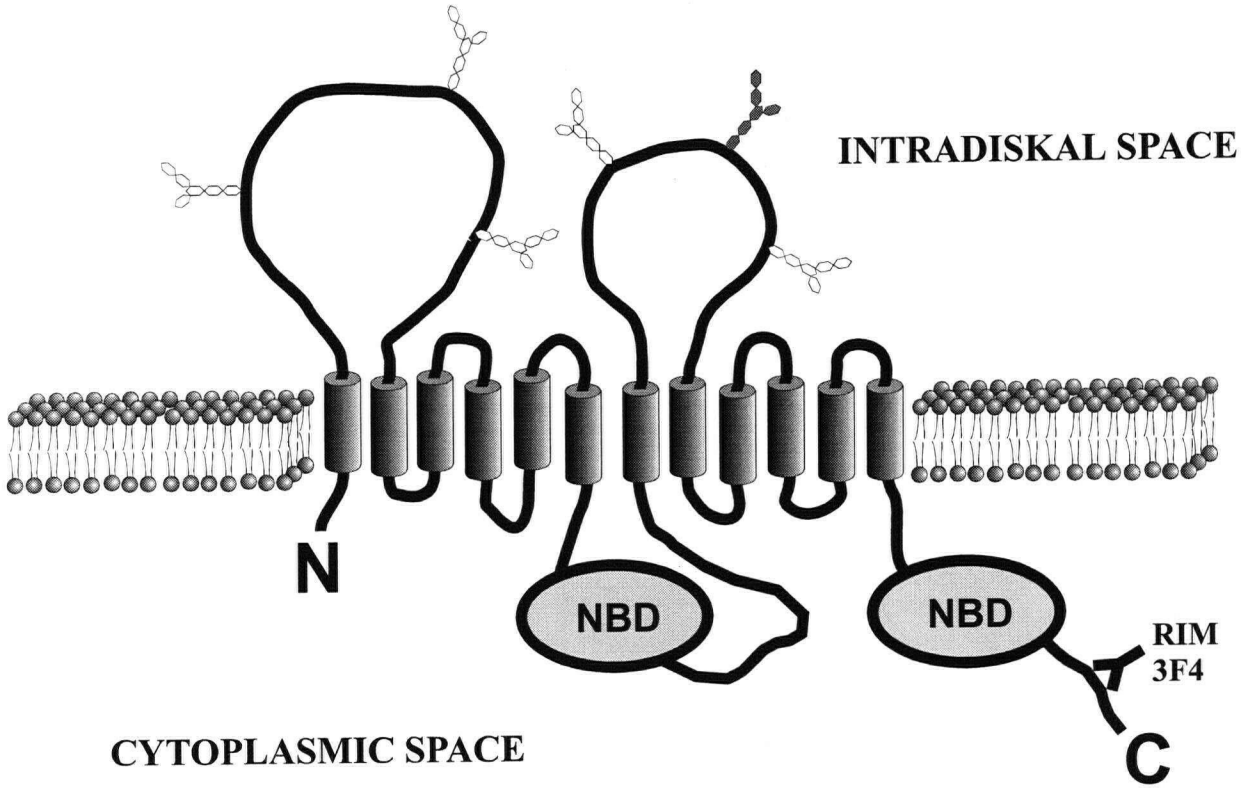

Fig 29. Model for the topological organization of the ROS rim protein in the disk membrane. The model shows twelve transmembrane segments and two nucleotide binding domains (*NBD*) localized on the cytoplasmic side of the membrane. The location of consensus sequences for N-linked glycosylation along the large putative intradiskal loops are indicated by *hexagons*. The site of N-linked glycosylation (Asn1586) predicted from peptide sequencing is represented by *filled hexagons*. The epitope for the Rim 3F4 monoclonal antibody near the C-terminus is indicated.

subunits (Bascom *et al.*, 1992; Connell and Molday, 1990) and have been suggested to be involved in the formation and stabilization of the highly curved rim region of the disk membranes.

4.5 The Bovine Rim Protein is an Orthologue of the Human ABCR *Gene Product Implicated in Stargardt's Disease and Age-Related Macular Degeneration:*

The rod ABC transporter appeared to be a good candidate for a protein which could be involved in human retinal diseases due to its relatively high quantity in the outer segments and its presence in the rims and incisures of the disk membranes. Clones containing the human orthologue of the bovine rod ABC transporter were identified and used to localize the gene to chromosome 1 and specifically sub-band 1p22 (Nasonkin *et al.*, 1997). At the same time, Allikmets and co-workers reported the cloning of a photoreceptor-specific ABC transporter and its implication in autosomal recessive Stargardt's disease (Allikmets *et al.*, 1997a). Comparison of the amino acid sequences of this protein with that of the human rod ABC transporter indicates that they are the same protein. The open reading frame of the human cDNA (Nasonkin *et al.*, 1997) encodes a protein which is 2273 amino acids long and is 90% identical and 94% similar to the predicted bovine amino acid sequence (**Fig 30**). More recently, the mouse orthologue has been cloned (Azarian and Travis, 1997) and also found to display a high degree of similarity to the bovine (87% identical, 92% similar) and human sequences (88% identical and 93% similar; **Fig 30**). Among the three sequences, there is an 85% identity and 91% similarity in the amino acid sequences and nine conserved N-linked glycosylation sites. One of these conserved sites corresponds to Asn1586 of the bovine sequence, providing further evidence for the membrane topology that has been proposed.

Macular dystrophy, a progressive retinal degenerative disease that affects the central or macular region of the retina, is a major cause of blindness in Western civilization. To date only a few genes have been linked to various monogenic forms of

Fig 30. Alignment of the human (H), bovine (B), and mouse (M) rod rim ABC transporter protein sequence. An 85% identity (*colon*) and an additional 6% similarity (*dot*) is observed amongst the three proteins (CLUSTAL program; PC Gene, IntelliGentics, Inc.). Conserved stretches that are possible transmembrane domains (Kyte and Doolittle, 1982; Eisenberg *et al.*, 1984) are indicated by a *single overtype line*. The epitope of the Rim 3F4 monoclonal antibody is shown by an *underline*. The ABC domains are *highlighted in boxes* and the Walker A and B regions and the active transport signature (ATS) are indicated within the ABC domains. Conserved consensus sequences for N-linked glycosylation are marked by an *asterisk* (*). The human sequence is from Nasonkin *et al.* (1997) and the mouse sequence is from Azarian and Travis (1997).

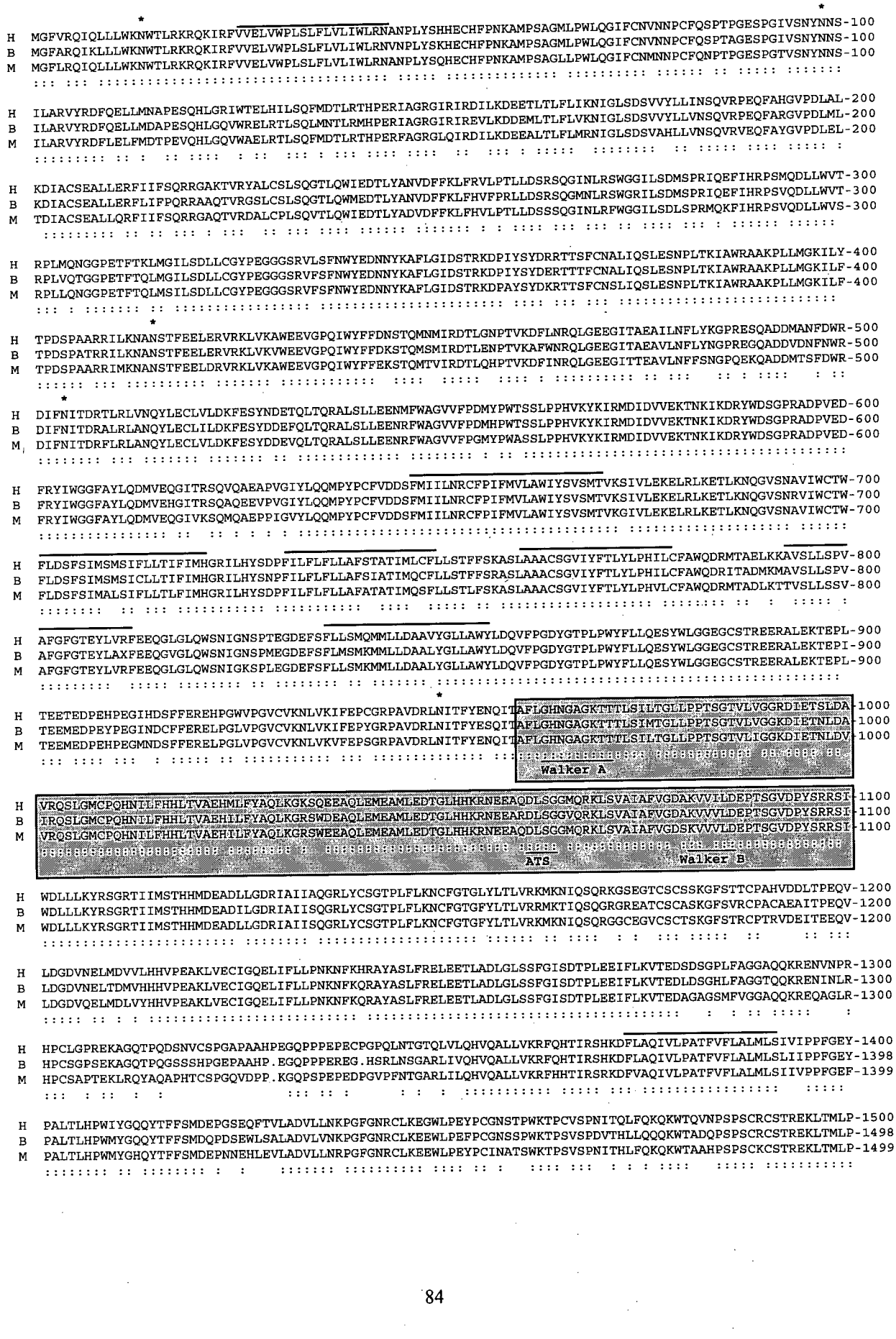
Walker A
ATS
Walker B

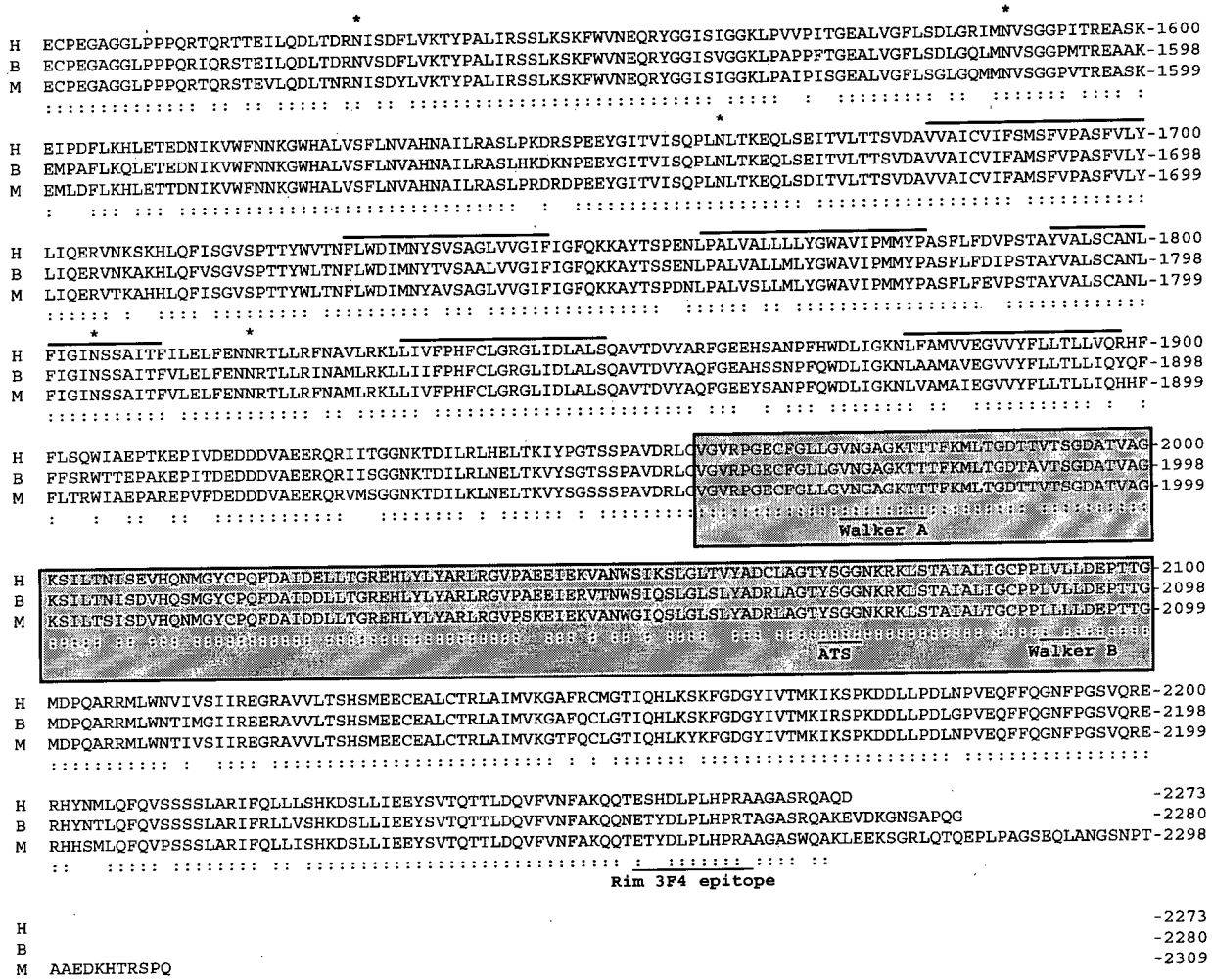
Walker A
ATS
Walker B
Rim 3F4 epitope

this disease. Mutations in the gene for TIMP3, an extracellular tissue inhibitor of metalloproteinases, have been implicated in Sorsby's fundus dystrophy (Weber *et al.*, 1994). Selected mutations in peripherin/rds, a membrane glycoprotein localized to the rim region of rod and cone outer segment disk membranes (Molday *et al.*, 1987), have been linked to various forms of autosomal dominant macular dystrophy including butterfly dystrophy, adult vitelliform macular dystrophy, and fundus flavimaculatus (Nichols *et al.*, 1993; Wells *et al.*, 1993; Weleber *et al.*, 1993). Two studies (Allikmets *et al.*, 1997a; Nasonkin *et al.*, 1997) have now implicated mutations in *ABCR*, the gene encoding the rod ABC transporter, to Stargardt's disease. Therefore, *ABCR* is the second gene encoding a protein expressed exclusively in the outer segments which has been linked to macular degeneration.

Age-related macular degeneration (AMD) is the most common cause of acquired visual impairment in the elderly and shows many of the phenotypes associated with Stargardt's disease. In a recent study, 16% of patients with AMD were found to have a mutation in one copy of *ABCR*, making it a dominant susceptibility locus (Allikmets *et al.*, 1997b). Interestingly, some of these patients had a relative with Stargardt's disease who in addition to the first mutation, had a mutation in their second copy of *ABCR*.

Although the rim protein is expressed in rods, but not cones, mutations in its gene (**Fig 31**) appear to be responsible for two diseases which affect the macular region of the retina where there is an abundance of cone photoreceptors. The reason for this is not yet clear, but is likely linked to its apparent functional activity as a transporter (see section 4.8). Interestingly, the mutations in Stargardt's map primarily to the NBDs while those in AMD are missense mutations lying outside the NBDs (**Fig 31**; Allikmets *et al.*, 1997b). Further comparison of the genotypes and phenotypes of patients with Stargardt's and AMD are needed to determine the significance of this observation.

Fig 31. Model of the human rim ABC transporter. The locations of the mutations identified in Stargardt's disease (Allikmets *et al.*, 1997a, Nasonkin *et al.*, 1997) are shown in *red* while those found in age-related macular degeneration (Allikmets *et al.*, 1997b) are shown in *green*. Mutations occurring in both diseases are shown in *blue*. The model shows twelve transmembrane segments and two nucleotide binding domains (*NBD*) localized on the cytoplasmic side of the membrane. The site of N-linked glycosylation is represented by *filled hexagons*. FS, frame shift mutation.

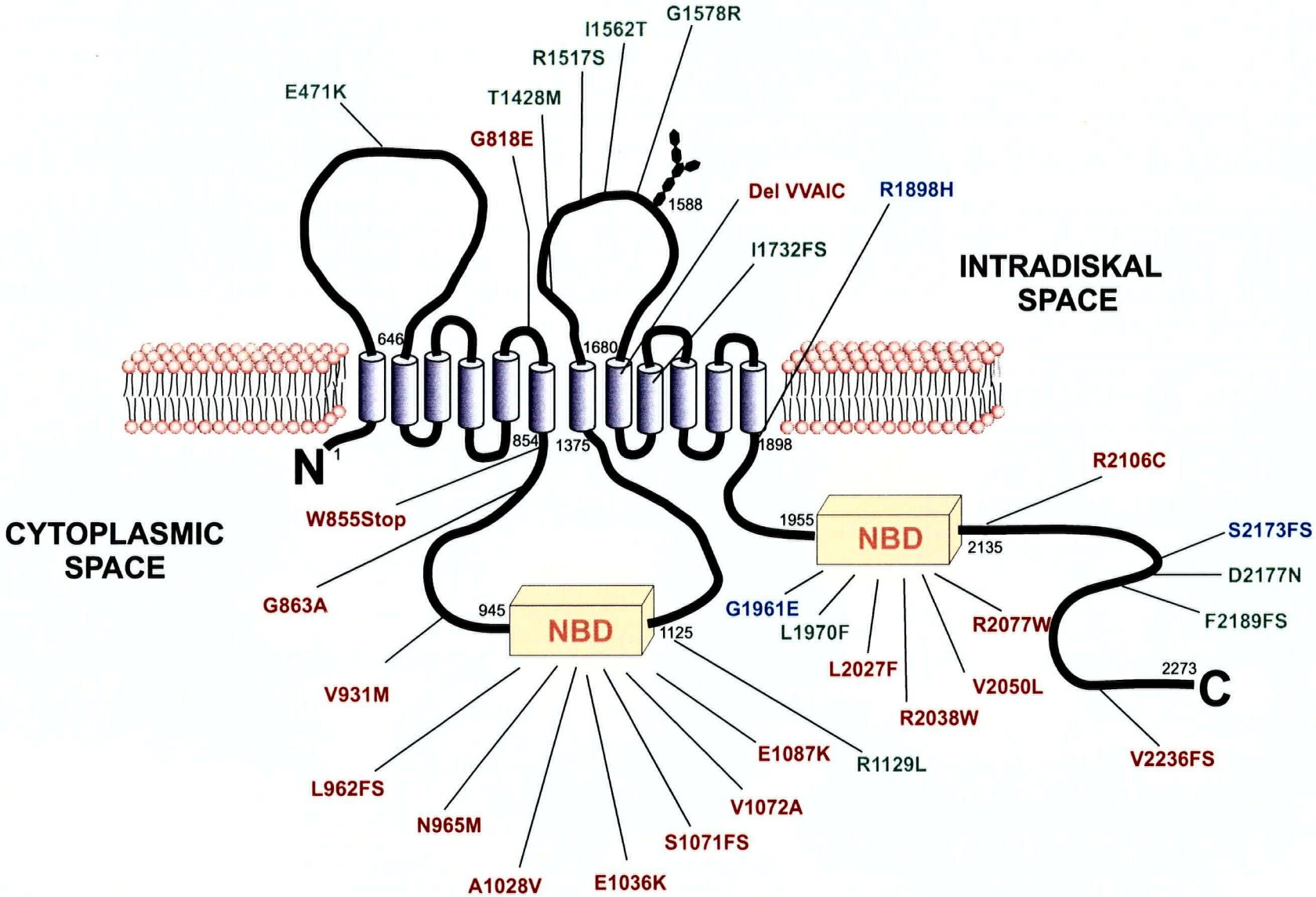
G1578R
I1562T
R1517S
E471K
T1428M
G818E
1588
Del VVAIC
R1898H
I1732FS
INTRADISKAL SPACE
646
1680
854
1375
1898
N
1
CYTOPLASMIC SPACE
W855Stop
R2106C
1955
NBD
2135
S2173FS
D2177N
F2189FS
G863A
945
NBD
1125
G1961E
L1970F
R2077W
L2027F
V2050L
2273
C
V931M
R2038W
E1087K
R1129L
V2236FS
L962FS
V1072A
N965M
S1071FS
A1028V
E1036K

4.6 Relationship of the Rod ABC Transporter to Other ABC Proteins:

The rod rim protein is most closely related to ABC1 and ABC2 transporters of macrophages (Luciani *et al.*, 1994) as shown in the dendrogram comparing the C-terminal NBDs of representative ABC transporters (**Fig 32**). Other related proteins include an ABC-c protein recently cloned from a human medullary thyroid carcinoma cell line (Klugbauer and Hofmann, 1996), the NodI protein involved in nodulation of plant roots by *Rhizobium* (Evans and Downie, 1986), and the YLH4 putative transporter from *Caenorhabditis elegans* (Wilson *et al.*, 1994). The rim protein is more distantly related to MDR1, involved in the active extrusion of drugs from cells (Chen *et al.*, 1986), and CFTR, which functions as a chloride channel and has been linked to cystic fibrosis (Riordan *et al.*, 1989).

4.7 Both Nucleotide Binding Domains of the Bovine Rod ABC Transporter Exhibit Nucleotidase Activity:

As a first step in determining the functional properties of the rod ABC transporter, the two cytoplasmic fragments of the protein, each of which contains one of the NBDs, were expressed as fusion proteins with GST. A significant fraction of both GST-fusion proteins was recovered in the soluble fraction of the cell lysate and exhibited nucleotidase activity after purification, indicating that the NBDs fold into a native-like conformation. The expressed NDBs hydrolyze both ATP and GTP with similar efficiency. This result is consistent with photoaffinity labeling studies which have shown that the rod ABC transporter binds both nucleotides with similar affinities (section 3.9.3; Shuster *et al.*, 1988). In rod outer segments, ATP and GTP are present at similar concentrations (Robinson and Hagins, 1979); therefore, it is possible that both nucleotides may play a role in the putative transport function of the rod ABC transporter.

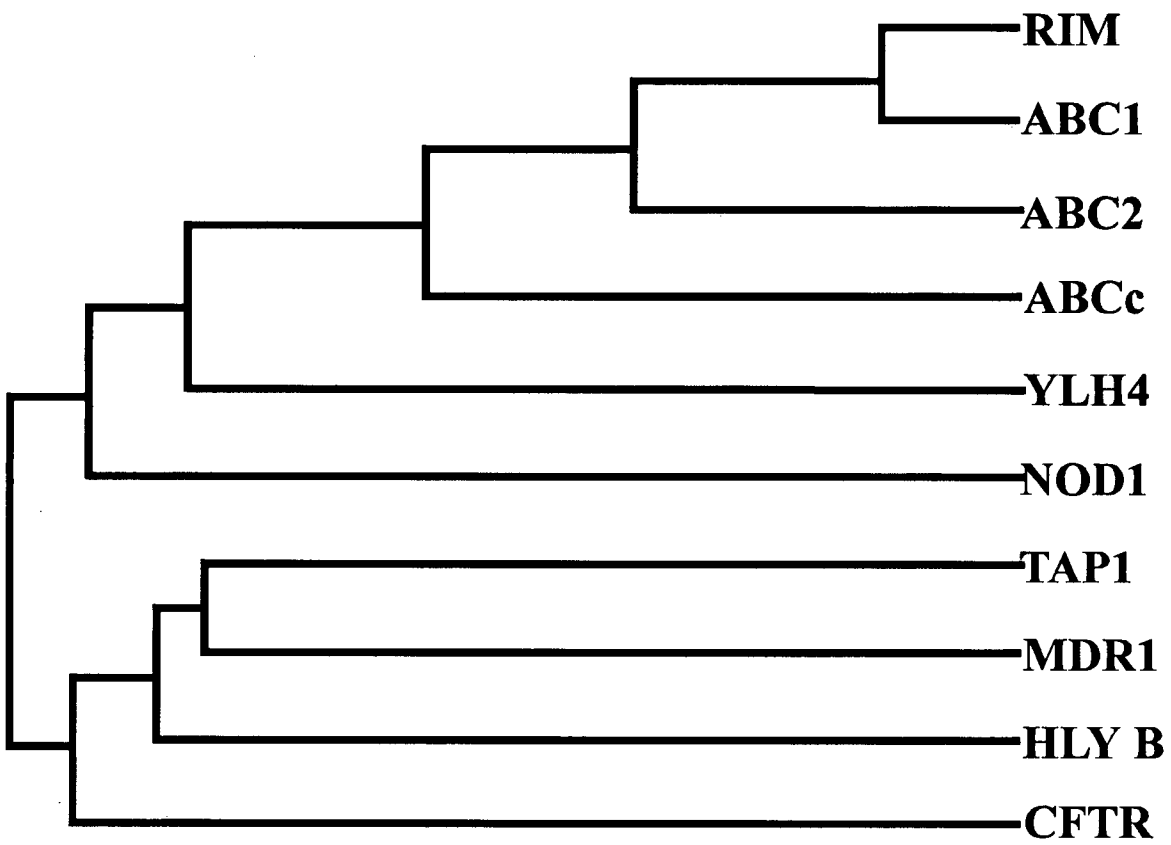

Fig 32. Dendrogram showing the relationship of the ROS rim protein to other ABC transporters. The relationship of the C-terminal ATP-binding cassettes of the proteins was calculated by the unweighted pair group method with arithmetic mean (CLUSTAL program; PC Gene, IntelliGenetics, Inc.). Distances along the horizontal axis are proportional to the differences between the sequences. The following sequences were compared: YLH4, putative ABC transporter in *ced-7* locus of *Caenorhabditis elegans* (Wilson *et al.*, 1994); NODI, involved in root nodulation by *Rhizobium* (Evans and Downie, 1986); TAP1, mouse antigen-processing-associated transporter (Monaco *et al.*, 1990); MDR1, human multi-drug resistance transporter (Chen *et al.*, 1986); HLYB, hemolysin exporter in *E. coli* (Juranka *et al.*, 1992); CFTR, human cystic fibrosis transmembrane conductance regulator (Riordan *et al.*, 1989); ABC1 and ABC2, from a mouse macrophage cell line (Luciani *et al.*, 1994); and ABC-c, from a human medullary thyroid carcinoma cell line (Klugbauer and Hofmann, 1996).

Expression of cytoplasmic NBDs of other members of the ABC transporter superfamily have met with mixed success. The prokaryotic OppF subunit of the oligopeptide permease and MalK from the maltose permease both formed inclusion bodies upon expression; however, after renaturation, MalK was shown to exhibit ATPase activity (Gallagher *et al.*, 1989; Walter *et al.*, 1992). HisP of the histidine permease was soluble when overexpressed with a histidine tag and was able to hydrolyze ATP (Nikaido *et al.*, 1997). Short peptides (67 amino acids long) in the two NBDs of CFTR were soluble and both bound ATP analogs, but did not display nucleotidase activity (Thomas *et al.*, 1991; Ko *et al.*, 1994). However, constructs containing the entire NBD1 (Ko *et al.*, 1993; Ko and Pedersen, 1995) or NBD2 (Randak *et al.*, 1997) of CFTR fused to the maltose binding protein both exhibited ATPase activity. The NBDs of P-glycoprotein have also been expressed in various forms. A C-terminal construct containing NBD2 and fused to maltose binding protein was expressed as a soluble, enzymatically active protein. However, when the same C-terminal construct was expressed with a His-tag, the protein was found in inclusion bodies (Sharma and Rose, 1995). On the other hand, NBD1 of P-glycoprotein was expressed with a His-tag and recovered as a soluble protein with an active ATPase (Dayan *et al.*, 1996). From these studies, cytosolic domains of ABC transporters can generally be expressed as fusion proteins and bind ATP, although the extent of expression as soluble, enzymatically active proteins is dictated by the size of the construct and nature of the fusion partner.

The ATPase activity of several ABC transporters and their expressed NBDs are summarized in **Table 6**. The Km and Vmax values for the NBD1 and NBD2 of the rod ABC transporter are similar to each other and to those measured for the NBDs of CFTR, P-glycoprotein and the maltose and histidine permease. This suggests that the conformation of these NBDs is similar despite considerable differences in amino acid sequence. In the case of CFTR, the activities of the NBDs are also similar to the activity observed for the full-length protein (Li *et al.*, 1996) suggesting that the structure of the

TABLE 6

ATPase activity of ABC transporters and their isolated NBDs.

ABC transporter	NBD1		NBD2		protein[a]			
					-substrate		+substrate	
	Vmax (nmoles/ min/mg)	Km (mM)	Vmax (nmoles/ min/mg)	Km (mM)	Vmax (nmoles/ min/mg)	Km (mM)	Vmax (nmoles/ min/mg)	Km (mM)
Maltose permease[b]	75	ND	—	—	0	ND	860	0.10
Histidine permease[c]	155	0.2	—	—	140	0.6	1-2 $\times 10^3$	0.6
CFTR[d]	30	0.11	~5	0.86	50	1.0	?	?
P-glycoprotein[e]	25	2.1	24	20	1-1.4 $\times 10^3$	0.8-1.4	2-9 $\times 10^3$	0.8-1.4
rod ABC transporter	116	0.97	80	0.44	ND	ND	?	?

[a] activity of the whole transporter;
[b] ref: Walter *et al.*, 1992; Davidson *et al.*, 1992;
[c] ref: Petronilli and Ames, 1991; Lui *et al.*, 1997; Nikaido *et al.*, 1997;
[d] ref: Ko and Pedersen, 1995; Li *et al.*, 1996; Randak *et al.*, 1997;
[e] ref: Dayan *et al.*, 1996; Sharma and Rose, 1995; Al-Shawi and Senior, 1993; Loo and Clarke, 1994; Sarkadi *et al.*, 1992; Shapiro and Ling, 1994,

ND, not determined; ?, unknown substrate

expressed NBDs resemble that of the NBDs contained within the full length protein. The ATPase activity of P-glycoprotein, on the other hand, is about 50 times higher than that of the isolated NBDs (Sarkadi *et al.*, 1992; Al-Shawi and Senior 1993; Loo and Clarke 1994; Shapiro and Ling 1994) suggesting that interactions within the protein greatly affect the activity of the NBD. In coexpression studies using HEK 293 cells, Loo and Clarke (1995) have shown that the two halves of P-glycoprotein interact with each other, both through their NBDs and their membrane spanning domains. In addition, each NBD interacts with its corresponding membrane-spanning domain. In a more recent study, the HisP subunit of the histidine permease was expressed and shown to be active as a dimer (Nikaido *et al.*, 1997). In the present study, interactions between fusion proteins containing the NBD1 and NBD2 of the rod ABC transporter have not been observed. It is possible that interaction and modulation of activity may require coexpression of these domains or expression of constructs containing both the NBDs and the membrane spanning domains. The domains may be forming dimers like HisP and, therefore, are unavailable to interact after purification.

Although photoaffinity labeling studies have shown that the rod ABC transporter binds both ATP and GTP (section 3.9.3; Shuster *et al.*, 1988), the nucleotidase activity of the isolated protein has yet to be systematically measured and the putative substrate transported by this protein has not been identified. It is possible that the nucleotidase activity of the rod ABC transporter may be dependent on the presence of substrate as observed for P-glycoprotein and prokaryotic permeases (**Table 6**). The nucleotidase activity of the rod ABC transporter may provide the energy for the active transport of substrates across the disk membranes.

4.8 Proposed Functions of the Rod ABC Transporter:

The function of the rim protein is not currently known. On the basis of its large size and location along the disk rims, it had been generally believed that this protein

constitutes the filamentous structures that link adjacent disks together and/or connects disks to the plasma membrane (Roof and Heuser, 1982; Corless and Schneider, 1987). The finding that the rim protein is a member of the ABC transporter superfamily makes this less likely. The rim protein, however, could play a role in anchoring such filaments to the disk rim membrane (**Fig 33**).

In a number of cases, ABC transporters have been shown to be involved in the active transport of a variety of hydrophobic molecules across membranes including drugs (Endicott and Ling, 1989), lipids (Hettema *et al.*, 1996), metabolites (Ewart *et al.*, 1994) and peptides (Trowsdale *et al.*, 1990; Powis *et al.*, 1992). The mouse MDR2 and its human counterpart (MDR3) have also been reported to function as a flippase promoting the transfer of phosphotidylcholine from the inner to the outer leaflet of the plasma membranes of hepatocytes (Smit *et al.*, 1993). It is possible that the rim protein may also function in the transport of specific hydrophobic substrates between the cytoplasm and intradiskal side of the disk membrane. Retinal derivatives which are important in phototransduction are hydrophobic and might be considered as possible substrates for translocation into or out of the disk lumen. However, there is no evidence that retinal derivatives accumulate inside the disks or require an active process for transport across cell membranes. Other possible substrates include lipids or peptides which, after translocation to the intradiskal space, may interact with regions of proteins exposed on the lumen side of the disk membrane.

Some ABC transporters have been reported to be involved in morphological processes. The ABC1 protein of mouse macrophage and the *ced-7* protein of *Caenorhabditis elegans* have been implicated in the process of engulfment of cell corpses generated by apoptotic cell death (Ellis *et al.*, 1991; Luciani and Chimini, 1996) and the NodI protein has been linked to the process of *Rhizobium* nodulation in roots (Evans and Downie, 1986). The rod ABC transporter, being more similar in structure to these proteins, may function in the morphogenesis of the rim region of disk membranes.

Fig 33. Model of the membranes and proteins of the rod photoreceptor outer segment. The disk and plasma membranes are indicated as well as the highly structured rim region where the ABC transporter and the peripherin/rds-rom-1 complex (Molday *et al.*, 1987; Bascom *et al.*, 1992) are localized. Disease associated proteins are accompanied by a *box* (STGD, Stargardt's disease; MD, macular dystrophy; ADRP, Autosomal dominant retinitis pigmentosa; ARRP, Autosomal recessive retinitis pigmentosa; LCA1, Leber's congenital amaurosis). Figure modified from R.S. Molday.

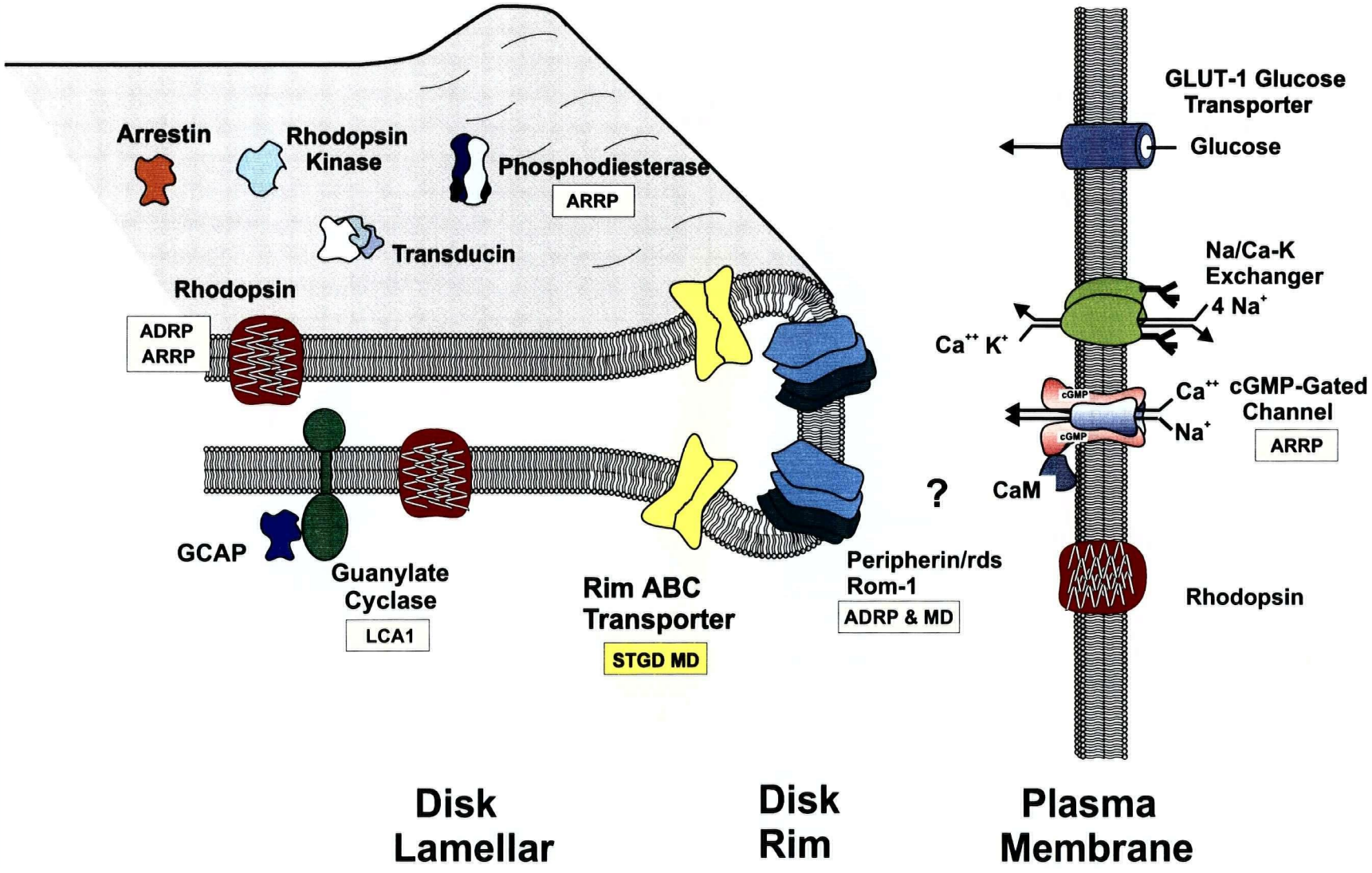
Arrestin
Rhodopsin Kinase
Phosphodiesterase
ARRP
Transducin
Rhodopsin
ADRP
ARRP
GCAP
Guanylate Cyclase
LCA1
Rim ABC Transporter
STGD MD
Peripherin/rds
Rom-1
ADRP & MD
?
CaM
GLUT-1 Glucose Transporter
Glucose
Na/Ca-K Exchanger
4 Na+
Ca++ K+
Ca++ cGMP-Gated Channel
Na+
ARRP
cGMP
cGMP
Rhodopsin
Disk Lamellar
Disk Rim
Plasma Membrane

Both peripherin/rds-rom-1 and the rod ABC transporter are found exclusively at the rims of the disks and are predicted to have large intradiskal loops which may be responsible for the highly curved membrane in this region (**Fig 33**). This curvature may be responsible for the proper alignment of the disks, which is likely important in the transduction and regeneration processes.

A closer examination of the etiology of the diseases in which the rod ABC transporter has been implicated may shed some light on its function. In Stargardt's disease and AMD, a defective rod ABC transporter could lead to an accumulation or deficiency of a substrate required for normal rod outer segment morphogenesis and structure or simply cause a disruption of the structure. The resulting defective rod outer segments could lead to abnormal phagocytosis by the underlying retinal pigment epithelial cells. Clinical features of these diseases including pigmentary deposits and loss in central vision may be a manifestation of the secondary effects on the retinal pigment epithelial cells and cone photoreceptors caused by defective rod ABC transporter activity.

For example, the substrate of the ABC transporter may be one of the derivatives of retinal. There is no evidence that any of the retinal derivatives requires transport; however, it seems unlikely that such an important process would occur solely by diffusion. If the substrate is all-*trans* retinol (*i.e.* after reduction by retinol dehydrogenase), its accumulation in the disk membranes would occur. Initially, diffusion of the retinol would proceed, but slower than normal. Eventually the system would be overwhelmed and cells would begin to die. If all-*trans* retinal is the substrate, another transporter would likely be required to return 11-*cis* retinal to the disk membranes since all of the transporters studied to date transport only in one direction (Higgins, 1992). Accumulation of retinoids would account for the lipofuscin deposits observed in patients.

Fatty acids or lipids may also be the substrate of the ABC transporter. Lipid composition analysis indicates a difference in phospholipid and cholesterol content of the plasma and disk membranes (Boesze-Battaglia and Albert, 1992). The plasma membrane is rich in phosphotidylcholine (65%) and phosphotidylserine (24%) and only 5% of the fatty acids are docasahexanoic acid (22:6). The disks have almost equal amounts of phosphotidylethanolamine (41%) and phosphotidylcholine (45%) and 35% of the fatty acids are docasahexanoic acid. In addition, the cholesterol to phospholipid mole ratio is 0.38 for the plasma and 0.1 for the disk membrane. Studies have indicated that the disk membrane phospholipid content is independent of the age of the disks while the cholesterol phospholipid mole ratio falls from 0.38 to 0.1 as the disks mature (Boesze-Battaglia *et al.*, 1990). It is possible that the ABC transporter is involved in sorting of the phospholipids or in the removal of cholesterol from the disks as they age. Failure to perform either of these tasks could lead to an accumulation of lipids and deposits of lipofuscin observed in patients. Alternatively, the amount of cholesterol in the disks may be a signal for phagocytosis by the RPE; however, disruption of this mechanism would more likely cause immediate and not degenerate damage to the cells.

The time of onset of AMD and Stargardt's disease correlates with the amount of mutant protein. AMD patients have one wild-type copy of the protein and retain vision until much later in life than the Stargardt's patients with no wild-type protein. The cells in the macular region of the retina are more susceptible to this degeneration than those in the periphery. This region is less vascularized than the periphery of the retina, which may indicate that the blood may at least partially compensate for the accumulation or depletion of a substrate. Clearly, more studies are required to determine the role of the rim protein in outer segment structure and function.

4.9 Summary and Future Directions:

In order to identify new proteins which may be involved in human retinal disease, a high molecular weight glycoprotein in the bovine rod outer segment was cloned and characterized. It is a member of the ABC transporter superfamily whose structure consists of a tandem repeat with a multiple membrane-spanning region followed by a cytosolic region containing a nucleotide binding domain. Through immunohistochemistry and biochemical techniques, this ABC transporter has been shown to localize to the rims of the disk membranes in a pattern similar to peripherin/rds-rom-1 and the frog rim protein (Papermaster *et al.*, 1978; Papermaster *et al.*, 1982). The protein has been shown be glycosylated, most likely with one N-linked glycosylation occurring at Asn1586. Based on this result, a topological model for the protein was proposed which predicts a large intradiskal loop in each half of the protein. A large intradiskal loop has also been predicted in models of both peripherin/rds (Connell and Molday, 1990) and rom-1 (Bascom *et al.*, 1992). The co-localization of these proteins to the rims of the disks and the presence of these large intradiskal domains may indicate a role for both of these proteins in the morphology of the disks and a possible role in the structure of the outer segments of photoreceptor cells. The apparent absence of the rod ABC transporter in cone cells may represent one of the morphological differences between the photoreceptor types or may be due to a yet unidentified cone homologue. Animal models of rod ABC transporter knock-outs are currently being developed and may help identify the protein's role in the structure of the photoreceptors.

The human orthologue of the bovine ABC transporter was identical to the recently cloned *ABCR* gene product which has been implicated in Stargardt's disease and AMD (Allikmets *et al.*, 1997a and 1997b). AMD is the most common cause of blindness in elderly people and affects over 11 million North Americans. Mutations associated with Stargardt's disease appear to cluster in the NBDs of the protein, while those responsible for AMD are more likely to be found outside these domains. Mutations in

ABCR have also been linked to fundus flavimaculatus, a disorder clinically similar to Stargardt's disease. There is no clear correlation between the phenotypes of these diseases and the mutations in *ABCR*, making this an area which needs to be studied.

The bovine rod ABC transporter has been shown to bind both ATP and GTP with relatively equal affinity; however, nucleotidase activity has yet to be reported for the whole protein. The expressed NBD1 and NBD2 of the rod ABC transporter exhibit both ATPase and GTPase activity and the ATPase activity is comparable to the activity of the NBDs of other members of the ABC superfamily. Other transporters including P-glycoprotein and the prokaryotic permeases have ATPase activities which are stimulated upon transport of their substrates. Inclusion of the substrate in the assay system may be necessary before nucleotidase activity of the whole rod ABC transporter can be measured.

The nucleotidase activity of the NBDs most likely provides the energy for transport of a substance across the disk membrane and its identification will be the focus of many investigations. The etiology of the diseases associated with this protein indicates that the accumulation or depletion of a substance leads to the degeneration of the photoreceptor cells. Likely candidates to be tested include the retinoids, fatty acids and/or lipids, and other compounds involved in the visual transduction process. The mechanism of substrate transport by the rod ABC transporter may be similar to that proposed for P-glycoprotein ("hydrophobic vacuum cleaner") if its substrate is hydrophobic and partitions into the membrane. Alternatively, the protein may function as a channel whose mechanism is similar to that proposed for CFTR, although channel activity in the disk membranes has not been reported. Sequence comparisons suggest that the rod ABC transporter is less related to P-glycoprotein and CFTR than it is to other ABC transporters. Therefore, identification of the function of the rod ABC transporter will be essential before a mechanism of action can be proposed.

These studies have identified and characterized the bovine rod ABC transporter, a major component of the photoreceptor outer segment, and found it to be the orthologue to the gene product of *ABCR*, implicated in Stargardt's disease and AMD. The present study serves as a basis for beginning to define the role of this protein in rod photoreceptor structure and function and elucidating the molecular basis for how specific mutations in the *ABCR* gene, particularly those in the NBD, lead to either Stargardt's disease or AMD.

REFERENCES

Aebersold, R.H., Leavitt, J., Saavendra, R.A., Hood, L.E., and Kent, S.B.H. (1987) Internal amino acid sequence analysis of proteins separated by one- or two-dimensional gel electrophoresis after *in situ* protease digestion on nitrocellulose. *Proc. Natl. Acad. Sci. USA*. **84**, 6970-6974.

Aguilar-Bryan, L., Nichols, C.G., Wechsler, S.W., Clement, J.P. 4th., Boyd, A.E. 3rd., Gonzalez, G., Herrera-Sosa, H., Nguy, K., Bryan, J., and Nelson, D.A. (1995) Cloning of the beta cell high-affinity sulfonylurea receptor: a regulator of insulin secretion. *Science.* **268,** 423-426.

Allikmets, R., Singh, N., Sun, H., Shroyer, N.F., Hutchinson, A., Chidambaram, A., Gerrard, B., Baird, L., Stauffer, D., Peiffer, A., Rattner, A., Smallwood, P., Li, Y., Anderson, K.L., Lewis, R.A., Nathans, J., Leppert, M., Dean, M., and Lupski, J.R. (1997a) A photoreceptor cell-specific ATP-binding transporter gene (*ABCR*) is mutated in recessive Stargardt macular dystrophy. *Nature Genet.* **15,** 236-246.

Allikmets, R., Shroyer, N.F., Singh, N., Seddon, J.M., Lewis, R.A., Bernstein, P.S., Peiffer, A., Zabriskie, N.A., Li, Y.X., Hutchinson, A., Dean, M., Lupski, J.R., and Leppert, M. (1997b) Mutation of the Stargardt-disease gene (*ABCR*) in age-related macular degeneration. *Science.* **277,** 1805-1807.

Al-Shawi, M.K. and Senior, A.E. (1993) Characterization of the adenosine triphosphatase activity of Chinese hamster P-glycoprotein. *J. Biol. Chem.* **268**, 4197-4206.

Anderson, M.P., Berger, H.A., Rich, D.P., Gregory, R.J., Smith, A.E., and Welsh, M.J. (1991) Nucleoside triphosphates are required to open the CFTR chloride channel. *Cell.* **67,** 775-784.

Ausubel, F., Brent, R., Kingston, R.E., Moore, D.D. Serdwan, J.G., Smith, J.A., and Struhl, K. eds. (1994) Current protocols in molecular biology. John Wiley & Sons, Inc., New York.

Azarian, S.M. and Travis, G.H. (1997) The photoreceptor rim protein is an ABC transporter encoded by the gene for recessive Stargardt's disease (*ABCR*). *FEBS Lett.* **409,** 247-252.

Bascom, R.A., Manara, S., Collins, L., Molday, R.S., Kalnins, V.I., and McInnes, R.R. (1992) Cloning of the cDNA for a novel photoreceptor membrane protein (rom-1) identifies a disk rim protein family implicated in human retinopathies. *Neuron.* **8**, 1171-1184.

Beaudet, L. and Gros, P. (1995) Functional dissection of P-glycoprotein nucleotide-binding domains in chimeric and mutant proteins. Modulation of drug resistance profiles. *J. Biol. Chem.* **270,** 17159-17170.

Benton, W.D. and Davis, R.W. (1977) Screening λgt recombinant clones by hybridization to single plaques *in situ*. *Science.* **196,** 180-182.

Birnbach, C.D., Järveläinen, M., Possin, D.E., and Milam, A.H. (1994) Histopathology and immunocytochemistry of the neurosensory retina in fundus flavimaculatus. *Ophthalmol.* **101**, 1211-1219.

Boesze-Battaglia, K. and Albert, A.D. (1992) Phospholipid distribution among bovine rod outer segment plasma membrane and disk membranes. *Exp. Eye Res.* **54,** 821-823.

Boesze-Battaglia, K., Fliesler, S.J., and Albert, A.D. (1990) Relationship of cholesterol content to spatial distribution and age of disc membranes in retinal rod outer segments. *J. Biol. Chem.* **265**, 18867-18870.

Bok, D. (1993) The retinal pigment epithelium: a versatile partner in vision. *J. Cell Sci.* **17**, 189-195.

Bönigk, W., Altenhofen, W., Müller, F., Dosé, A., Illing, M. Molday, R.S., and Kaupp, U.B. (1993) Rod and cone photoreceptor cells express distinct genes for cGMP-gated channels. *Neuron.* **10,** 865-877.

Burton, M.D., Onstott, L.T. and Polans, A.S. (1989) The use of gold reagents to quantitate antibodies eluted from nitrocellulose blots: application to electron microscopic immunocytochemistry. *Anal. Biochem.* **183**, 225-230.

Chen, C.J., Chin, J.E., Ueda, K., Clark, D.P. Pastan, I., Gottesman, M.M., and Roninson, I.B. (1986) Internal duplication and homology with bacterial transport proteins in the MDR1 (P-glycoprotein) gene from multidrug-resistant human cells. *Cell.* **47**, 381-389.

Chen, C.K., Wieland, T., and Simon, M.I. (1996) RGS-r, a retinal specific RGS protein, binds an intermediate conformation of transducin and enhances recycling. *Proc. Natl. Acad. Sci. USA.* **93**, 12885-12889.

Chirgwin, J.M., Przybyla, A.E., MacDonald, R.J., and Rutter, W.J. (1979) Isolation of biologically active ribonucleic acid from sources enriched in ribonuclease. *Biochemistry.* **18,** 5294-5299.

Cole, S.P., Bhardwaj, G., Gerlach, J.H., Mackie, J.E., Grant, C.E., Almquist, K.C., Stewart A.J., Kurz, E.U., Duncan, A.M., and Deeley, R.G. (1992) Overexpression of a transporter gene in a multidrug-resistant human lung cancer cell line. *Science.* **258**, 1650-1654.

Connell, G.J. and Molday, R.S. (1990) Molecular cloning, primary structure, and orientation of the vertebrate photoreceptor cell protein peripherin in the rod outer segment disk membrane. *Biochemistry.* **29**, 4691-4698.

Converse, C.A. (1979) The large intrinsic membrane protein in rod outer segments: in vitro synthesis in cattle, and comparison in humans and rabbits. *Exp. Eye Res.* **29**, 409-416.

Cook, N.J., Hanke, W., and Kaupp, U.B. (1987) Identification, purification, and functional reconstitution of the cyclic GMP-dependent channel from rod photoreceptors. *Proc. Natl. Acad. Sci. USA.* **84**, 585-589.

Cook, N.J., Molday, L.L., Reid, D., Kaupp, U.B., and Molday, R.S. (1989) The cGMP-gated channel of bovine rod photoreceptors is localized exclusively in the plasma membrane. *J. Biol. Chem.* **264**, 6996-6999.

Corless, J.M. and Schneider, T.G. (1987) Patterns of interdisk connections within the lamellar domains of retinal rod outer segment disks: observations relevant to the axial propagation of incisures. *Exp. Eye. Res.* **45**, 883-905.

Cuatrecasas, P. (1970) Protein purification by affinity chromatography. Derivatizations of agarose and polyacrylamide beads. *J. Biol. Chem.* **245**, 3059-3065.

Davidson, A.L., Shuman, H.A., and Nikaido, H. (1992) Mechanism of maltose transport in *Escherichia coli*: transmembrane signaling by periplasmic binding proteins. *Proc. Natl. Acad. Sci. USA.* **89**, 2360-2364.

Dayan, G., Baubichon-Cortay, H., Jault, J.-M., Cortay, J.-C., Deléage, G., and Di Pietro, A. (1996) Recombinant N-terminal nucleotide-binding domain from mouse P-glycoprotein. Overexpression, purification, and role of cysteine 430. *J. Biol. Chem.* **271**, 11652-11658.

Dizhoor, A.M., Olshevskaya, E.V., Henzel, W.J., Wong, S.C., Stults, J.T., Ankoudinova, I., and Hurley, J.B. (1995) Cloning, sequencing, and expression of a 24-kDa Ca^{2+}-binding protein activating photoreceptor guanylyl cyclase. *J. Biol. Chem.* **270**, 25200-25206.

Doige, C.A. and Ames, G.F. (1993) ATP-dependent transport systems in bacteria and humans: relevance to cystic fibrosis and multidrug resistance. *Ann. Rev. Micro.* **47**, 291-319.

Dosé, A.C. (1995) Molecular characterization of the cyclic nucleotide-gated cation channel of bovine rod outer segments. *PHd thesis*. University of British Columbia.

Dryja, T.P., Finn, J.T., Peng, Y.W., McGee, T.L., Berson, E.L., and Yau, K.W. (1995) Mutations in the gene encoding the alpha subunit of the rod cGMP-gated channel in autosomal recessive retinitis pigmentosa. *Proc. Natl. Acad. Sci. USA.* **92**, 10177-10181.

Dryja, T.P., Hahn, L.B., Cowley, G.S., McGee, T.L., and Berson, E.L. (1991) Mutation spectrum of the rhodopsin gene among patients with autosomal dominant retinitis pigmentosa. *Proc. Natl. Acad. Sci. USA.* **88**, 9370-9374.

Dryja, T.P., McGee, T.L., Reichel, E., Hahn, L.B., Cowley, G.S., Yandell, D.W., Sandberg, M.A., and Berson, E.L. (1990) A point mutation of the rhodopsin gene in one form of retinitis pigmentosa. *Nature.* **343**, 364-366.

Eisenberg, D., Schwarz, E., Komaromy, M., and Wall, R. (1984) Analysis of membrane and surface protein sequences with the hydrophobic moment plot. *J. Mol. Biol.* **179**, 125-142.

Ellis, R.E., Jacobson, D.M., and Horvitz, H.R. (1991) Genes required for the engulfment of cell corpses during programmed cell death in *Caenorhabditis elegans*. *Genetics.* **129**, 79-94.

Endicott, J.A. and Ling, V. (1989) The biochemistry of P-glycoprotein-mediated multidrug resistance. *Annu. Rev. Biochem.* **58**, 137-171.

Evans, I.J. and Downie, J.A. (1986) The nodI gene product of *Rhizobium leguminosarum* is closely related to ATP-binding bacterial transport proteins; nucleotide sequence analysis of the nodI and nodJ genes. *Gene.* **43**, 95-101.

Ewart, G.D., Cannell, D., Cox, G.B. and Howells, A.J. (1994) Mutational analysis of the traffic ATPase (ABC) transporters involved in uptake of eye pigment precursors in *Drosophila melanogaster*. Implications for structure-function relationships. *J. Biol. Chem.* **269**, 10370-10377.

Farrar, G.J., Kenna, P., Jordan, S.A., Kumar-Singh, R., Humphries, M.M., Sharp, E.M., Sheils, D.M., and Humphries, P. (1991) A three-base-pair deletion in the peripherin-RDS gene in one form of retinitis pigmentosa. *Nature.* **354,** 478-480.

Faurobert, E. and Hurley, J.B. (1997) The core domain of a new retina specific RGS protein stimulates the GTPase activity of transducin *in vitro*. *Proc. Natl. Acad. Sci. USA.* **94,** 2945-2950.

Fiske C.H. and Subarrow, Y. (1925) The colorimetric determination of phosphorous. *J. Biol. Chem.* **66**, 375-400.

Fung, B.K., Hurley, J.B., and Stryer, L. (1981) Flow of information in the light-triggered cyclic nucleotide cascade of vision. *Proc. Natl. Acad. Sci. USA.* **78,** 152-156.

Galfre, G., Milstein, C., and Wright, B. (1979) Rat x rat hybrid myelomas and a monoclonal anti-Fd portion of mouse IgG. *Nature.* **277**, 131-133.

Gallagher, M.P., Pearce, S.R., and Higgins, C.F. (1989) Identification and localization of the membrane-associated, ATP-binding subunit of the oligopeptidepermease of *Salmonella typhimurium*. *Eur. J. Biochem.* **180**, 133-141.

Goding J.W. ed. (1986) Monoclonal Antibodies. Principals and Practice. 2nd ed. Academic Press, London.

Goldberg, A.F. and Molday, R.S. (1996) Subunit composition of the peripherin/rds-rom-1 disk rim complex from rod photoreceptors: hydrodynamic evidence for a tetrameric quaternary structure. *Biochemistry.* **35**, 6144-6149.

Goldberg, A.F., Moritz, O.L., and Molday, R.S. (1995) Heterologous expression of photoreceptor peripherin/rds and Rom-1 in COS-1 cells: assembly, interactions, and localization of multisubunit complexes. *Biochemistry.* **34**, 14213-14219.

Gray-Keller, M.P., Polans, A.S., Palczewski, K., and Detwiler, P.B. (1993) The effect of recoverin-like calcium-binding proteins on the photoresponse of retinal rods. *Neuron.* **10,** 523-531.

Gros, P., Dhir, R., Croop, J., and Talbot, F. (1991) A single amino acid substitution strongly modulates the activity and substrate specificity of the mouse mdr1 and mdr3 drug efflux pumps. *Proc. Natl. Acad. Sci. USA.* **88,** 7289-7293.

Grunstein, M. and Hogness, D.S. (1975) Colony hybridization: A method for the isolation of cloned cDNAs that contain a specific gene. *Proc. Natl. Acad. Sci. USA*. **72**, 3961-3965.

Hartman, J., Huang, Z., Rado, T.A., Peng, S., Jilling, T., Muccio, D.D., and Sorscher, E.J. (1992) Recombinant synthesis, purification, and nucleotide binding characteristics of the first nucleotide binding domain of the cystic fibrosis gene product. *J. Biol. Chem.* **267**, 6455-6458.

Helfman, D.M., Feramisco, J.R., Fiddes, J.C., Thomas, G.P., and Hughes, S.H. (1983) Identification of clones that encode chicken tropomyosin by direct immunological screening of a cDNA expression library. *Proc. Natl. Acad. Sci. USA*. **80**, 31-35.

Hettema, E.H., van Roermund, C.W., Distel, B., van den Berg, M., Vilela, C., Rodrigues-Pousada, C., Wanders, R.J. and Tabak, H.F. (1996) The ABC transporter proteins Pat1 and Pat2 are required for import of long-chain fatty acids into peroxisomes of *Saccharomyces cerevisiae*. *EMBO J.* **15**, 3813-3822.

Higgins, C.F. (1992) ABC transporters: from microorganisms to man. *Ann. Rev. Cell Biol.* **8**, 67-113.

Higgins, C.F., Hiles, I.D., Salmond, G.P., Gill, D.R., Downie, J.A., Evans, I.J., Holland, I.B., Gray, L., Buckel, S.D., Bell, A.W., and Hermodson, M.A. (1986) A family of related ATP-binding subunits coupled to many distinct biological processes in bacteria. *Nature*. **323**, 448-450.

Hipfner, D.R., Almquist, K.C., Leslie, E.M., Gerlach, J.H., Grant, C,E., Deeley, R.G., and Cole, S.P.C. (1997) Membrane topology of the multidrug resistance protein (MRP) - a study of glycosylation-site mutants reveals an extracytosolic NH2 terminus. *J. Biol. Chem.* **272**, 23623-23630.

Hsu, S-C. and Molday, R.S. (1991) Glycolytic enzymes and a GLUT-1 glucose transporter in the outer segments of rod and cone photoreceptor cells. *J. Biol. Chem.* **266**, 21745-21752.

Hsu, Y.T. and Molday, R.S. (1993) Modulation of the cGMP-gated channel of rod photoreceptor cells by calmodulin. *Nature*. **361**, 76-79.

Huang, S.H., Pittler, S.J., Huang, X., Oliveira, L., Berson, E.L., and Dryja, T.P. (1995) Autosomal recessive retinitis pigmentosa caused by mutations in the alpha subunit of rod cGMP phosphodiesterase. *Nature Genet.* **11**, 468-471.

Hughes, A.L. (1994) Evolution of the ATP-binding cassette transmembrane transporters of vertebrates. *Mol. Biol. Evol.* **11**, 899-910.

Hurwitz, R.L., Bunt-Milam, A.H., Chang, M.L., and Beavo, J.A. (1985) cGMP phosphodiesterase in rod and cone outer segments of the retina. *J. Biol. Chem.* **260**, 568-573.

Hyde, S.C., Emsley, P., Hartshorn, M.J., Mimmack, M.M., Gileadi, U., Pearce, S.R., Gallagher, M.P., Gill, D.R., Hubbard, R.E., and Higgins, C.F. (1990) Structural model of ATP-binding proteins associated with cystic fibrosis, multidrug resistance and bacterial transport. *Nature.* **346**, 362-365.

Illing, M., Molday, L.L., and Molday, R.S. (1997) The 220-kDa rim protein of retinal rod outer segments is a member of the ABC transporter superfamily. *J. Biol. Chem.* **272**, 10303-10310.

Juranka, P., Zhang, F., Kulpa, J., Endicott, J.A., Blight, M., Holland, I.B., and Ling, V. (1992) Characterization of the hemolysin transporter, HlyB, using an epitope insertion. *J. Biol. Chem.* **267**, 3764-3770.

Kajiwara, K., Berson, E.L., and Dryja, T.P. (1994) Digenic retinitis pigmentosa due to mutations at the unlinked peripherin/RDS and ROM1 loci. *Science.* **264,** 1604-1608.

Kajiwara, K., Hahn, L.B., Mukai, S., Travis, G.H., Berson, E.L., and Dryja, T.P. (1991) Mutations in the human retinal degeneration slow gene in autosomal dominant retinitis pigmentosa. *Nature.* **354**, 480-483.

Kaplan, J. Gerber, S., Larget-Piet, D., Rozet, J.M., Dollfus, H., Dufier, J.L., Odent, S., Postel-Vinay, A., Janin, N., Briard, M.L., Frézal, J., and Munnich, A. (1993) A gene for Stargardt's disease (fundus flavimaculatus) maps to the short arm of chromosome 1. *Nature Genet.* **5,** 308-311.

Keen, T.J., Inglehearn, C.F., Lester, D.H., Bashir, R., Jay, M., Bird, A.C., Jay, B., and Bhattacharya, S.S. (1991) Autosomal dominant retinitis pigmentosa: four new mutations in rhodopsin, one of them in the retinal attachment site. *Genomics.* **11,** 199-205.

Klugbauer, N. and Hofmann, F. (1996) Primary structure of a novel ABC transporter with a chromosomal localization on the band encoding the multidrug resistance-associated protein. *FEBS Lett.* **391**, 61-65.

Ko, Y.H. and Pedersen, P.L. (1995) The cystic fibrosis transmembrane conductance regulator. Nucleotide binding to a synthetic peptide segment from the second predicted nucleotide binding fold. *J. Biol. Chem.* **270**, 22093-22096.

Ko, Y.H., Thomas, P.J., Delannoy, M.R., and Pedersen, P.L. (1993) The cystic fibrosis transmembrane conductance regulator. Overexpression, purification, and characterization of wild type and delta F508 mutant forms of the first nucleotide binding fold in fusion with the maltose-binding protein. *J. Biol. Chem.* **268**, 24330-24338.

Ko, Y.H., Thomas, P.J., and Pedersen, P.L. (1994) The cystic fibrosis transmembrane conductance regulator. Nucleotide binding to a synthetic peptide segment from the second predicted nucleotide binding fold. *J. Biol. Chem.* **269,** 14584-14588.

Koch, K.W. (1995) Control of photoreceptor proteins by Ca^{2+}. *Cell Calcium.* **18**, 314-321.

Kolb, H. (1994) The architecture of functional neural circuits in the vertebrate retina. *Inves. Ophth. Vis. Sci.* **35**, 2385-2404.

Körschen, H.G., Illing, M., Seifert, R., Sesti, F., Williams, A., Gotzes, S., Colville, C., Muller, F., Dosé, A., Molday. L.L., Godde, M., Molday, R.S. and Kaupp, U.B. (1995) A 240 kDa protein represents the complete beta subunit of the cyclic nucleotide-gated channel from rod photoreceptor. *Neuron.* **15**, 627-636.

Kozak, M. (1991) An analysis of vertebrate mRNA sequences: intimations of translational control. *J. Cell. Biol.* **115**, 887-903.

Kyte, J. and Doolittle, R.F. (1982) A simple method for displaying the hydropathic character of a protein. *J. Mol. Biol.* **157,** 105-132.

Laemmli, U.K. (1970) Cleavage of structural proteins during the assembly of the head of bacteriophage T4. *Nature.* **227,** 680-685.

Lerea, C.L., Somers, D.E., Hurley, J.B., Klock, I.B., and Bunt-Milam, A.H. (1986) Identification of specific transducin alpha subunits in retinal rod and cone photoreceptors. *Science.* **234**, 77-80.

Lewis, G.P., Erickson, P.A., Anderson, D.H., and Fisher, S.K. (1991) Opsin distribution and protein incorporation in photoreceptors after experimental retinal detachment. *Exp. Eye Res.* **53**, 629-640.

Li, C., Ramjeesingh, M., Wang, W., Garami, E., Hewryk, M., Lee, D., Rommens, J.M., Galley, K., and Bear, C.E. (1996) ATPase activity of the cystic fibrosis transmembrane conductance regulator. *J. Biol. Chem.* **271**, 28463-28468.

Liu, C.E., Liu, P.Q., and Ames, G.F.-L. (1997) Characterization of the adenosine triphosphatase activity of the periplasmic histidine permease, a traffic ATPase (ABC transporter). *J. Biol. Chem.* **272,** 21883-21891.

Liu, X., Seno, K., Nishizawa, Y., Hayashi, F., Yamazaki, A., Matsumoto, H., Wakabayashi, and Usukura, J. (1994) Ultrastructural localization of retinal guanylate cyclase in human and monkey retinas. *Exp. Eye Res.* **59**, 761-768.

Loo, T.W. and Clarke, D.M. (1994) Reconstitution of drug-stimulated ATPase activity following co-expression of each half of human P-glycoprotein as separate polypeptides. *J. Biol. Chem.* **269**, 7750-7755.

Loo, T.W. and Clarke, D.M. (1995) P-glycoprotein. Associations between domains and between domains and molecular chaperones. *J. Biol. Chem.* **270,** 21839-21844.

Loo, T.W. and Clarke, D.M. (1996) Mutational analysis of the predicted first transmembrane segment of each homologous half of human P-glycoprotein suggests that they are symmetrically arranged in the membrane. *J. Biol. Chem.* **271,** 15414-15419.

Lowe, D.G., Dizhoor, A.M., Liu, K., Gu, Q., Spencer, M., Laura, R., Lu, L., and Hurley, J.B. (1995) Cloning and expression of a second photoreceptor-specific membrane retina guanylyl cyclase (RetGC), RetGC-2. *Proc. Natl. Acad. Sci. USA*. **92,** 5535-5539.

Luciani, M-F. and Chimini, G. (1996) The ATP binding cassette transporter ABC1, is required for the engulfment of corpses generated by apoptotic cell death. *EMBO J.* **15**, 226-235.

Luciani, M-F., Denizot, F., Savary, S., Mattei, M.G., and Chimini, G. (1994) Cloning of two novel ABC transporters mapping on human chromosome 9. *Genomics* **21**, 150-159.

Ma, J., Zhao, J., Drumm, M.L., Xie, J., and Davis, P.B. (1997) Function of the R domain in the cystic fibrosis transmembrane conductance regulator chloride channel. *J. Biol. Chem.* **272**, 28133-28141.

MacKenzie, D. and Molday, R.S. (1982) Organization of rhodopsin and a high molecular weight glycoprotein in rod photoreceptor disc membranes using monoclonal antibodies. *J. Biol. Chem.* **257**, 7100-7105.

Massey, S.C. and Maguire, G. (1995) The role of glutamate in retinal circuitry. Excitory amino acids and synaptic transmission. 2nd ed. Academic Press, London.

McGrath, J.P. and Varshavsky, A. (1989) The yeast STE6 gene encodes a homologue of the mammalian multidrug resistance P-glycoprotein. *Nature.* **340,** 400-404.

McLaughlin, M.E., Sandberg, M.A., Berson, E.L., and Dryja, T.P. (1993) Recessive mutations in the gene encoding the beta-subunit of rod phosphodiesterase in patients with retinitis pigmentosa. *Nature Genet.* **4,** 130-134.

Meindl, A., Dry, K., Herrmann, K., Manson, F., Ciccodicola, A., Edgar, A., Carvalho, M.R., Achatz, H., Hellebrand, H., Lennon, A., Migliaccio, C., Porter, K., Zrenner, E., Bird, A., Jay, M., Lorenz, B., Wittwer, B., D'Urso, M., Meitinger, T., and Wright, A. (1996) A gene (RPGR) with homology to the RCC1 guanine nucleotide exchange factor is mutated in X-linked retinitis pigmentosa (RP3). *Nature Genet.* **13,** 35-42.

Merrifield, R.B. (1963) Solid phase peptide synthesis. I. The synthesis of a tetrapeptide. *J. Am. Chem. Soc.* **85**, 2149-2154.

Molday, L.L., Cook, N.J., Kaupp, U.B., and Molday, R.S. (1990) The cGMP-gated cation channel of bovine rod photoreceptor cells is associated with a 240-kDa protein exhibiting immunochemical cross-reactivity with spectrin. *J. Biol. Chem.* **265**, 18690-18695.

Molday, R.S., Hicks, D., and Molday, L.L. (1987) Peripherin. A rim-specific membrane protein of rod outer segment discs. *Invest. Ophth. Vis. Sci.* **28**, 50-61.

Molday, R.S. and Molday, L.L. (1979) Identification and characterization of multiple forms of rhodopsin and minor proteins in frog and bovine rod outer segment disc membranes. Electrophoresis, lectin labeling, and proteolysis studies. *J. Biol. Chem.* **254**, 4653-4660.

Molday, R.S. and Molday, L.L. (1987) Differences in the protein composition of bovine retinal rod outer segment disk and plasma membranes isolated by a ricin-gold-dextran density perturbation method. *J. Cell Biol.* **105**, 2589-2601.

Molday, R.S. and Molday, L.L. (1993) Isolation and characterization of rod outer segment disk and plasma membranes. *Methods in Neurosci.* **15**, 131-150.

Monaco, J.J., Cho, S., and Attaya, M. (1990) Transport protein genes in the murine MHC: possible implications for antigen processing. *Science.* **250**, 1723-1726.

Moritz, O.L. and Molday, R.S. (1996) Molecular cloning, membrane topology, and localization of bovine rom-1 in rod and cone photoreceptor cells. *Invest. Ophth. Vis. Sci.* **37**, 352-362.

Nasonkin, I., Illing, M., Koehler, M.R., Schmid, M., Molday, R.S., and Weber, B.H.F. (1997) The human homologue of the bovine rim ABC transporter of rod photoreceptor outer segments maps to 1p22 and is mutated in Stargardt's disease. *Hum. Genet.* (in press).

Nathans J. (1989) The genes for color vision. *Sci. American.* **260,** 42-49.

Nichols, B.E., Drack, A.V., Vandenburgh, K., Kimura, A.E., Sheffield, V.C., and Stone E.M. (1993) A 2 base pair deletion in the *RDS* gene associated with butterfly-shaped pigment dystrophy of the fovea. *Hum. Mol. Genet.* **2,** 601-603.

Nikaido, H. (1994) Maltose transport system of *Escherichia coli*: an ABC-type transporter. *FEBS Lett.* **346,** 55-58.

Nikaido, K., Liu, P.-Q., and Ames, G.F.-L. (1997) Purification and characterization of HisP, the ATP-binding subunit of a traffic ATPase (ABC transporter), the histidine permease of *Salmonella typhimurium*. Solubility, dimerization, and ATPase activity. *J. Biol. Chem.* **272**, 27745-27752.

Osterberg, G. (1935) Topography of the layer of rods and cones in the human retina. *Acta Ophthalmol. (Copenh.)* **6**, 1-102.

Palczewski, K. (1994) Is vertebrate phototransduction solved? New insights into the molecular mechanism of phototransduction. *Invest. Ophth. Vis. Sci.* **35,** 3577-3581.

Palczewski, K., Hargrave, P.A., McDowell, J.H., and Ingebritsen, T.S., (1989) The catalytic subunit of phosphatase 2A dephosphorylates rhodopsin. *Biochemistry.* **28,** 415-419.

Palczewski, K., Subbaraya, I., Gorczyca, W.A., Helekar, B.S., Ruiz, C.C., Ohguro, H., Huang, J., Zhao, X., Crabb, J.W., and Johnson, R.S. (1994) Molecular cloning and characterization of retinal photoreceptor guanylyl cyclase-activating protein. *Neuron.* **13,** 395-404.

Papermaster, D.S., Reilly, P., and Schneider, B.G. (1982) Cone lamellae and red and green rod outer segment disks contain a large intrinsic membrane protein on their margins: an ultrastructural immunocytochemical study of frog retinas. *Vis. Res.* **22**, 1417-1428.

Papermaster, D.S., Schneider, B.G., Zorn, M.A., and Kraehenbuhl, J.P. (1978) Immunocytochemical localization of a large intrinsic membrane protein to the incisures and margins of frog rod outer segment disks. *J. Cell Biol.* **78**, 415-425.

Perrault, I., Rozet, J.M., Calvas, P., Gerber, S., Camuzat, A., Dollfus, H., Chatelin, S., Souied, E., Ghazi, I., Leowski, C., Bonnemaison, M., Le Paslier, D., Frezal, J., Dufier, J.L., Pittler, S., Munnich, A., and Kaplan, J. (1996) Retinal-specific guanylate cyclase gene mutations in Leber's congenital amaurosis. *Nature Genet.* **14**, 461-464.

Petronilli, V., and Ames, G.F.-L. (1991) Binding protein-independent histidine permease mutants. Uncoupling of ATP hydrolysis from transmembrane signaling. *J. Biol. Chem.* **266,** 16293-16296.

Polans, A., Baehr, W., and Palczewski, K. (1996) Turned on by Ca^{2+}: The physiology and pathology of Ca($^{2+}$)-binding proteins in the retina. *TINS.* **19**, 547-554.

Powis, S.J., Deverson, E.V., Coadwell, W.J., Ciruela, A., Huskisson, N.S., Smith, H., Butcher, G.W., and Howard, J.C. (1992) Effect of polymorphism of an MHC-linked transporter on the peptides assembled in a class I molecule. *Nature.* **357,** 211-215.

Pugh, E.N. Jr. and Lamb, T.D. (1993) Amplification and kinetics of the activation steps in phototransduction. *Acta Biochim. Biophys.* **1141,** 111-149.

Randak, C., Neth, P., Auerswald, E.A., Eckerskorn, C., Assfalg-Machleidt, I., and Machleidt, W. (1997) A recombinant polypeptide model of the second nucleotide-binding fold of the cystic fibrosis transmembrane conductance regulator functions as an active ATPase, GTPase and adenylate kinase. *FEBS Letters.* **410**, 180-186.

Reid, D.M., Friedel, U., Molday, R.S., and Cook, N.J. (1990) Identification of the sodium-calcium exchanger as the major ricin-binding glycoprotein of bovine rod outer segments and its localization to the plasma membrane. *Biochemistry.* **29**, 1601-1607.

Reilander, H., Achilles, A., Friedel, U., Maul, G., Lottspeich, F., and Cook, N.J. (1992) Primary structure and functional expression of the Na/Ca,K-exchanger from bovine rod photoreceptors. *EMBO J.* **11,** 1689-1695.

Riordan, J.R., Rommens, J.M., Kerem, B., Alon, N., Rozmahel, R., Grzelczak, Z., Zielenski, J., Lok, S., Plavsic, N., Chou, J.L., Drumm, M.L., Iannuzzi, M.C., Collins, F.S., and Tsui, L.-C. (1989) Identification of the cystic fibrosis gene: cloning and characterization of complementary DNA. *Science.* **245,** 1066-1073.

Robinson. W.E. and Hagins, W.A. (1979) GTP hydrolysis in intact rod outer segments and the transmitter cycle in visual excitation. *Nature.* **280,** 398-400.

Roof, D.J. and Heuser, J.E. (1982) Surfaces of rod photoreceptor disk membranes: integral membrane components. *J. Cell Biol.* **95**, 487-500.

Rosenfeld, P.J., Cowley, G.S., McGee, T.L., Sandberg, M.A., Berson, E.L., and Dryja, T.P. (1992) A null mutation in the rhodopsin gene causes rod photoreceptor dysfunction and autosomal recessive retinitis pigmentosa. *Nature Genet.* **1,** 209-213.

Sambrook, J., Fritsch, E.F., and Maniatis, T. (1989) Molecular cloning: A laboratory manual. 2nd ed. Cold Spring Harbor Press, New York.

Sanger, F., Niklen, S., and Coulson, A.R. (1977) DNA sequencing with chain-terminating inhibitors. *Proc. Natl. Acad. Sci. USA.* **74,** 5463-5467.

Sarkadi, B., Price, E.M., Boucher, R.C., Germann, U.A., and Scarborough, G.A. (1992) Expression of the human multidrug resistance cDNA in insect cells generates a high activity drug-stimulated membrane ATPase. *J. Biol. Chem.* **267,** 4854-4858.

Sauer, C.G., Gehrig, A., Warnekewittstock, R., Marquardt, A., Ewing, C.C., Gibson, A., Lorenz, B., Jurklies, B., and Weber, B.H.F. (1997) Positional cloning of the gene associated with X-linked juvenile retinoshisis. *Nature Genet.* **17,** 164-170.

Senior, A.E., Al-Shawi, M.K., and Urbatsch, I.L. (1995) The catalytic cycle of P-glycoprotein. *FEBS Lett.* **377,** 285-289.

Shapiro, A.B. and Ling, V. (1994) ATPase activity of purified and reconstituted P-glycoprotein from Chinese hamster ovary cells. *J. Biol. Chem.* **269,** 3745-3754.

Shapiro, A.B. and Ling, V. (1995) Using purified P-glycoprotein to understand multidrug resistance. *J. Bioener. Biomem.* **27,** 7-13.

Sharma, S. and Rose, D.R. (1995) Cloning, overexpression, purification, and characterization of the carboxyl-terminal nucleotide binding domain of P-glycoprotein. *J. Biol. Chem.* **270,** 14085-14093.

Shuster, T.A., Nagy, A.K., and Farber, D.B. (1988) Nucleotide binding to the rod outer segment rim protein. *Exp. Eye. Res.* **46,** 647-655.

Shyamala, V., Baichwal, V., Beall, E., and Ames, G.F. (1991) Structure-function analysis of the histidine permease and comparison with cystic fibrosis mutations. *J. Biol. Chem.* **266,** 18714-18719.

Shyjan, A.W., de Sauvage, F.J., Gillett, N.A., Goeddel, D.V., and Lowe, D.G. (1992) Molecular cloning of a retina-specific membrane guanylyl cyclase. *Neuron.* **9,** 727-737.

Smit, J.J., Schinkel, A.H., Oude Elferink, R.P., Groen, A.K., Wagenaar, E., van Deemter, L., Mol, C.A., Ottenhoff, R., van der Lugt, N.M., van Roon, M.A., van der Valk, M.A., Offerhaus, G.J.A., Berns, A.J.M., and Borst, P. (1993) Homozygous disruption of the murine MDR2 P-glycoprotein gene leads to a complete absence of phospholipid from bile and to liver disease. *Cell.* **75,** 451-462.

Smith, D.B. and Johnson, K.S. (1988) Single-step purification of polypeptides expressed in *Escherichia coli* as fusions with glutathione-S-transferase. *Gene* **67,** 31-40.

Spalton, D.J., Hitchings, R.A., and Hunter, P.A. eds. (1994) Atlas of clinical ophthalmology. 2nd ed. Wolfe Publishing, London.

Steinberg, R.H., Fisher, S.K. and Anderson, D.H. (1980) Disc morphogenesis in vertebrate photoreceptors. *J. Comp. Neurol.* **190**, 501-518.

Sun, H. and Nathans, J. (1997) Stargardt's *ABCR* is localized to the disc membrane of retinal rod outer segments. *Nature Genet.* **17,** 15-16.

Sung, C.H., Davenport, C.M., Hennessey, J.C., Maumenee, I.H., Jacobson, S.G., Heckenlively, J.R., Nowakowski, R., Fishman, G., Gouras, P., and Nathans, J. (1991) Rhodopsin mutations in autosomal dominant retinitis pigmentosa. *Proc. Natl. Acad. Sci. USA.* **88,** 6481-6485.

Szuts, E.Z. (1985) Light stimulates phosphorylation of two large membrane proteins in frog photoreceptors. *Biochemistry.* **24**, 4176-4184.

Thomas, P.J., Shenbagamurthi, P., Ysern, X., and Pedersen, P.L. (1991) Cystic fibrosis transmembrane conductance regulator: nucleotide binding to a synthetic peptide. *Science.* **251,** 555-557.

Towbin, H., Staehelin, T., and Gordon, J. (1979) Electrophoretic transfer of proteins from polyacrylamide gels to nitrocellulose sheets: procedure and some applications. *Proc. Natl. Acad. Sci. USA.* **76**, 4350-4354.

Trowsdale, J., Hanson, I., Mockridge, I., Beck, S., Townsend, A., and Kelly, A. (1990) Sequences encoded in the class II region of the MHC related to the ABC superfamily of transporters. *Nature.* **348**, 741-744.

Tusnády, G.E., Bakos, E., Váradi, A., and Sarkadi, B. (1997) Membrane topology distinguishes a subfamily of the ATP-binding cassette (ABC) transporters. *FEBS Lett.* **402**, 1-3.

Usukura, J. and Yamada, E. (1981) Molecular organization of the rod outer segment. A deep-etching study with rapid freezing using unfixed frog retina. *Biomed. Res.* **2**, 177-193.

Walker, J.E., Saraste, M., Runswick, M.J., and Gay, N.J. (1982) Distantly related sequences in the alpha- and beta-subunits of ATP synthase, myosin, kinases and other ATP-requiring enzymes and a common nucleotide binding fold. *EMBO J.* **1**, 945-951.

Walter, C., Höner zu Bentrup, K., and Schneider, E. (1992) Large scale purification, nucleotide binding properties, and ATPase activity of the MalK subunit of *Salmonella typhimurium* maltose transport complex. *J. Biol. Chem.* **267**, 8863-8869.

Weber, B.H.F., Sander, S., Kopp, C., Walker, D., Eckstein, A., Wissinger, B., Zrenner, E., and Grimm, T., (1996) Analysis of 21 Stargardt's disease families confirms a major locus on chromosome 1p with evidence for non-allelic heterogeneity in a minority of cases. *Brit. J. Ophthal.* **80,** 745-749.

Weber, B.H.F., Vogt, G., Stohr, H., Sander, S., Walker, D., and Jones, C. (1994) High-resolution meiotic and physical mapping of the best vitelliform macular dystrophy (VMD2) locus to pericentromeric chromosome 11. *Am. J. Hum. Genet.* **55,** 1182-1187.

Weil, D., Blanchard, S., Kaplan, J., Guilford, P., Gibson, F., Walsh, J., Mburu, P., Varela, A., Levilliers, J., Weston, M.D., Kelly, P.M., Kimberling, W.J., Wagenaar, M., Levi-Acobas, F., Larget-Piet, D., Munnich, A., Steel, K.P., Brown, S.D.M., and Petit, C. (1995) Defective myosin VIIA gene responsible for Usher syndrome type 1B. *Nature.* **374,** 60-61.

Weleber, R.G., Carr, R.E., Murphey, W.H., Sheffield, V.C., and Stone, E.M. (1993) Phenotypic variation including retinitis pigmentosa, pattern dystrophy, and fundus flavimaculatus in a single family with a deletion of codon 153 or 154 of the peripherin/RDS gene. *Arch. Ophthalmol.* **111,** 1531-1542.

Wells, J., Wroblewski, J., Keen, J., Inglehearn, C., Jubb, C., Eckstein, A., Jay, M., Arden, G., Bhattacharya, S., Fitzke, F., and Bird A.C. (1993) Mutations in the human retinal degeneration slow (RDS) gene can cause either retinitis pigmentosa or macular dystrophy. *Nature Genet.* **3,** 213-218.

Wilden, U., Hall, S.W., and Kühn, H. (1986) Phosphodiesterase activation by photoexcited rhodopsin is quenched when rhodopsin is phosphorylated and binds the intrinsic 48-kDa protein of rod outer segments. *Proc. Natl. Acad. Sci. USA.* **83,** 1174-1178.

Wilson, R., Ainscough, R., Anderson, K., Baynes, C., Berks, M., Bonfield, J., Burton, J., Connell, M., Copsey, T., Cooper, J., Coulson, A., Craxton, M., Dear, S., Du, Z., Durbin, R., Favello, A., Fraser, A., Fulton, L., Gardner, A., Green, P., Hawkins, T., Hillier, L., Jier, M., Johnston, L., Jones, M., Kershaw, J., Kirsten, J., Laisster, N., Latreille, P., Lightning, J., Lloyd, C., Mortimore, B., O'Callaghan, M., Parsons, J., Percy, C., Rifkin, L., Roopra, A., Saunders, D., Shownkeen, R., Sims, M., Smaldon, N., Smith, A., Smith, M., Sonnhammer, E., Staden, R., Sulston, J., Thierry-Mieg, J., Thomas, K., Vaudin, M., Vaughan, K., Waterson, R., Watson, A., Weinstock, L., Wilkinson-Sproat, J., and Wohldman, P. (1994) 2.2 Mb of contiguous nucleotide sequence from chromosome III of *C. elegans*. *Nature.* **368,** 32-38.

Winter, M.C. and Welsh, M.J. (1997) Stimulation of CFTR activity by its phosphorylated R domain. *Nature.* **389,** 294-296.

APPENDIX Buffers

HT (100X):

Hypoxanthine	136 mg
Thymidine	39 mg

per 100 ml of H_2O, filter sterilize
For HT medium: dilute to 1X into IMDM 10% FBS

HAT (100X):

Aminopterin	0.9 mg
100 X HT media	50 ml
1 M NaOH	dropwise, with stirring, until aminopterin dissolves

filter sterilize
For HAT medium: dilute to 1X into IMDM 10% FBS

LB medium:

tryptone	10 g
yeast extract	5 g
NaCl	10 g

per liter of H_2O

LB/Amp: 50 μg ampicillin per ml LB

Phosphate buffered saline (PBS):

NaCl	8 g
KCl	0.2 g
KH_2PO_4	0.2 g
Na_2HPO_4	1.15 g

per liter of H_2O

PBST: PBS with 0.05% Tween 20

20X SSC:

NaCl	175.6 g
sodium citrate , pH 7.0	88.2 g

per liter of H_2O

SM buffer:

NaCl	5.8 g
$MgSO_4 \cdot 7H_2O$	2 g
2% gelatin solution	5 ml
Tris·HCl, pH7.5	50 mM

per liter of H_2O